Charmless non-leptonic B_s decays to PP, PV and VV final states in the pQCD approach

Ahmed Ali[a], Gustav Kramer[b]

[a] *Deutsches Elektronen-Synchrotron DESY, 22607 Hamburg, Germany*

[b] *II. Institut für Theoretische Physik,*

Universität Hamburg, 22761 Hamburg, Germany

Ying Li, Cai-Dian Lü, Yue-Long Shen, Wei Wang and Yu-Ming Wang

Institute of High Energy Physics, CAS,

P.O. Box 918(4), 100049, P.R. China

(Dated: August 21, 2007)

Abstract

We calculate the CP-averaged branching ratios and CP-violating asymmetries of a number of two-body charmless hadronic decays $\overline{B_s^0} \to PP, PV, VV$ in the perturbative QCD (pQCD) approach to leading order in α_s (here P and V denote light pseudo-scalar and vector mesons, respectively). The mixing-induced CP violation parameters are also calculated for these decays. We also predict the polarization fractions of $B_s \to VV$ decays and find that the transverse polarizations are enhanced in some penguin dominated decays such as $\overline{B_s^0} \to K^*\overline{K^*}$, $K^*\rho$. Some of the predictions worked out here can already be confronted with the recently available data from the CDF collaboration on the branching ratios for the decays $\overline{B_s^0} \to K^+\pi^-$, $\overline{B_s^0} \to K^+K^-$ and the CP-asymmetry in the decay $\overline{B_s^0} \to K^+\pi^-$, and are found to be in agreement within the current errors. A large number of predictions for the branching ratios, CP-asymmetries and vector-meson polarizations in $\overline{B_s^0}$ decays, presented in this paper and compared with the already existing results in other theoretical frameworks, will be put to stringent experimental tests in forthcoming experiments at Fermilab, LHC and Super B-factories.

I. INTRODUCTION

There has been remarkable progress in the study of exclusive charmless $\overline{B_d^0} \rightarrow h_1 h_2$ and $B^\pm \rightarrow h_1 h_2$ decays, where h_1, h_2 are light pseudo-scalar and/or vector mesons. Historically, these decays were calculated in the so-called naive factorization approach [1], which was improved by including some perturbative QCD contributions [2, 3]. Currently, there are three popular theoretical approaches to study the dynamics of these decays, which go under the name QCD factorization (QCDF) [4], perturbative QCD (pQCD) [5], and soft-collinear effective theory (SCET) [6]. All three are based on power expansion in $1/m_b$, where m_b is the b-quark mass. Factorization of the hadronic matrix elements $\langle h_1 h_2 | \mathcal{O}_i | B \rangle$, where $\mathcal{O}_i$ is typically a four-quark or a magnetic moment type operator, is shown to exist in the leading power in $1/m_b$ in a class of decays. In addition, these approaches take into account some contributions in the decays $B \rightarrow h_1 h_2$ not included in the earlier attempts [1, 2, 3], in particular the so-called hard spectator graphs.

Despite being embedded in the Λ/m_b approach, justified by both the large mass, $m_b = O(5$ GeV$)$, and a large energy release in the decay, with $E_{h_i} = m_B/2$, these methods differ significantly from each other in a number of important aspects. For example, these differences pertain to whether one takes into account the collinear degrees of freedom only as in QCDF and SCET, or includes also the transverse momenta implemented using the Sudakov formalism, as followed in the pQCD method. Also, in pQCD, the power counting is different from the one in QCDF, which makes some amplitudes differ significantly in the two approaches. The other differing feature of pQCD and QCDF is the scale at which strong interaction effects, including the Wilson coefficients, are calculated. In pQCD, this scale is low, typically of order $1 - 2$ GeV. In QCDF, typical scales for the Wilson coefficients are taken as $O(m_b)$, following arguments based on factorization. There also exist detailed differences between QCDF and SCET, despite the fact that dedicated studies in the context of SCET have allowed to gain a better understanding of the QCDF framework. These differences, though not inherent, lie in how practically the calculations are done in the two approaches and involve issues such as the treatment of the so-called charming penguin contributions [7] to the decays $B \rightarrow h_1 h_2$. These are argued to be power-suppressed in QCDF, and left as phenomenological parameters to be determined by data in SCET. Likewise, the treatment of the hard spectator contribution in these two approaches is also different. We recall that a generic factorization formula [8]

$$\langle h_1 h_2 | \mathcal{O}_i | B \rangle = \Phi_{h_2}(u) * \left(T^I(u) F^{Bh_1}(0) + C^{II}(\tau, u) * \Xi^{Bh_1}(\tau, 0) \right) \tag{1}$$

involves the QCD form factor $F^{Bh_1}(0)$ and an unknown, non-local form factor $\Xi^{Bh_1}(\tau, 0)$. In QCDF, this non-local form factor factorizes into light-cone distribution amplitudes and a jet function $J(\tau, \omega, v)$, when the hard-collinear scale $\sqrt{m_b\Lambda}$ is integrated out. This interpretation of the hard spectator contribution was not at hand in the BBNS papers [4], but was gained subsequently in the SCET-analysis of the form factors [9]. Amusingly, this SCET-result is not used in the SCET-based phenomenology in $B \to h_1 h_2$ decays, for example in the works of Bauer et al. [10], where the use of perturbation theory at the scale $\sqrt{m_b\Lambda}$ is avoided. Detailed comparisons of their predictions with the data for the decays of the $\overline{B_d^0}$ (and its charge conjugate) and $B^{\pm}$-mesons have been made in the literature. We also refer to a recent critique [8] of the underlying theoretical assumptions in the three methods. Data from the B-factory experiments, BABAR and BELLE, as well as the CDF collaboration at the Tevatron, do provide some discrimination among them. With the advent of the LHC physics program, and the steadily improving experimental precision at the existing facilities, it should be possible to disentangle the underlying dynamics in hadronic B-decays.

The experimental program to study non-leptonic decays $\overline{B_s^0} \to h_1 h_2$ has also started [11], with first measurements for the branching ratios $\overline{B_s^0} \to K^+\pi^-$ and $\overline{B_s^0} \to K^+K^-$ made available recently by the CDF collaboration [12, 13] at the proton-antiproton collider Tevatron. Remarkably, the first direct CP asymmetry involving the decay $\overline{B_s^0} \to K^+\pi^-$ and its CP conjugate mode has also been reported by CDF [13], which is found to be large, with $A_{\mathrm{CP}}(\overline{B_s^0} \to K^+\pi^-) = (39 \pm 15 \pm 8)\%$. This is in agreement with the predictions of the pQCD approach, as we also quantify in this paper. With the ongoing B-Physics program at the Tevatron, but, in particular, with the onset of the LHC experiments, as well as the Super B-factories being contemplated for the future, we expect a wealth of data involving the decays of the hitherto less studied $\overline{B_s^0}$ meson. The charmless $\overline{B_s^0} \to h_1 h_2$ decays are important for the CP asymmetry studies and the determination of the inner angles of the unitarity triangle, in particular γ (or ϕ_3), which has not yet been precisely measured. In addition, a number of charmless decays $\overline{B_s^0} \to h_1 h_2$ can be related to the $\overline{B_d^0} \to h_1 h_2$ decays using SU(3) (or U-spin) symmetry, and hence data on these decays can be combined to test the underlying standard model and search for physics beyond the SM under less (dynamical) model-dependent conditions. Anticipating the experimental developments, many studies have been devoted to the interesting charmless $\overline{B_s^0} \to h_1 h_2$ decays. Among others, they include detailed estimates undertaken in the naive factorization framework [14], the so-called generalized factorization approach [15], QCDF [16, 17, 18], pQCD [19] and SCET [20]. There are

3

also many studies [21] undertaken, parameterizing the various parts of the decay amplitudes using distinct topologies and the flavor symmetries to relate the $\overline{B_s^0} \to h_1 h_2$ and $\overline{B_d^0} \to h_1 h_2$ decays. Possible New Physics effects in these decays have also been explored [22].

In the applications of the pQCD approach to $\overline{B_s^0} \to h_1 h_2$ decays, the currently available works concentrate on specific decays. However, a comprehensive study of the decays $\overline{B_s^0} \to h_1 h_2$, which have been undertaken in QCDF and SCET, to the best of our knowledge, is still lacking in pQCD. Our aim is to fill in this gap and provide a ready reference to the existing and forthcoming experiments to compare their data with the predictions in the pQCD approach. In doing this, we have included the current information on the CKM matrix elements, updated some input hadronic parameters and have calculated the decay form factors in the pQCD approach. Since these form factors have to be provided from outside in QCDF and SCET (such as by resorting to QCD sum rules), there is already a potential source of disagreement among these approaches on this count. However, we remark that the estimates presented here for the cases $B_s \to PP, PV, VV$ are rather similar to the corresponding ones in the existing literature on the light cone QCD sum rules. Thus, theoretical predictions presented in this work reflect the detailed assumptions about the dynamics endemic to pQCD, such as the effective scales which are generated by the strong interaction aspects of the weak non-leptonic two-body decays, setting the relative strengths of the various competing amplitudes in magnitudes and phases. As we work in the leading order (LO) in α_s, there is considerable uncertainty related to the scale-dependence, which we quantify in the estimates of the branching ratios, CP-asymmetries and polarization fractions for the decays considered in this paper. Likewise, parametric uncertainties in the numerical estimates of these quantities resulting from other input parameters are worked out. Together, they quantify the theoretical imprecision in $\overline{B_s^0} \to h_1 h_2$ decays at the current stage in the pQCD approach. We have made detailed comparison of our predictions with the existing literature on the decays $\overline{B_s^0} \to h_1 h_2$ and in some benchmark decay widths and rate asymmetries in the corresponding $\overline{B_d^0} \to h_1 h_2$ decays. Whenever available, we have also compared our predictions with the data and found that they are generally compatible with each other.

We also present numerical results for some selected ratios of the branching ratios involving the decays $\overline{B_s^0} \to K^+ K^-$, $\overline{B_s^0} \to K^+ \pi^-$, $\overline{B_d^0} \to \pi^+ \pi^-$ and $\overline{B_d^0} \to K^- \pi^+$, which are related by SU(3) and U-spin symmetries. For comparison with other approaches, we also give in Table IV the contributions of the various topologies for these decays. The ratios worked out numerically are: $R_1 \equiv \frac{BR(\overline{B_s^0} \to K^+ K^-)}{BR(\overline{B_d^0} \to \pi^+ \pi^-)}$, $R_2 \equiv \frac{BR(\overline{B_s^0} \to K^+ K^-)}{BR(\overline{B_d^0} \to K^- \pi^+)}$, and two more, called R_3 and Δ, defined in Eq. (72)

4

and (73), respectively, which involve the decays $\overline{B_d^0} \to K^- \pi^+$ and $\overline{B_s^0} \to K^+ \pi^-$ and their charge conjugates. All these ratios have been measured experimentally and the pQCD-based estimates presented here are in agreement with the data, except possibly the ratio R_1 which turns out too small. Whether this reflects an intrinsic limitation of the pQCD approach or the inadequacy of the LO framework remains to be seen, as complete next-to-leading order (NLO) calculations of all the relevant pieces of the $B \to h_1 h_2$ decay matrix elements are still not in place. However, there are sound theoretical arguments why the ratios R_2, R_3 and Δ are protected against higher order QCD corrections, such as the charge conjugation invariance of the strong interactions (for R_3 and Δ), and the dominance of the decay amplitudes in the numerator and denominator in the ratio R_2 by a single decay topology. The agreement between the pQCD approach and data in these quantities is, therefore, both non-trivial and encouraging.

This paper is organized as follows: In section II, we briefly review the pQCD approach and give the essential input quantities that enter the pQCD approach, including the operator basis used subsequently and the numerical values of the Wilson coefficients together with their scale dependence. The wave function of the $\overline{B_s^0}$-meson, the distribution amplitudes for the light pseudo-scalar and vector mesons and the input values of the various mesonic decay constants are also given here. Section III contains the calculation of the $\overline{B_s^0} \to PP$ mesons, making explicit the contributions from the so-called emission and annihilation diagrams. Numerical results for the charge-conjugated averages of the decay branching ratios, direct CP-asymmetries, the time-dependent CP asymmetries S_f and the observables H_f in the time-dependent decay rates are tabulated in Tables III, V and VI, respectively. These tables also contain detailed comparisons of our work with the corresponding numerical results obtained in the QCDF and SCET approaches, as well as with the available data. Section IV contains the numerical results for the decays $\overline{B_s^0} \to PV$. They are presented in Tables VII, VIII and IX for the charge-conjugated averages of the decay branching ratios, time-integrated CP-asymmetries, the time-dependent CP asymmetries S_f and the observables H_f in the time-dependent decay rates, respectively. We also show the corresponding results from the QCDF approach in Tables VII and VIII. Section V is devoted to a study of the decays $\overline{B_s^0} \to VV$, making explicit the amplitudes for the longitudinal (L), normal (N) and transverse (T) polarization components of the vector mesons. Numerical results for the CP-averaged branching ratios are presented in Table X, and compared with the corresponding results from the QCDF approach, updated recently in Ref. [18], and available data. Results for the three polarization fractions f_0, $f_\parallel$, $f_\perp$, the relative strong phases $\phi_\parallel(rad)$, $\phi_\perp(rad)$ and the CP-asymmetries are

displayed in Table XI. Appendix A contains the various functions that enter the factorization formulae in the pQCD approach. Appendix B gives the analytic formulae for the $\overline{B_s^0} \to PP$ decays used in the numerical calculations, while the details of the formulae for the decays $\overline{B_s^0} \to PV$ and $\overline{B_s^0} \to VV$ are relegated to Appendix C and D, respectively.

II. THE EFFECTIVE HAMILTONIAN AND THE INPUT QUANTITIES

A. Notations and Conventions

We specify the weak effective Hamiltonian [23]:

$$\mathcal{H}_{eff} = \frac{G_F}{\sqrt{2}}\left\{V_{ub}V_{uq}^*\left[C_1(\mu)Q_1^u(\mu) + C_2(\mu)Q_2^u(\mu)\right] - V_{tb}V_{tq}^*\left[\sum_{i=3}^{10}C_i(\mu)Q_i(\mu)\right]\right\} + \text{H.c.}, \quad (2)$$

where $q = d, s$. The functions Q_i $(i = 1, ..., 10)$ are the local four-quark operators:

- current–current (tree) operators

$$Q_1^u = (\bar{u}_\alpha b_\beta)_{V-A}(\bar{q}_\beta u_\alpha)_{V-A}, \qquad Q_2^u = (\bar{u}_\alpha b_\alpha)_{V-A}(\bar{q}_\beta u_\beta)_{V-A}, \qquad (3)$$

- QCD penguin operators

$$Q_3 = (\bar{q}_\alpha b_\alpha)_{V-A}\sum_{q'}(\bar{q}'_\beta q'_\beta)_{V-A}, \qquad Q_4 = (\bar{q}_\beta b_\alpha)_{V-A}\sum_{q'}(\bar{q}'_\alpha q'_\beta)_{V-A}, \qquad (4)$$

$$Q_5 = (\bar{q}_\alpha b_\alpha)_{V-A}\sum_{q'}(\bar{q}'_\beta q'_\beta)_{V+A}, \qquad Q_6 = (\bar{q}_\beta b_\alpha)_{V-A}\sum_{q'}(\bar{q}'_\alpha q'_\beta)_{V+A}, \qquad (5)$$

- electro-weak penguin operators

$$Q_7 = \frac{3}{2}(\bar{q}_\alpha b_\alpha)_{V-A}\sum_{q'}e_{q'}(\bar{q}'_\beta q'_\beta)_{V+A}, \quad Q_8 = \frac{3}{2}(\bar{q}_\beta b_\alpha)_{V-A}\sum_{q'}e_{q'}(\bar{q}'_\alpha q'_\beta)_{V+A}, \qquad (6)$$

$$Q_9 = \frac{3}{2}(\bar{q}_\alpha b_\alpha)_{V-A}\sum_{q'}e_{q'}(\bar{q}'_\beta q'_\beta)_{V-A}, \quad Q_{10} = \frac{3}{2}(\bar{q}_\beta b_\alpha)_{V-A}\sum_{q'}e_{q'}(\bar{q}'_\alpha q'_\beta)_{V-A}, \qquad (7)$$

where α and β are the color indices and q' are the active quarks at the scale m_b, i.e. $q' = (u, d, s, c, b)$. The left handed current is defined as $(\bar{q}'_\alpha q'_\beta)_{V-A} = \bar{q}'_\alpha \gamma_\nu(1 - \gamma_5)q'_\beta$ and the right handed current $(\bar{q}'_\alpha q'_\beta)_{V+A} = \bar{q}'_\alpha \gamma_\nu(1 + \gamma_5)q'_\beta$. The combinations a_i of Wilson coefficients are defined as usual [3]:

$$a_1 = C_2 + C_1/3, \ a_3 = C_3 + C_4/3, \ a_5 = C_5 + C_6/3, \ a_7 = C_7 + C_8/3, \ a_9 = C_9 + C_{10}/3,$$

$$a_2 = C_1 + C_2/3, \ a_4 = C_4 + C_3/3, \ a_6 = C_6 + C_5/3, \ a_8 = C_8 + C_7/3, \ a_{10} = C_{10} + C_9/3. \quad (8)$$

6

TABLE I: Numerical values of the combinations of Wilson coefficients defined in the text at different scales (μ).

μ (GeV)	2.5	2.0	1.5	1.0
a_1	1.1	1.1	1.1	1.1
$a_2 (\times 10^{-2})$	1.1	-2.8	-8.7	-19.4
$a_3 (\times 10^{-3})$	6.2	7.5	9.7	14.4
$a_4 (\times 10^{-3})$	-32.0	-35.8	-41.4	-51.3
$a_5 (\times 10^{-3})$	-5.6	-7.4	-10.5	-17.6
$a_6 (\times 10^{-3})$	-46.8	-54.9	-68.2	-95.6
$a_7 (\times 10^{-4})$	12.6	12.7	13.2	14.0
$a_8 (\times 10^{-4})$	9.6	10.6	12.2	15.7
$a_9 (\times 10^{-4})$	-84.3	-85.4	-87.2	-91.0
$a_{10} (\times 10^{-4})$	-0.87	2.3	7.0	15.5

Since we work in the leading order of perturbative QCD ($O(\alpha_s)$), it is consistent to use the leading order Wilson coefficients. The scale μ characterizes the typical scale for the hard scattering, and for four different values of this scale the results of the Wilson coefficients are listed in Table I. It is seen that the coefficient a_2 and the penguin operator Wilson coefficients a_3, a_5 have a large dependence on the scale which will give large uncertainties to those channels highly dependent on them, such as the color-suppressed QCD penguin dominant processes. This situation is typical of leading order estimates; the reduction in the scale-dependence requires the calculation of next-to-leading order results which are beyond the theoretical accuracy to which we are working.

We consider the $\bar{B}_s^0 \to M_2 M_3$ decay. In the emission type diagrams with the spectator quark $\bar{s}$ from the initial state $\bar{B}_s$ recombining to form the meson M_3, we denote the emitted meson as M_2 while the recoiling meson is M_3. The factorization formula is then denoted as $F_{\bar{B}_s \to M_3}$. It is convenient to define two light-like vectors: n and v. These two vectors satisfy $n^2 = v^2 = 0$ and $n \cdot v = 1$. The meson M_2 is moving along the direction of $n = (1, 0, \mathbf{0}_T)$ and M_3 is on $v = (0, 1, \mathbf{0}_T)$, we use x_i to denote the momentum fraction of the anti-quark in each meson, $k_{i\perp}$ to denote the
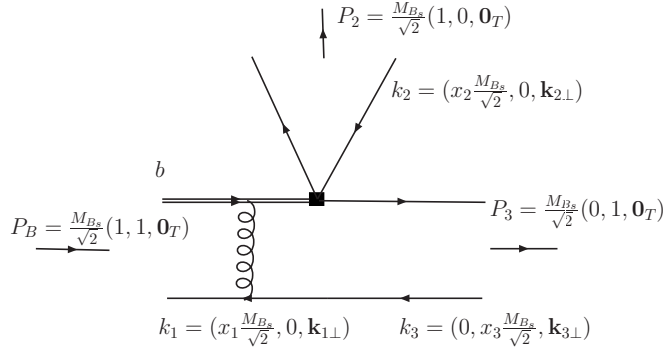
FIG. 1: The notation in our calculation

transverse momentum of the anti-quark:

$$
\begin{aligned}
P_B &= \frac{M_{B_s}}{\sqrt{2}}(1, 1, \mathbf{0}_T), \quad P_2 = \frac{M_{B_s}}{\sqrt{2}}(1, 0, \mathbf{0}_T), \quad P_3 = \frac{M_{B_s}}{\sqrt{2}}(0, 1, \mathbf{0}_T), \\
k_1 &= (x_1 \frac{M_{B_s}}{\sqrt{2}}, 0, \mathbf{k}_{1\perp}), \quad k_2 = (x_2 \frac{M_{B_s}}{\sqrt{2}}, 0, \mathbf{k}_{2\perp}), \quad k_3 = (0, x_3 \frac{M_{B_s}}{\sqrt{2}}, \mathbf{k}_{3\perp}),
\end{aligned}
\tag{9}
$$

which are shown in Figure 1.

B. Wave Functions of the B_s Meson

In order to calculate the analytic formulas of the decay amplitude, we use the light cone wave functions $\Phi_{M,\alpha\beta}$ decomposed in terms of the spin structure. In general, $\Phi_{M,\alpha\beta}$ with Dirac indices α, β can be decomposed into 16 independent components, $1_{\alpha\beta}$, $\gamma^\mu_{\alpha\beta}$, $\sigma^{\mu\nu}_{\alpha\beta}$, $(\gamma^\mu \gamma_5)_{\alpha\beta}$, $\gamma_{5\alpha\beta}$. If the considered meson M is the B_s meson, a heavy pseudo-scalar meson, the B_s meson light-cone matrix element can be decomposed as [24, 25]

$$
\begin{aligned}
&\int d^4 z e^{ik_1 \cdot z} \langle 0 | \bar{b}_\alpha(0) s_\beta(z) | B_s(P_{B_s}) \rangle \\
&= \frac{i}{\sqrt{6}} \left\{ (\slashed{P}_{B_s} + M_{B_s}) \gamma_5 \left[\phi_{B_s}(k_1) - \frac{\slashed{n} - \slashed{v}}{\sqrt{2}} \bar{\phi}_{B_s}(k_1) \right] \right\}_{\beta\alpha}.
\end{aligned}
\tag{10}
$$

From the above equation, one can see that there are two Lorentz structures in the B_s meson distribution amplitudes. They obey the following normalization conditions

$$
\int \frac{d^4 k_1}{(2\pi)^4} \phi_{B_s}(k_1) = \frac{f_{B_s}}{2\sqrt{6}}, \quad \int \frac{d^4 k_1}{(2\pi)^4} \bar{\phi}_{B_s}(k_1) = 0.
\tag{11}
$$

In general, one should consider these two Lorentz structures in the calculations of B_s meson decays. However, it is found that the contribution of $\bar{\phi}_{B_s}$ is numerically small [26], thus its

8

contribution can be neglected. With this approximation, we only retain the first term in the square bracket from the full Lorentz structure in Eq. (10)

$$\Phi_{B_s} = \frac{i}{\sqrt{6}}(\not{P}_{B_s} + M_{B_s})\gamma_5\phi_{B_s}(k_1). \tag{12}$$

In the next section, we will see that the hard part is always independent of one of the k_1^+ and/or k_1^-, if we make the approximations shown in the next section. The B_s meson wave function is then a function of the variables k_1^- (or k_1^+) and $k_1^\perp$ only,

$$\phi_{B_s}(k_1^-, k_1^\perp) = \int \frac{dk_1^+}{2\pi}\phi_{B_s}(k_1^+, k_1^-, k_1^\perp) . \tag{13}$$

Then, the B_s meson's wave function in the b-space can be expressed by

$$\Phi_{B_s}(x, b) = \frac{i}{\sqrt{6}}\left[\not{P}_{B_s}\gamma_5 + M_{B_s}\gamma_5\right]\phi_{B_s}(x, b), \tag{14}$$

where b is the conjugate space coordinate of the transverse momentum $k^\perp$.

In this study, we use the model function similar to that of the B meson which is

$$\phi_{B_s}(x, b) = N_{B_s}x^2(1-x)^2 \exp\left[-\frac{M_{B_s}^2 \, x^2}{2\omega_b^2} - \frac{1}{2}(\omega_b b)^2\right], \tag{15}$$

with N_{B_s} the normalization factor. In recent years, a lot of studies have been performed for the B_d^0 and $B^\pm$ decays in the pQCD approach [5]. The parameter $\omega_b = 0.40$ GeV has been fixed there using the rich experimental data on the B_d^0 and $B^\pm$ mesons. In the SU(3) limit, this parameter should be the same in B_s decays. Considering a small SU(3) breaking, the s quark momentum fraction here should be a little larger than that of the u or d quark in the lighter B mesons, since the s quark is heavier than the u or d quark. The shape of the distribution amplitude is shown in Fig.2 for $\omega_B = 0.45$ GeV, 0.5 GeV, and 0.55 GeV. It is easy to see that the larger ω_b gives a larger momentum fraction to the s quark. We will use $\omega_b = 0.50 \pm 0.05$ GeV in this paper for the B_s decays.

C. Distribution Amplitudes of Light Pseudo-scalar Mesons

The decay constant f_P of the pseudo-scalar meson is defined by the matrix element of the axial current:

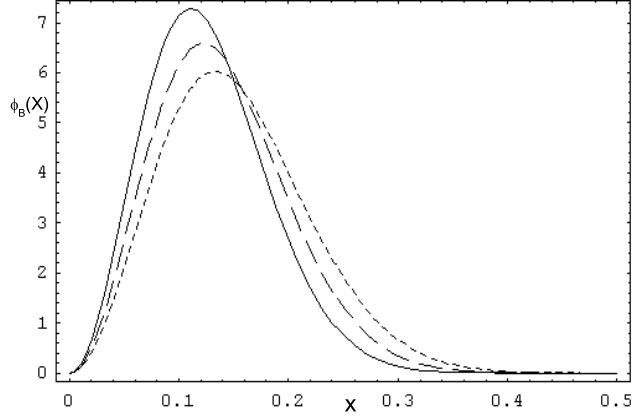$$\langle 0|\bar{q}_1\gamma_\mu\gamma_5 q_2|P(P)\rangle = if_P P_\mu. \tag{16}$$

FIG. 2: B_s meson distribution amplitudes. The solid-, dashed-, and tiny-dashed- lines correspond to $\omega_B = 0.45$ GeV, 0.5 GeV, and 0.55 GeV.

TABLE II: Input values of the decay constants of the pseudo-scalar and vector mesons (in MeV) [27, 28]

f_π	f_K	f_ρ	f_ρ^T	f_ω	f_ω^T	f_{K^*}	$f_{K^*}^T$	f_ϕ	f_ϕ^T
131	160	209 ± 2	165 ± 9	195 ± 3	145 ± 10	217 ± 5	185 ± 10	231 ± 4	200 ± 10

The pseudo-scalar decay constants are shown in table II, taken from the Particle Data Group [28]. The vector meson longitudinal decay constants are extracted from the data on $\tau^- \to (\rho^-, K^{*-})\nu_\tau$ [28] and the transverse decay constants are taken from QCD sum rules [29, 30]. The input values given in table II are very similar to the ones used in [16].

The light-cone distribution amplitudes are defined by the matrix elements of the non-local light-ray operators at the light-like separation z_μ with $z^2 = 0$, and sandwiched between the vacuum and the meson state. The two-particle light-cone distribution amplitudes of an outgoing pseudo-scalar meson P, up to twist-3 accuracy, are defined by [31]:

$$\langle P(P)|\bar{q}_2(z)\gamma_\mu\gamma_5 q_1(0)|0\rangle = -if_P P_\mu \int_0^1 dx e^{ixP\cdot z}\phi_2(x), \tag{17}$$

$$\langle P(P)|\bar{q}_2(z)\gamma_5 q_1(0)|0\rangle = -if_P m_0 \int_0^1 dx e^{ixP\cdot z}\phi_3^P(x) , \tag{18}$$

$$\langle P(P)|\bar{q}_2(z)\sigma_{\mu\nu}\gamma_5 q_1(0)|0\rangle = \frac{i}{6}f_P m_0(P_\mu z_\nu - P_\nu z_\mu) \int_0^1 dx e^{ixP\cdot z}\phi_3^\sigma(x) . \tag{19}$$

where we have omitted the Wilson line connecting the two space-time points. $\phi_2(x)$, $\phi_3^P(x)$ and $\phi_3^\sigma(x)$ have unit normalization. M_P is the mass of the pseudo-scalar meson, m_0 is the chiral scale parameter which is defined using the meson mass and the quark masses as $m_0 = \frac{M_P^2}{m_{q_1}+m_{q_2}}$:

10

$m_0^\pi = 1.4$ GeV and $m_0^K = 1.9$ GeV, x is the momentum fraction associated with the quark q_2. It is easy to observe that the contribution from $\phi_2(x)$, independent of the mass, is twist-2. The contributions from $\phi_3^P(x)$ and $\phi_3^\sigma(x)$, proportional to $r = m_0/M_{B_s}$, are twist-3.

The above definitions can be collected as

$$\langle P(P)|\bar{q}_{2\beta}(z)q_{1\alpha}(0)|0\rangle = -\frac{i}{\sqrt{6}}\int_0^1 dx e^{ixP\cdot z}\left[\gamma_5 \not{P}\phi^A(x) + m_0\gamma_5\phi^P(x) - m_0\sigma^{\mu\nu}\gamma_5 P_\mu z_\nu \frac{\phi^\sigma(x)}{6}\right]_{\alpha\beta}$$
$$= -\frac{i}{\sqrt{6}}\int_0^1 dx e^{ixP\cdot z}\left[\gamma_5 \not{P}\phi^A(x) + \gamma_5 m_0\phi^P(x) + m_0\gamma_5(\not{n}\not{v} - 1)\phi^T(x)\right]_{\alpha\beta} ,$$

(20)

with the redefinitions of the distribution amplitudes:

$$\phi^A(x) = \frac{f_P}{2\sqrt{6}}\phi_2(x),\ \ \phi^P(x) = \frac{f_P}{2\sqrt{6}}\phi_3^P(x),\ \ \phi^\sigma(x) = \frac{f_P}{2\sqrt{6}}\phi_3^\sigma(x),$$

(21)

and we have performed the integration by parts for the third terms and $\phi^T(x) = \frac{1}{6}\frac{d}{dx}\phi^\sigma(x)$.

In the pQCD approach, the only non-perturbative inputs are the meson decay constants and meson light cone distribution amplitudes, and they are both channel independent. The meson decay constants are either measured through the leptonic decays of the mesons and the semileptonic decays of the τ-lepton or calculated from the measured ones using broken SU(3) symmetry. Therefore there is not much uncertainty in them. The wave functions depend on the factorization scale and also the factorization scheme. In principle, they should be determined by experiment. Although there is no direct experimental measurement for the moments yet, the non-leptonic B^0 and $B^\pm$ decays already give much information on them [5, 33]. Since the pQCD approach gives very good results for these decays, especially the direct CP asymmetries in $B^0 \to \pi^+\pi^-$ and $B^0 \to K^+\pi^-$ decays [34], we will use the well constrained light cone distribution amplitudes of the mesons in these papers [31] (see [32] for a summary and update of the LCDAs):

$$\phi_\pi^A(x) = \frac{3f_\pi}{\sqrt{6}}x(1-x)[1 + 0.44C_2^{3/2}(t)],$$

(22)

$$\phi_\pi^P(x) = \frac{f_\pi}{2\sqrt{6}}[1 + 0.43C_2^{1/2}(t)],$$

(23)

$$\phi_\pi^T(x) = -\frac{f_\pi}{2\sqrt{6}}[C_1^{1/2}(t) + 0.55C_3^{1/2}(t)],$$

(24)

$$\phi_K^A(x) = \frac{3f_K}{\sqrt{6}}x(1-x)[1 + 0.17C_1^{3/2}(t) + 0.2C_2^{3/2}(t)],$$

(25)

$$\phi_K^P(x) = \frac{f_K}{2\sqrt{6}}[1 + 0.24C_2^{1/2}(t)],$$

(26)

$$\phi_K^T(x) = -\frac{f_K}{2\sqrt{6}}[C_1^{1/2}(t) + 0.35C_3^{1/2}(t)],$$

(27)

11

with Gegenbauer polynomials defined as:

$$
\begin{aligned}
C_1^{1/2}(t) &= t, & C_1^{3/2}(t) &= 3t \\
C_2^{1/2}(t) &= \tfrac{1}{2}(3t^2 - 1), & C_2^{3/2}(t) &= \tfrac{3}{2}(5t^2 - 1), \\
C_3^{1/2}(t) &= \tfrac{1}{2}t(5t^2 - 3) \ ,
\end{aligned}
\tag{28}
$$

and $t = 2x - 1$. In the LCDAs for $\phi_\pi^A(x)$, $\phi_\pi^P(x)$ and $\phi_K^P(x)$, we have dropped the terms proportional to $C_4^{1/2,3/2}$, and take into account only the first two terms in their expansion, consistently with the rest of the LCDAs. These distribution amplitudes are very close to the previous QCD sum rule results [31]. In recent years, there have been continuing updates of the light cone distribution amplitudes [35]. However, the changes in the coefficients of the Gegenbauer polynomials do not affect our results significantly, as shown in the next section. We also point out that the default value of the scale at which the Gegenbauer coefficients are given above is 1 GeV. However, the scale of the perturbative calculation in the pQCD approach where these LCDAs enter is typically 2 GeV. The LCDAs can be scaled up, as the required anomalous dimensions are known. We have done this and find that the resulting numerical differences are small. Strictly speaking, these differences are part of the NLO corrections. With the current theoretical accuracy, they can be absorbed in the uncertainties on the input Gegenbauer coefficients in the numerical calculations.

As for the mixing of η and η', we use the quark flavor basis proposed by Feldmann, Kroll and Stech [36], i.e. these two mesons are made of $\bar{n}n = (\bar{u}u + \bar{d}d)/\sqrt{2}$ and $\bar{s}s$:

$$
\begin{pmatrix} |\eta\rangle \\ |\eta'\rangle \end{pmatrix} = U(\phi) \begin{pmatrix} |\eta_n\rangle \\ |\eta_s\rangle \end{pmatrix},
\tag{29}
$$

with the matrix,

$$
U(\phi) = \begin{pmatrix} \cos\phi & -\sin\phi \\ \sin\phi & \cos\phi \end{pmatrix},
\tag{30}
$$

where the mixing angle $\phi = 39.3° \pm 1.0°$. In principle, this mixing mechanism is equivalent to the singlet and octet formalism, as discussed in [36], and the advantage here is that explicitly only two decay constants are needed:

$$
\begin{aligned}
\langle 0|\bar{n}\gamma^\mu\gamma_5 n|\eta_n(P)\rangle &= \frac{i}{\sqrt{2}} f_n P^\mu \ , \\
\langle 0|\bar{s}\gamma^\mu\gamma_5 s|\eta_s(P)\rangle &= i f_s P^\mu \ .
\end{aligned}
\tag{31}
$$

We assume that the distribution amplitudes of $\bar{n}n$ and $\bar{s}s$ are the same as the distribution amplitudes of π, except for the different decay constants and the chiral scale parameters. We

use [36]

$$f_n = (1.07 \pm 0.02)f_\pi = 139.1 \pm 2.6 \text{ MeV}, \quad f_s = (1.34 \pm 0.06)f_\pi = 174.2 \pm 7.8 \text{ MeV}, \quad (32)$$

as the averaged results from the experimental data. The chiral enhancement factors are chosen as

$$m_0^{\bar{n}n} = \frac{1}{2m_n}[m_\eta^2 \cos^2\phi + m_{\eta'}^2 \sin^2\phi - \frac{\sqrt{2}f_s}{f_n}(m_{\eta'}^2 - m_\eta^2)\cos\phi\sin\phi], \quad (33)$$

$$m_0^{\bar{s}s} = \frac{1}{2m_s}[m_{\eta'}^2 \cos^2\phi + m_\eta^2 \sin^2\phi - \frac{f_n}{\sqrt{2}f_s}(m_{\eta'}^2 - m_\eta^2)\cos\phi\sin\phi]. \quad (34)$$

There are gluonic contributions which have been investigated in [37], with the result that these parts do not change the numerical results significantly. So, we will not consider this kind of contribution in this work.

D. Distribution Amplitudes of Light Vector Mesons

We choose the vector meson momentum P with $P^2 = M_V^2$, which is mainly in the plus direction. The polarization vectors ϵ, satisfying $P \cdot \epsilon = 0$, include one longitudinal polarization vector ϵ_L and two transverse polarization vectors ϵ_T. Following a similar procedure as for the pseudo-scalar mesons, we can derive the vector meson distribution amplitudes up to twist-3 [38]:

$$\langle V(P, \epsilon_L^*)|\bar{q}_{2\beta}(z)q_{1\alpha}(0)|0\rangle = \frac{1}{\sqrt{6}}\int_0^1 dx e^{ixP\cdot z}\left[M_V \not\epsilon_L^* \phi_V(x) + \not\epsilon_L^* \not P \phi_V^t(x) + M_V \phi_V^s(x)\right]_{\alpha\beta} (35)$$

$$\langle V(P, \epsilon_T^*)|\bar{q}_{2\beta}(z)q_{1\alpha}(0)|0\rangle = \frac{1}{\sqrt{6}}\int_0^1 dx e^{ixP\cdot z}\left[M_V \not\epsilon_T^* \phi_V^v(x) + \not\epsilon_T^* \not P \phi_V^T(x) \right.$$
$$\left. + M_V i\epsilon_{\mu\nu\rho\sigma}\gamma_5\gamma^\mu\epsilon_T^{*\nu}n^\rho v^\sigma \phi_V^a(x)\right]_{\alpha\beta}, \quad (36)$$

for longitudinal polarization and transverse polarization, respectively. Here x is the momentum fraction associated with the q_2 quark. We adopt the convention $\epsilon^{0123} = 1$ for the Levi-Civita tensor $\epsilon^{\mu\nu\alpha\beta}$.

The twist-2 distribution amplitudes for a longitudinally polarized vector meson can be parameterized as:

$$\phi_\rho(x) = \frac{3f_\rho}{\sqrt{6}}x(1-x)\left[1 + a_{2\rho}^\| C_2^{3/2}(t)\right], \quad (37)$$

$$\phi_\omega(x) = \frac{3f_\omega}{\sqrt{6}}x(1-x)\left[1 + a_{2\omega}^\| C_2^{3/2}(t)\right], \quad (38)$$

$$\phi_{K^*}(x) = \frac{3f_{K^*}}{\sqrt{6}}x(1-x)\left[1 + a_{1K^*}^\| C_1^{3/2}(t) + a_{2K^*}^\| C_2^{3/2}(t)\right], \quad (39)$$

$$\phi_\phi(x) = \frac{3f_\phi}{\sqrt{6}}x(1-x)\left[1 + a_{2\phi}^\| C_2^{3/2}(t)\right]. \quad (40)$$

13

Here f_V is the decay constant of the vector meson with longitudinal polarization, whose values are shown in table II. The Gegenbauer moments have been studied extensively in the literatures [38, 39], here we adopt the following values from the recent updates [29, 30, 40]:

$$a_{1K^*}^{||} = 0.03 \pm 0.02, \quad a_{2\rho}^{||} = a_{2\omega}^{||} = 0.15 \pm 0.07, \quad a_{2K^*}^{||} = 0.11 \pm 0.09, \quad a_{2\phi}^{||} = 0.18 \pm 0.08, \quad (41)$$

and we use the asymptotic form [41]:

$$\phi_V^t(x) = \frac{3f_V^T}{2\sqrt{6}}t^2, \quad \phi_V^s(x) = \frac{3f_V^T}{2\sqrt{6}}(-t) . \quad (42)$$

The twist-2 transversely polarized distribution amplitudes ϕ_V^T have a similar form as the longitudinally polarized ones in eq.(37-40), with the moments [29, 30]:

$$a_{1K^*}^{\perp} = 0.04 \pm 0.03, \quad a_{2\rho}^{\perp} = a_{2\omega}^{\perp} = 0.14 \pm 0.06, \quad a_{2K^*}^{\perp} = 0.10 \pm 0.08, \quad a_{2\phi}^{\perp} = 0.14 \pm 0.07. \quad (43)$$

The asymptotic form of the twist-3 distribution amplitudes ϕ_V^v and ϕ_V^a are

$$\phi_V^v(x) = \frac{3f_V}{8\sqrt{6}}(1 + t^2), \quad \phi_V^a(x) = \frac{3f_V}{4\sqrt{6}}(-t). \quad (44)$$

The above choices of vector meson distribution amplitudes can essentially explain the measured $B \to K^*\phi$, $B \to K^*\rho$ and $B \to \rho\rho$ polarization fractions [41, 42, 43, 44], together with the right branching ratios.

E.   A Brief Review of the pQCD Approach

The basic idea of the pQCD approach is that it takes into account the transverse momentum of the valence quarks in the hadrons which results in the Sudakov factor in the decay amplitude. As an example, taking the first diagram in Fig. 3, the emitted particle M_2 in the decay can be factored out (in terms of the appropriate vacuum to M_2 transition matrix element) and the rest of the amplitude can be expressed as the convolution of the wave functions ϕ_{B_s}, ϕ_{M_3} and the hard scattering kernel T_H, integrated over the longitudinal and the transverse momenta. Thus,

$$\mathcal{M} \propto \int_0^1 dx_1 dx_3 \int \frac{d^2\vec{k}_{1T}}{(2\pi)^2} \frac{d^2\vec{k}_{3T}}{(2\pi)^2} \phi_B(x_1, \vec{k}_{1T}, p_1, t) T_H(x_1, x_3, \vec{k}_{1T}, \vec{k}_{3T}, t) \phi_V(x_3, \vec{k}_{3T}, p_3, t) . \quad (45)$$

It is convenient to calculate the decay amplitude in coordinate space. Through the Fourier transformation, the above equation can be expressed as:

$$\mathcal{M} \propto \int_0^1 dx_1 dx_3 \int d^2\vec{b}_1 d^2\vec{b}_3 \phi_B(x_1, \vec{b}_1, p_1, t) T_H(x_1, x_3, \vec{b}_1, \vec{b}_3, t) \phi_V(x_3, \vec{b}_3, p_3, t) . \quad (46)$$

14

Loop effects can, in principle, be taken into account in the above expression. In general, individual higher order diagrams suffer from two types of infrared divergences: soft and collinear. Soft divergence arise from the region of a loop momentum where all it's components in the light-cone coordinate vanish:

$$l^\mu = (l^+, l^-, \vec{l}_T) = (\Lambda, \Lambda, \vec{\Lambda}). \tag{47}$$

Collinear divergence originates from the gluon momentum region which is parallel to the massless quark momentum,

$$l^\mu = (l^+, l^-, \vec{l}_T) \sim (m_B, \Lambda^2/m_B, \vec{\Lambda}). \tag{48}$$

In both cases, the loop integration corresponds to $\int d^4 l/l^4 \sim \log \Lambda$, so logarithmic divergences are generated. It has been shown order by order in perturbation theory that these divergences can be separated from the hard perturbative kernel and absorbed into the meson wave functions using the eikonal approximation [45] . One also encounters double logarithm divergences when soft and collinear momenta overlap. These large double logarithm can be re-summed into the Sudakov factor and the explicit form is given in Appendix A.

Loop corrections to the weak decay vertex also give rise to double logarithms. For example, the first diagram in Fig. 3 gives an amplitude proportional to $1/(x_3^2 x_1)$. In the threshold region with $x_3 \to 0$, additional collinear divergences are associated with the internal quark. The QCD loop corrections to the weak vertex can produce the double logarithm $\alpha_s \ln^2 x_3$ and the re-summation of this type of double logarithms leads to the Sudakov factor $S_t(x_3)$. Similarly, the re-summation of $\alpha_s \ln^2 x_1$ due to loop corrections in the other diagram lead to the Sudakov factor $S_t(x_1)$. These double logarithm can also be factored out from the hard part and grouped into the quark jet function [46]. This type of factor decreases faster than any power of x as $x \to 0$, so it removes the endpoint singularity. For simplicity, this factor has been parameterized in a form which is independent of the decay channels, twist and flavors [47].

Combining all the elements together, the typical factorization formula in the pQCD approach reads as:

$$\mathcal{M} \propto \int_0^1 dx_1 dx_3 \int d^2\vec{b}_1 d^2\vec{b}_3 \phi_B(x_1, \vec{b}_1, p_1, t)$$
$$\times T_H(x_1, x_3, \vec{b}_1, \vec{b}_3, t)\phi_{M_3}(x_3, \vec{b}_3, p_3, t)S_t(x_3)\exp[-S_B(t) - S_3(t)] . \tag{49}$$

The threshold Sudakov function $S_t(x_3)$ and the Sudakov exponents $S_B(t)$, $S_2(t)$ and $S_3(t)$ are given in Appendix A. Again, strictly speaking, the Sudakov improvements result from higher
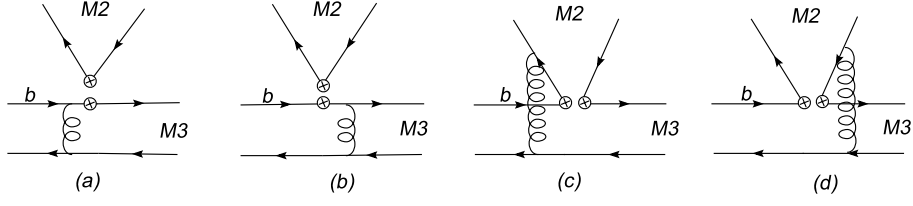
FIG. 3: The Feynman diagrams for emission contribution, with possible four-quark operator insertions

order contributions. However, they are included traditionally in the pQCD approach, though in most applications, the perturbative function $T_H(x_1, x_3, \vec{b}_1, \vec{b}_3, t)\phi_{M_3}(x_3, \vec{b}_3, p_3, t)$ is calculated only in the leading order in α_s .

III.   CALCULATION OF THE $B_s \to PP$ DECAY AMPLITUDES IN THE PQCD APPROACH

In the following we will give the general factorization formulae for $\bar{B}_s \to PP$ decays, and the pQCD functions can be found in Appendix A. We will use LL to denote the contribution from $(V-A)(V-A)$ operators, LR to denote the contribution from $(V-A)(V+A)$ operators and SP to denote the contribution from $(S-P)(S+P)$ operators which result from the Fierz transformation of the $(V-A)(V+A)$ operators.

A.   Emission Diagram

The emission diagrams are depicted in Figure 3. The first two diagrams are called factorizable. They will give the $B \to M_3$ decay form factor, if we factor out the corresponding Wilson coefficients a_i.

- $(V-A)(V-A)$ operators:

$$
\begin{aligned}
f_{M_2} F_{B_s \to M_3}^{LL}(a_i) &= 8\pi C_F M_{B_s}^4 f_{M_2} \int_0^1 dx_1 dx_3 \int_0^\infty b_1 db_1 b_3 db_3 \phi_{B_s}(x_1, b_1) \Big\{ a_i(t_a) E_e(t_a) \\
&\times \Big[(1+x_3)\phi_3^A(x_3) + r_3(1-2x_3)(\phi_3^P(x_3) + \phi_3^T(x_3))\Big] h_e(x_1, x_3, b_1, b_3) \\
&+ 2r_3\phi_3^P(x_3) a_i(t_a') E_e(t_a') h_e(x_3, x_1, b_3, b_1) \Big\},
\end{aligned}
$$

(50)

- $(V-A)(V+A)$ operators:

$$
F_{B_s \to M_3}^{LR}(a_i) = -F_{B_s \to M_3}^{LL}(a_i),
$$

(51)

16

- $(S - P)(S + P)$ operators:

$$f_{M_2} F^{SP}_{B_s \to M_3}(a_i) = 16\pi r_2 C_F M^4_{B_s} f_{M_2} \int_0^1 dx_1 dx_3 \int_0^\infty b_1 db_1 b_3 db_3 \phi_{B_s}(x_1, b_1) \Big\{ a_i(t_a) E_e(t_a)$$
$$\times \Big[\phi_3^A(x_3) + r_3(2 + x_3)\phi_3^P(x_3) - r_3 x_3 \phi_3^T(x_3) \Big] h_e(x_1, x_3, b_1, b_3)$$
$$+ 2r_3 \phi_3^P(x_3) a_i(t'_a) E_e(t'_a) h_e(x_3, x_1, b_3, b_1) \Big\}, \tag{52}$$

with $C_F = 4/3$ and a_i the corresponding Wilson coefficients for specific channels. In the above functions, $r_i = m_{0i}/m_{B_s}$, where m_{0i} is the chiral scale parameter. The functions E_i, the definitions of the factorization scales t_i and the hard functions h_i are given in Appendix A.

The last two diagrams in Fig.3 (c)(d) are the non-factorizable diagrams, whose contributions are

- $(V - A)(V - A)$ operators:

$$M^{LL}_{B_s \to M_3}(a_i) = 32\pi C_F M^4_{B_s}/\sqrt{6} \int_0^1 dx_1 dx_2 dx_3 \int_0^\infty b_1 db_1 b_2 db_2 \phi_{B_s}(x_1, b_1) \phi_2^A(x_2)$$
$$\times \Big\{ \Big[(1 - x_2)\phi_3^A(x_3) - r_3 x_3(\phi_3^P(x_3) - \phi_3^T(x_3)) \Big] a_i(t_b) E'_e(t_b)$$
$$\times h_n(x_1, 1 - x_2, x_3, b_1, b_2) + h_n(x_1, x_2, x_3, b_1, b_2)$$
$$\times \Big[- (x_2 + x_3)\phi_3^A(x_3) + r_3 x_3(\phi_3^P(x_3) + \phi_3^T(x_3)) \Big] a_i(t'_b) E'_e(t'_b) \Big\}, \tag{53}$$

- $(V - A)(V + A)$ operators:

$$M^{LR}_{B_s \to M_3}(a_i) = 32\pi C_F M^4_{B_s} r_2/\sqrt{6} \int_0^1 dx_1 dx_2 dx_3 \int_0^\infty b_1 db_1 b_2 db_2 \phi_{B_s}(x_1, b_1)$$
$$\times \Big\{ h_n(x_1, 1 - x_2, x_3, b_1, b_2) \Big[(1 - x_2)\phi_3^A(x_3) \left(\phi_2^P(x_2) + \phi_2^T(x_2) \right)$$
$$+ r_3 x_3 \left(\phi_2^P(x_2) - \phi_2^T(x_2) \right) \left(\phi_3^P(x_3) + \phi_3^T(x_3) \right)$$
$$+ (1 - x_2) r_3 \left(\phi_2^P(x_2) + \phi_2^T(x_2) \right) \left(\phi_3^P(x_3) - \phi_3^T(x_3) \right) \Big] a_i(t_b) E'_e(t_b)$$
$$- h_n(x_1, x_2, x_3, b_1, b_2) \Big[x_2 \phi_3^A(x_3)(\phi_2^P(x_2) - \phi_2^T(x_2))$$
$$+ r_3 x_2(\phi_2^P(x_2) - \phi_2^T(x_2))(\phi_3^P(x_3) - \phi_3^T(x_3))$$
$$+ r_3 x_3(\phi_2^P(x_2) + \phi_2^T(x_2))(\phi_3^P(x_3) + \phi_3^T(x_3)) \Big] a_i(t'_b) E'_e(t'_b) \Big\}, \tag{54}$$
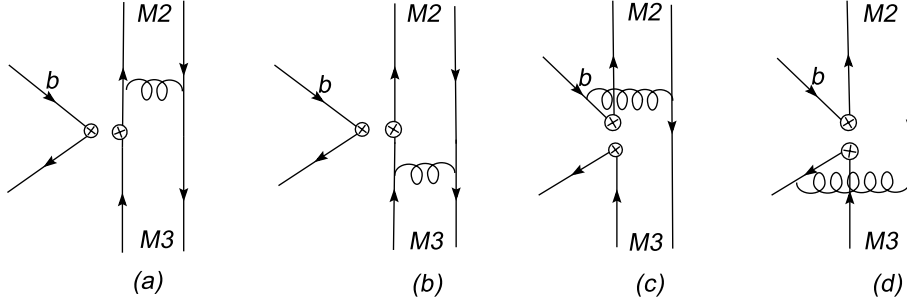
FIG. 4: The Feynman diagrams for annihilation contribution, with possible four-quark operator insertions

- $(S-P)(S+P)$ operators:

$$
\begin{aligned}
M^{SP}_{B_s \to M_3}(a_i) =\ & 32\pi C_F M^4_{B_s}/\sqrt{6} \int_0^1 dx_1 dx_2 dx_3 \int_0^\infty b_1 db_1 b_2 db_2 \phi_{B_s}(x_1, b_1)\phi_2^A(x_2) \\
& \times \Bigg\{ \Big[(x_2 - x_3 - 1)\phi_3^A(x_3) + r_3 x_3(\phi_3^P(x_3) + \phi_3^T(x_3)) \Big] \\
& \times a_i(t_b)E'_e(t_b)h_n(x_1, 1 - x_2, x_3, b_1, b_2) + a_i(t'_b)E'_e(t'_b) \\
& \times \Big[x_2\phi_3^A(x_3) + r_3 x_3(\phi_3^T(x_3) - \phi_3^P(x_3)) \Big] h_n(x_1, x_2, x_3, b_1, b_2) \Bigg\}.
\end{aligned}
\tag{55}
$$

From these formulas we can see that there are cancellations between the two diagrams of Fig.3 (c) and (d). If the Wilson coefficients are the same, the non-factorizable contributions (proportional to the small x_i) are power suppressed compared to the factorizable emission diagram contributions in eq.(50-52).

B. Annihilation type Diagrams

We group all the W annihilation and W-exchange, space-like penguin and time-like penguin annihilation diagrams together and refer to them as the annihilation type diagrams. In Fig.4, the first two diagrams are the factorizable annihilation diagrams, whose contributions are

- $(V - A)(V - A)$ operators:

$$
\begin{aligned}
f_{B_s} F_{ann}^{LL}(a_i) =\ & 8\pi C_F M_{B_s}^4 f_{B_s} \int_0^1 dx_2 dx_3 \int_0^\infty b_2 db_2 b_3 db_3 \Big\{ a_i(t_c) E_a(t_c) \\
& \times \Big[(x_3 - 1)\phi_2^A(x_2)\phi_3^A(x_3) - 4r_2 r_3 \phi_2^P(x_2)\phi_3^P(x_3) \\
& + 2r_2 r_3 x_3 \phi_2^P(x_2)(\phi_3^P(x_3) - \phi_3^T(x_3)) \Big] h_a(x_2, 1 - x_3, b_2, b_3) \\
& + \Big[x_2 \phi_2^A(x_2)\phi_3^A(x_3) + 2r_2 r_3 (\phi_2^P(x_2) - \phi_2^T(x_2))\phi_3^P(x_3) \\
& + 2r_2 r_3 x_2 (\phi_2^P(x_2) + \phi_2^T(x_2))\phi_3^P(x_3) \Big] a_i(t_c') E_a(t_c') h_a(1 - x_3, x_2, b_3, b_2) \Big\}. (56)
\end{aligned}
$$

There is a big cancellation between the two factorizable diagrams Fig.4(a) and (b), such that they are highly power suppressed, which agrees with the long time argument that the annihilation contributions are negligible. Especially, if the two final state mesons are identical, the formula of eq.(56) gives exactly zero.

- $(V - A)(V + A)$ operators:

$$
F_{ann}^{LR}(a_i) = F_{ann}^{LL}(a_i), \tag{57}
$$

- $(S - P)(S + P)$ operators:

$$
\begin{aligned}
f_{B_s} F_{ann}^{SP}(a_i) =\ & 16\pi C_F M_{B_s}^4 f_{B_s} \int_0^1 dx_2 dx_3 \int_0^\infty b_2 db_2 b_3 db_3 \Big\{ \Big[2r_2 \phi_2^P(x_2)\phi_3^A(x_3) \\
& + (1 - x_3) r_3 \phi_2^A(x_2)(\phi_3^P(x_3) + \phi_3^T(x_3)) \Big] a_i(t_c) E_a(t_c) h_a(x_2, 1 - x_3, b_2, b_3) \\
& + \Big[2r_3 \phi_2^A(x_2)\phi_3^P(x_3) + r_2 x_2 (\phi_2^P(x_2) - \phi_2^T(x_2))\phi_3^A(x_3) \Big] \\
& \times a_i(t_c') E_a(t_c') h_a(1 - x_3, x_2, b_3, b_2) \Big\}. \tag{58}
\end{aligned}
$$

It is interesting to see that the two diagrams Fig.4 (a) and (b) give constructive contributions here. Furthermore, they are not power suppressed as the $(V - A)(V - A)$ operator contribution in eq.(56) (proportional to the small x_i), but proportional to $2r_2$ or $2r_3$. This gives the chirally enhanced contributions in the annihilation type diagrams. The operator O_6-induced space-like penguin contributions produce a large strong phase, which is essential to explain the large direct CP asymmetry in the $B^0 \to \pi^+\pi^-$ and $B^0 \to K^+\pi^-$ decays [34].

The last two diagrams in Fig.4 are the non-factorizable annihilation diagrams, whose contributions are

- $(V - A)(V - A)$ operators:

$$M_{ann}^{LL}(a_i) = 32\pi C_F M_{B_s}^4/\sqrt{6} \int_0^1 dx_1 dx_2 dx_3 \int_0^\infty b_1 db_2 b_2 db_2 \phi_{B_s}(x_1, b_1)$$

$$\times \Big\{ h_{na}(x_1, x_2, x_3, b_1, b_2) \Big[- x_2 \phi_2^A(x_2)\phi_3^A(x_3) - 4r_2 r_3 \phi_2^P(x_2)\phi_3^P(x_3)$$

$$+ r_2 r_3 (1 - x_2)(\phi_2^P(x_2) + \phi_2^T(x_2))(\phi_3^P(x_3) - \phi_3^T(x_3))$$

$$+ r_2 r_3 x_3 (\phi_2^P(x_2) - \phi_2^T(x_2))(\phi_3^P(x_3) + \phi_3^T(x_3)) \Big] a_i(t_d) E_a'(t_d)$$

$$+ h_{na}'(x_1, x_2, x_3, b_1, b_2) \Big[(1 - x_3)\phi_2^A(x_2)\phi_3^A(x_3)$$

$$+ (1 - x_3)r_2 r_3 (\phi_2^P(x_2) + \phi_2^T(x_2))(\phi_3^P(x_3) - \phi_3^T(x_3))$$

$$+ x_2 r_2 r_3 (\phi_2^P(x_2) - \phi_2^T(x_2))(\phi_3^P(x_3) + \phi_3^T(x_3)) \Big] a_i(t_d') E_a'(t_d') \Big\}, \qquad (59)$$

- $(V - A)(V + A)$ operators:

$$M_{ann}^{LR}(M_2, M_3, a_i) = 32\pi C_F M_{B_s}^4/\sqrt{6} \int_0^1 dx_1 dx_2 dx_3 \int^\infty b_1 db_1 b_2 db_2 \phi_{B_s}(x_1, b_1)$$

$$\times \Big\{ h_{na}(x_1, x_2, x_3, b_1, b_2) \Big[r_2(2 - x_2)(\phi_2^P(x_2) + \phi_2^T(x_2))\phi_3^A(x_3)$$

$$- r_3(1 + x_3)\phi_2^A(x_2)(\phi_3^P(x_3) - \phi_3^T(x_3)) \Big] a_i(t_d) E_a'(t_d)$$

$$+ h_{na}'(x_1, x_2, x_3, b_1, b_2) \Big[r_2 x_2 \left(\phi_2^P(x_2) + \phi_2^T(x_2) \right) \phi_3^A(x_3)$$

$$+ r_3(x_3 - 1)\phi_2^A(x_2)(\phi_3^P(x_3) - \phi_3^T(x_3)) \Big] a_i(t_d') E_a'(t_d') \Big\}, \qquad (60)$$

- $(S - P)(S + P)$ operators:

$$M_{ann}^{SP}(a_i) = 32\pi C_F M_{B_s}^4/\sqrt{6} \int_0^1 dx_1 dx_2 dx_3 \int_0^\infty b_1 db_1 b_2 db_2 \phi_{B_s}(x_1, b_1)$$

$$\times \Big\{ a_i(t_d) E_a'(t_d) h_{na}(x_1, x_2, x_3, b_1, b_2) \Big[(x_3 - 1)\phi_2^A(x_2)\phi_3^A(x_3)$$

$$- 4r_2 r_3 \phi_2^P(x_2)\phi_3^P(x_3) + r_2 r_3 x_3 (\phi_2^P(x_2) + \phi_2^T(x_2))(\phi_3^P(x_3) - \phi_3^T(x_3))$$

$$+ r_2 r_3 (1 - x_2)(\phi_2^P(x_2) - \phi_2^T(x_2))(\phi_3^P(x_3) + \phi_3^T(x_3)) \Big]$$

$$+ a_i(t_d') E_a'(t_d') h_{na}'(x_1, x_2, x_3, b_1, b_2) \Big[x_2 \phi_2^A(x_2)\phi_3^A(x_3)$$

$$+ x_2 r_2 r_3 (\phi_2^P(x_2) + \phi_2^T(x_2))(\phi_3^P(x_3) - \phi_3^T(x_3))$$

$$+ r_2 r_3 (1 - x_3)(\phi_2^P(x_2) - \phi_2^T(x_2))(\phi_3^P(x_3) + \phi_3^T(x_3)) \Big] \Big\}. \qquad (61)$$

They are all power suppressed compared to the factorizable emission diagrams.

C. Results for $B_s \to PP$ decays

First we give the numerical results in the pQCD approach for the form factors at maximal recoil. For the form factors, we obtain:

$$F_0^{B \to \pi} = 0.23^{+0.05+0.00}_{-0.04-0.00}, \quad F_0^{B \to K} = 0.28^{+0.06+0.00}_{-0.05-0.00}, \tag{62}$$

$$F_0^{B_s \to K} = 0.24^{+0.05+0.00}_{-0.04-0.01}, \tag{63}$$

where $f_B = 0.19 \pm 0.02$ GeV, $\omega_B = 0.40$ GeV (for the $B^\pm$ and B_d^0 mesons) and $f_{B_s} = 0.23 \pm 0.02$ GeV, $\omega_{B_s} = 0.50 \pm 0.05$ GeV (for the B_s^0 meson) have been used. They quantify the SU(3)-symmetry breaking effects in the form factors in the pQCD approach. The input values for f_B and f_{B_s} are in agreement with the unquenched lattice results [48] $f_B = 0.216 \pm 0.022$ GeV and $f_{B_s} = 0.259 \pm 0.032$ GeV, and with the results from the QCD sum rules [49, 50]. We also mention in passing that a recent calculation of the distribution amplitudes for the pion and kaon with the QCD sum rules [51], which includes a new logarithmic divergent term in the twist-3 distribution amplitudes, leads to very large SU(3)-breaking effects in the form factors, calculating the form factors in the standard pQCD approach [52]. This has also been observed in [27]. Whether this feature also emerges in the light-cone sum rule approach is not clear to us.

For the CKM matrix elements, we adopt the updated results from [53] and drop the (small) errors on V_{ud}, V_{us}, V_{ts} and V_{tb}:

$$
\begin{aligned}
&|V_{ud}| = 0.974, &&|V_{us}| = 0.226, &&|V_{ub}| = (3.68^{+0.11}_{-0.08}) \times 10^{-3}, \\
&|V_{td}| = (8.20^{+0.59}_{-0.27}) \times 10^{-3}, &&|V_{ts}| = 40.96 \times 10^{-3}, &&|V_{tb}| = 1.0, \\
&\alpha = (99^{+4}_{-9.4})^\circ, &&\gamma = (59.0^{+9.7}_{-3.7})^\circ, &&\arg[-V_{ts}V_{tb}^*] = 1.0^\circ.
\end{aligned}
\tag{64}
$$

The CKM factors mostly give an overall factor to the branching ratios. However, the CKM angles do give large uncertainties to the branching ratios of some decays and to all the non-zero CP asymmetries. We will discuss their effects separately.

The formulas of the decay amplitudes for the various channels in terms of above topologies are given in Appendix B. The CP-averaged branching ratios of $B_s \to PP$ decays are listed in Table III. The dominant topologies contributing to these decays are also indicated through the symbols T (tree), P (penguin), P_{EW} (electroweak penguins), C (color-suppressed tree), and ann (annihilation). The first error in these entries arises from the input hadronic parameters, which is dominated by the B_s-meson decay constant (taken as $f_{B_s} = 0.23 \pm 0.02$ GeV) and the B_s meson wave function shape parameter (taken as $\omega_b = 0.50 \pm 0.05$ GeV). The second error is from the

21

TABLE III: The CP-averaged branching ratios ($\times 10^{-6}$) of $B_s \to PP$ decays obtained in the pQCD approach (This work); the errors for these entries correspond to the uncertainties in the input hadronic quantities, from the scale-dependence, and the CKM matrix elements, respectively. We have also listed the current experimental measurements and upper limits (90% C.L.) wherever available [13]. For comparison, we also cite the theoretical estimates of the branching ratios in the QCD factorization framework [16], and in SCET [20], quoting two estimates in the latter case for some decays.

Modes	Class	QCDF	SCET	This work	Exp.
$\overline{B}_s^0 \to K^+\pi^-$	T	$10.2^{+4.5+3.8+0.7+0.8}_{-3.9-3.2-1.2-0.7}$	$4.9 \pm 1.2 \pm 1.3 \pm 0.3$	$7.6^{+3.2+0.7+0.5}_{-2.3-0.7-0.5}$	$5.0 \pm 0.75 \pm 1.0$
$\overline{B}_s^0 \to K^0\pi^0$	C	$0.49^{+0.28+0.22+0.40+0.33}_{-0.24-0.14-0.14-0.17}$	$0.76 \pm 0.26 \pm 0.27 \pm 0.17$	$0.16^{+0.05+0.10+0.02}_{-0.04-0.05-0.01}$	
$\overline{B}_s^0 \to K^+K^-$	P	$22.7^{+3.5+12.7+2.0+24.1}_{-3.2-8.4-2.0-9.1}$	$18.2 \pm 6.7 \pm 1.1 \pm 0.5$	$13.6^{+4.2+7.5+0.7}_{-3.2-4.1-0.2}$	$24.4 \pm 1.4 \pm 4.6$
$\overline{B}_s^0 \to K^0\overline{K}^0$	P	$24.7^{+2.5+13.7+2.6+25.6}_{-2.4-9.2-2.9-9.8}$	$17.7 \pm 6.6 \pm 0.5 \pm 0.6$	$15.6^{+5.0+8.3+0.0}_{-3.8-4.7-0.0}$	
$\overline{B}_s^0 \to \pi^0\eta$	P_{EW}	$0.075^{+0.013+0.030+0.008+0.010}_{-0.012-0.025-0.010-0.007}$	$0.014 \pm 0.004 \pm 0.005 \pm 0.004$	$0.05^{+0.02+0.01+0.00}_{-0.02-0.01-0.00}$	< 1000
			$0.016 \pm 0.0007 \pm 0.005 \pm 0.006$		
$\overline{B}_s^0 \to \pi^0\eta'$	P_{EW}	$0.11^{+0.02+0.04+0.01+0.01}_{-0.02-0.04-0.01-0.01}$	$0.006 \pm 0.003 \pm 0.002^{+0.064}_{-0.006}$	$0.11^{+0.05+0.02+0.00}_{-0.03-0.01-0.00}$	
			$0.038 \pm 0.013 \pm 0.016^{+0.260}_{-0.036}$		
$\overline{B}_s^0 \to K^0\eta$	C	$0.34^{+0.19+0.64+0.21+0.16}_{-0.16-0.27-0.07-0.08}$	$0.80 \pm 0.48 \pm 0.29 \pm 0.18$	$0.11^{+0.05+0.06+0.01}_{-0.03-0.03-0.01}$	
			$0.59 \pm 0.34 \pm 0.24 \pm 0.15$		
$\overline{B}_s^0 \to K^0\eta'$	C	$2.0^{+0.3+1.5+0.6+1.5}_{-0.3-1.1-0.3-0.6}$	$4.5 \pm 1.5 \pm 0.4 \pm 0.5$	$0.72^{+0.20+0.28+0.11}_{-0.16-0.17-0.05}$	
			$3.9 \pm 1.3 \pm 0.5 \pm 0.4$		
$\overline{B}_s^0 \to \eta\eta$	P	$15.6^{+1.6+9.9+2.2+13.5}_{-1.5-6.8-2.5-5.5}$	$7.1 \pm 6.4 \pm 0.2 \pm 0.8$	$8.0^{+2.6+4.7+0.0}_{-1.9-2.5-0.0}$	< 1500
			$6.4 \pm 6.3 \pm 0.1 \pm 0.7$		
$\overline{B}_s^0 \to \eta\eta'$	P	$54.0^{+5.5+32.4+8.3+40.5}_{-5.2-22.4-6.4-16.7}$	$24.0 \pm 13.6 \pm 1.4 \pm 2.7$	$21.0^{+6.0+10.0+0.0}_{-4.6-5.6-0.0}$	
			$23.8 \pm 13.2 \pm 1.6 \pm 2.9$		
$\overline{B}_s^0 \to \eta'\eta'$	P	$41.7^{+4.2+26.3+15.2+36.6}_{-4.0-17.2-8.5-15.4}$	$44.3 \pm 19.7 \pm 2.3 \pm 17.1$	$14.0^{+3.2+6.2+0.0}_{-2.7-3.9-0.0}$	
			$49.4 \pm 20.6 \pm 8.4 \pm 16.2$		
$\overline{B}_s^0 \to \pi^+\pi^-$	ann	$0.024^{+0.003+0.025+0.000+0.163}_{-0.003-0.012-0.000-0.021}$	—	$0.57^{+0.16+0.09+0.01}_{-0.13-0.10-0.00}$	< 1.36
$\overline{B}_s^0 \to \pi^0\pi^0$	ann	$0.012^{+0.001+0.013+0.000+0.082}_{-0.001-0.006-0.000-0.011}$	—	$0.28^{+0.08+0.04+0.01}_{-0.07-0.05-0.00}$	< 210

hard scale t, defined in Eqs. (A1) – (A8) in Appendix A, which we vary from $0.75t$ to $1.25t$, and from $\Lambda^{(5)}_{QCD} = 0.25 \pm 0.05$ GeV. The scale-dependent uncertainty can be reduced only if the next-to-leading order contributions in the pQCD approach are known. A part of this perturbative improvement coming from the Wilson coefficients in the NLO approximation can be implemented already. However, the complete NLO corrections to the hard spectator kernels are still missing. The third error is the combined uncertainty in the CKM matrix elements and the angles of the unitarity triangle.

For comparison, we also reproduce verbatim the corresponding numerical results evaluated in the framework of the QCD factorization (QCDF) [16], and the ones obtained using the Soft-Collinear-Effective-Theory (SCET) [20]. For the decays $B^0_s \to PP$ involving an η- and/or an η'-meson, Ref. [20] quotes two sets of values, which differ in the input values of the SCET parameters specific to the iso-singlet modes, describing gluonic contributions to the $B \to \eta^{(\prime)}$ form factors and the gluonic parts of the charming penguins. They are not too different from each other except for the electroweak-penguin-dominated decay $\overline{B^0_s} \to \pi^0 \eta'$. The errors quoted in the QCDF case correspond, respectively, to the assumed variation of the CKM parameters, variation of the renormalization scales, quark masses, decay constants, form factors and (whenever applicable) the η - η' mixing angle (collectively called "hadronic 1"), uncertainties in the expansion of the light-cone distribution amplitudes (called "hadronic 2"), and estimates of the power corrections. The errors shown in the case of the SCET-based results are due to the estimates of the SU(3)-breaking, $1/m_b$ corrections and the errors on the SCET-parameters. The last column gives the current experimental data from the CDF collaboration [12, 13], and the upper limits correspond to 90% C.L.

A number of remarks on the entries in Table III is in order. We note that there is general agreement among these methods in the tree and penguin-dominated $B^0_s \to PP$ decays, with the variations reflecting essentially the differences in the input quantities. This agreement is less marked for the color-suppressed and electroweak-penguin dominated decays. For the annihilation dominated decays, SCET has no predictions and QCDF has essentially no predictive power as indicated by the estimates for the decays $\overline{B^0_s} \to \pi^+ \pi^-$ and $\overline{B^0_s} \to \pi^0 \pi^0$, which vary over more than an order of magnitude once the parametric uncertainties are taken into account. First measurements of the tree-dominated decay $\overline{B^0_s} \to K^+ \pi^-$ and the penguin-dominated decay $\overline{B^0_s} \to K^+ K^-$ have been reported by the CDF collaboration, and are in the right ball-park of the predictions shown in Table III. A good number of the decays shown in this Table will be measured at the LHC

and Super B-factories, which would discriminate among the predictions of the three frameworks.

The decays $B \to \pi\pi$, $B \to K\pi$, $B_s \to K\pi$ and $B_s \to KK$ have received a lot of theoretical interest, as they can be related by SU(3)-symmetry, a question of considerable interest is the amount of SU(3)-breaking in various topologies (diagrams) contributing to these decays. To that end, we present in Table IV the magnitude of the decay amplitudes (squared, in units of GeV^2) involving the distinct topologies: $\mathcal{T}$, $\mathcal{P}$, $\mathcal{E}$, $\mathcal{P}_{\mathcal{A}}$ and $\mathcal{P}_{\mathcal{EW}}$ for the four decays modes of the B_d^0 and B_s^0 mesons. The two decays in the upper half of this table are related by U-spin symmetry $(d \to s)$ (likewise the two decays in the lower half). We note that the assumption of U-spin symmetry for the (dominant) tree ($\mathcal{T}$) and penguin ($\mathcal{P}$) amplitudes in the emission diagrams is quite good, it is less so in the other topologies, including the contributions from the W-exchange diagrams, denoted by $\mathcal{E}$ for which there are non-zero contributions for the flavor-diagonal states $\pi^+\pi^-$ and K^+K^- only. The U-spin breaking is large in the electroweak penguin induced amplitudes $\mathcal{P}_{\mathcal{EW}}$, and in the penguin annihilation amplitudes $\mathcal{P}_{\mathcal{A}}$ relating the decays $B_d \to K^+\pi^-$ and $B_s \to K^+K^-$. In the SM, however, the amplitudes $\mathcal{P}_{\mathcal{EW}}$ are negligibly small.

TABLE IV: Contributions from the various topologies to the decay amplitudes (squared) for the four indicated decays $B_d^0 \to \pi^+\pi^-$; $K^+\pi^-$ and $B_s^0 \to \pi^+K^-$; K^+K^-. Here, $\mathcal{T}$ is the contribution from the color favored emission diagrams; $\mathcal{P}$ is the penguin contribution from the emission diagrams; $\mathcal{E}$ is the contribution from the W-exchange diagrams; $\mathcal{P}_{\mathcal{A}}$ is the contribution from the penguin annihilation amplitudes; and $\mathcal{P}_{\mathcal{EW}}$ is the contribution from the electro-weak penguin induced amplitude. See text for their definitions.

mode (GeV^2)	$\|\mathcal{T}\|^2$	$\|\mathcal{P}\|^2$	$\|\mathcal{E}\|^2$	$\|\mathcal{P}_{\mathcal{A}}\|^2$	$\|\mathcal{P}_{\mathcal{EW}}\|^2$
$B_d \to \pi^+\pi^-$	0.8	4.8×10^{-3}	5.5×10^{-3}	1.6×10^{-3}	0.6×10^{-6}
$B_s \to \pi^+K^-$	1.0	5.4×10^{-3}	0	3.3×10^{-3}	0.8×10^{-6}
$B_d \to K^+\pi^-$	1.2	10.2×10^{-3}	0	2.3×10^{-3}	2.9×10^{-6}
$B_s \to K^+K^-$	1.5	11.3×10^{-3}	3.5×10^{-3}	7.3×10^{-3}	0.5×10^{-6}

The direct CP asymmetry of $\bar{B}_s \to f$ is defined as

$$A_{CP}^{dir} \equiv \frac{BR(\bar{B}_s^0 \to f) - BR(B_s^0 \to \bar{f})}{BR(\bar{B}_s^0 \to f) + BR(B_s^0 \to \bar{f})} = \frac{|A(\bar{B}_s \to f)|^2 - |A(B_s \to \bar{f})|^2}{|A(\bar{B}_s \to f)|^2 + |A(B_s \to \bar{f})|^2}. \tag{65}$$

The numerical results for the direct CP asymmetries in $B \to PP$ decays are shown in Table V. The first error is from the B_s meson wave function parameter $\omega_b = 0.50^{+0.05}_{-0.05}$ GeV. As f_{B_s} is an

overall factor, it drops out in the ratio and hence does not give any uncertainty in the estimates of the direct CP asymmetries. The second error is from the hard scale t varying from $0.75t$ to $1.25t$ (not changing $1/b_i$, $i = 1, 2, 3$) and $\Lambda_{QCD}^{(5)} = 0.25 \pm 0.05$ GeV. The third error is again from the combined uncertainty in the CKM matrix elements and the angles of the unitarity triangle. The observed CP asymmetry $A_{\text{CP}}^{\text{dir}}(\overline{B_s^0} \to K^+\pi^-)$ by the CDF collaboration is also shown in this table, and is found to be in agreement with the pQCD predictions.

Within (large) theoretical errors, the observed CP asymmetry is also in agreement with the SCET estimate but in stark disagreement with the QCDF prediction. This deserves a comment. As is well-known, the decay rates and CP-asymmetries in the decays $\overline{B_d^0} \to \pi^+\pi^-$ and $\overline{B_s^0} \to K^+\pi^-$ are related by SU(3) symmetry. The predicted CP asymmetry $A_{\text{CP}}^{\text{dir}}(\overline{B_s^0} \to K^+\pi^-)$ in the QCDF approach shown in Table V is very similar to the SU(3)-related CP asymmetry $A_{\text{CP}}^{\text{dir}}(\overline{B_d^0} \to \pi^+\pi^-)$. These CP-asymmetries are small in the QCDF approach and both are consistently in disagreement with the data, in magnitude and sign. Using SU(3)-symmetry, the CP-asymmetry $A_{\text{CP}}^{\text{dir}}(\overline{B_s^0} \to K^+\pi^-)$ in SCET, given in Table V, is identical to the values quoted in Ref. [20] for the CP-asymmetry $A_{\text{CP}}^{\text{dir}}(\overline{B_d^0} \to \pi^+\pi^-)$. As the dynamical hadronic quantities in the SCET framework are fitted using the B-factory data on $B \to \pi\pi$ and $B \to K\pi$ [20], it is not surprising that this phenomenological fit can account for the SU(3)-related observed CP-asymmetry in the B_s^0 decays, such as $A_{\text{CP}}^{\text{dir}}(\overline{B_s^0} \to K^+\pi^-)$. The fitted quantities, namely the SCET-specific functions ζ, ζ_J, differ from their corresponding QCDF analogs. But, crucially, also the contributions of the charming penguin [7], denoted as $|A_{\text{cc}}|$ and $\arg A_{\text{cc}}$ in [20], which are power-suppressed in QCDF, are found to be large using data and SCET. These differences lead to a different phenomenological profile of the $B \to h_1 h_2$ decays in SCET and QCDF. However, one has to stress that the charming penguin contribution, which is not yet shown to factorize in SCET, obviously is not on the same theoretical footing as the rest of the decay amplitudes, for which factorization is proven in the heavy quark limit. Thus, the predictions in SCET [20] essentially reflect the parameterization of the charming penguins from the available data.

In general, one has also to take into account the uncertainties caused by the Gegenbauer moments. In recent years, the light cone distribution amplitudes have been continually updated [35]. In order to check the sensitivity to the values on the Gegenbauer moments, we calculate the branching ratio for $\bar{B}_s \to K^+\pi^-$ with the following values for the twist-2 LCDAs:

$$a_1^K = 0.06 \pm 0.03, \quad a_2^{\pi,K} = 0.25 \pm 0.15, \tag{66}$$

instead of $a_1^K = 0.17$ and $a_2^K = 0.2$ from eq. (25) and $a_2^\pi = 0.44$ from eq. (22). Using the above values and the asymptotic forms for the twist-3 LCDAs, we obtain

$$\mathcal{BR}(\bar{B}_s^0 \to K^+\pi^-) = (7.2^{+3.0+0.7+0.4}_{-2.2-0.8-0.5}) \times 10^{-6}, \tag{67}$$

where the errors are to be interpreted as before. The agreement between this result with the corresponding number listed in Table III confirms our expectation that this branching ratio is not changed significantly. In our calculation, the parameters in the LCDAs are chosen at $\mu = 1$ GeV but as they are scale-dependent quantities, their value at $\mu = 2$ GeV, the typical scale which enters the perturbative calculation in pQCD, is required. At $\mu = 2$ GeV, the values for the Gegenbauer moments scaled from eq. (66) are:

$$a_1^K = 0.05 \pm 0.02, \quad a_2^{\pi,K} = 0.17 \pm 0.10. \tag{68}$$

Using these values, we obtain:

$$\mathcal{BR}(\bar{B}_s^0 \to K^+\pi^-) = (6.9^{+3.0+0.7+0.4}_{-2.1-0.7-0.5}) \times 10^{-6} . \tag{69}$$

We remark that the uncertainties caused by the scale dependence of the Gegenbauer moments are not large, compared with other uncertainties.

D. The Observables S_f and H_f in time-dependent decays $B_s^0(t) \to f$

Restricting the final state f to have definite CP-parity, the time-dependent decay width for the $B_s \to f$ decay is [54]:

$$\Gamma(B_s^0(t) \to f) = e^{-\Gamma t} \, \overline{\Gamma}(B_s \to f) \left[\cosh\left(\frac{\Delta\Gamma t}{2}\right) + H_f \sinh\left(\frac{\Delta\Gamma t}{2}\right) \right. $$
$$\left. - \mathcal{A}_{\mathrm{CP}}^{dir} \cos(\Delta m t) - S_f \sin(\Delta m t) \right], \tag{70}$$

where $\Delta m = m_H - m_L > 0$, $\overline{\Gamma}$ is the average decay width, and $\Delta\Gamma = \Gamma_H - \Gamma_L$ is the difference of decay widths for the heavier and lighter B_s^0 mass eigenstates. The time dependent decay width $\Gamma(\bar{B}_s^0(t) \to f)$ is obtained from the above expression by flipping the signs of the $\cos(\Delta m t)$ and $\sin(\Delta m t)$ terms. In the B_s system, we expect a much larger decay width difference $(\Delta\Gamma/\Gamma)_{B_s}$. This is estimated within the standard model to have a value $(\Delta\Gamma/\Gamma)_{B_s} = -0.12 \pm 0.05$ [55], updated recently in [56] to $(\Delta\Gamma/\Gamma)_{B_s} = -0.147 \pm 0.060$, while experimentally $(\Delta\Gamma/\Gamma)_{B_s} = -0.33^{+0.09}_{-0.11}$ [57],

TABLE V: The direct CP asymmetries (in %) in the $B_s \to PP$ decays, obtained in the pQCD approach (This work); the errors for these entries correspond to the uncertainties in the input hadronic quantities, from the scale-dependence, and the CKM matrix elements, respectively. The only measured CP asymmetry is also given [13]. For comparison, we also cite the theoretical estimates of the CP asymmetries in the QCD factorization framework [16], and in SCET [20].

Modes	Class	QCDF	SCET	This work	EXP
$\overline{B}_s^0 \to K^+\pi^-$	T	$-6.7^{+2.1+3.1+0.2+15.5}_{-2.2-2.9-0.4-15.2}$	$20\pm17\pm19\pm5$	$24.1^{+3.9+3.3+2.3}_{-3.6-3.0-1.2}$	$39\pm15\pm8$
$\overline{B}_s^0 \to K^0\pi^0$	C	$41.6^{+16.6+14.3+7.8+40.9}_{-12.0-13.3-14.5-51.0}$	$76\pm26\pm27\pm17$	$59.4^{+1.8+7.4+2.2}_{-4.0-11.3-3.5}$	
$\overline{B}_s^0 \to K^+K^-$	P	$4.0^{+1.0+2.0+0.5+10.4}_{-1.0-2.3-0.5-11.3}$	$-6\pm5\pm6\pm2$	$-23.3^{+0.9+4.9+0.8}_{-0.2-4.4-1.1}$	
$\overline{B}_s^0 \to K^0\overline{K}^0$	P	$0.9^{+0.2+0.2+0.1+0.2}_{-0.2-0.2-0.1-0.3}$	<10	0	
$\overline{B}_s^0 \to \pi^0\eta$	P_{EW}	——	—-	$-0.4^{+0.6+2.2+0.0}_{-0.7-2.2-0.0}$	
$\overline{B}_s^0 \to \pi^0\eta'$	P_{EW}	$27.8^{+6.0+9.6+2.0+24.7}_{-7.1+5.7-2.0-27.2}$	—-	$20.6^{+0.0+2.0+2.8}_{-0.7-2.5-1.2}$	
$\overline{B}_s^0 \to K^0\eta$	C	$46.8^{+18.5+28.6+5.2+34.6}_{-13.2-32.2-12.5-45.6}$	$-56\pm46\pm14\pm6$ $61\pm59\pm12\pm8$	$56.4^{+2.9+6.8+3.1}_{-3.4-8.0-3.4}$	
$\overline{B}_s^0 \to K^0\eta'$	C	$-36.6^{+8.6+6.0+3.8+19.3}_{-8.2-7.4-2.5-17.3}$	$-14\pm7\pm16\pm2$ $37\pm8\pm14\pm4$	$-19.9^{+1.6+5.1+1.4}_{-1.4-5.0-0.9}$	
$\overline{B}_s^0 \to \eta\eta$	P	$-1.6^{+0.5+0.6+0.4+2.2}_{-0.4-0.6-0.7-2.2}$	$7.9\pm4.9\pm2.7\pm1.5$ $-1.1\pm5.0\pm3.9\pm1.0$	$-0.6^{+0.2+0.6+0.0}_{-0.2-0.5-0.1}$	
$\overline{B}_s^0 \to \eta\eta'$	P	$0.4^{+0.1+0.3+0.1+0.4}_{-0.1-0.3-0.1-0.3}$	$0.04\pm0.14\pm0.39\pm0.43$ $2.7\pm0.9\pm0.8\pm7.6$	$-1.3^{+0.0+0.1+0.1}_{-0.0-0.2-0.1}$	
$\overline{B}_s^0 \to \eta'\eta'$	P	$2.1^{+0.5+0.4+0.2+1.1}_{-0.6-0.4-0.3-1.2}$	$0.9\pm0.4\pm0.6\pm1.9$ $-3.7\pm1.0\pm1.2\pm5.6$	$1.9^{+0.2+0.3+0.2}_{-0.2-0.4-0.1}$	
$\overline{B}_s^0 \to \pi^+\pi^-$	ann	——	—-	$-1.2^{+0.1+1.2+0.1}_{-0.4-1.2-0.1}$	
$\overline{B}_s^0 \to \pi^0\pi^0$	ann	——	—-	$-1.2^{+0.1+1.2+0.1}_{-0.4-1.2-0.1}$	

so that both S_f and H_f, can be extracted from the time dependent decays of B_s mesons. The definition of the various quantities in the above equation are as follows:

$$S_f = \frac{2Im[\lambda]}{1+|\lambda|^2}, \quad H_f = \frac{2Re[\lambda]}{1+|\lambda|^2},$$
(71)

with

$$\lambda = \eta_f e^{2i\epsilon} \frac{A(\bar{B}_s \to f)}{A(B_s \to \bar{f})},\tag{72}$$

where η_f is $+1(-1)$ for a CP-even (CP-odd) final state f and $\epsilon = \arg[-V_{cb}V_{ts}V_{cs}^*V_{tb}^*]$. With the convention $\arg[V_{cb}] = \arg[V_{cs}] = 0$, the parameter can be reduced to $\epsilon = \arg[-V_{ts}V_{tb}^*]$. The results of our calculations for the decays $B_s^0 \to PP$ are listed in Table VI and compared with the ones obtained in SCET [20].

E. Specific Tests of the pQCD predictions in $\overline{B_d^0} \to PP$ and $\overline{B_s^0} \to PP$ Decays

In this subsection, we confront the predictions of the pQCD approach to available data in the decay modes $\overline{B_s^0} \to PP$ and $\overline{B_d^0} \to PP$, in terms of the ratios of the branching ratios and CP-asymmetries. Restricted by the currently available data, we shall confine ourselves to the decay modes $\overline{B_s^0} \to K^+K^-$, $\overline{B_s^0} \to K^+\pi^-$, $\overline{B_d^0} \to \pi^+\pi^-$ and $\overline{B_d^0} \to K^-\pi^+$. The ratio of the branching ratios defined as $R_1 \equiv \frac{BR(\overline{B_s^0} \to K^+K^-)}{BR(\overline{B_d^0} \to \pi^+\pi^-)}$ has been studied at some length in the literature. In R_1, the numerator is dominated by the penguin amplitude, but the denominator is a mixture of tree and penguin amplitudes, and both the numerator and denominator have been measured experimentally. It has been argued that the ratio R_1 and the two CP asymmetries $S_{CP}(\bar{B}_d^0 \to \pi^+\pi^-)$ and $C_{CP}(\bar{B}_d^0 \to \pi^+\pi^-) = -A_{CP}^{dir}(\bar{B}_d^0 \to \pi^+\pi^-)$ of the $\bar{B}_d^0 \to \pi^+\pi^-$ channel depend, in the SU(3) limit, on only two quantities [58] which can be determined from data and compared with the various dynamical models to get a clear picture of two-body non-leptonic decays. However, not invoking the SU(3) limit, this system of observables has too many unknowns and a clean test of the dynamical models is bogged down in the details of the hadronic input. To enable getting cleaner theoretical handles on the underlying dynamics, we calculate the ratio $R_2 \equiv \frac{BR(\bar{B}_s^0 \to K^+K^-)}{BR(\bar{B}_d^0 \to \pi^+K^-)}$, the ratio R_3 and the quantity called Δ, defined later in this subsection. The last two (i.e. R_3 and Δ) have been advocated by Lipkin [60] invoking earlier work by Gronau [59] as precision tests of the SM.

The CDF collaboration has measured the branching ratio of $\overline{B_s^0} \to K^+K^-$ in the form [13]:

$$\frac{f_s \cdot BR(\overline{B_s^0} \to K^+K^-)}{f_d \cdot BR(\overline{B_d^0} \to \pi^+K^-)} = 0.324 \pm 0.019 \pm 0.041.\tag{73}$$

Using the results [57]

$$f_s = (10.4 \pm 1.4)\%, \quad f_d = (39.8 \pm 1.0)\%,\tag{74}$$

$$BR(\overline{B_d^0} \to \pi^+\pi^-) = (5.2 \pm 0.2) \times 10^{-6},\tag{75}$$

28

TABLE VI: The mixing-induced CP asymmetries S_f (the first row of each decay channel) and the observables H_f (the second row) in the $B_s \to PP$ decays calculated in the pQCD approach (This work). The errors for these entries correspond to the uncertainties in the input hadronic quantities, from the scale-dependence, and the CKM matrix elements, respectively. Estimates of these quantities in SCET [20] are also given, quoting two of these for the decays involving an η and/or an η'-meson.

Modes	SCET Theory I	SCET Theory II	This work
$\overline{B}_s^0 \to K_S\pi^0$	$-0.16 \pm 0.41 \pm 0.33 \pm 0.17$		$-0.61^{+0.08+0.23+0.01}_{-0.06-0.19-0.03}$
	$0.80 \pm 0.27 \pm 0.25 \pm 0.11$		$-0.52^{+0.04+0.22+0.03}_{-0.06-0.16-0.02}$
$\overline{B}_s^0 \to K^-K^+$	$0.19 \pm 0.04 \pm 0.04 \pm 0.01$		$0.28^{+0.03+0.04+0.02}_{-0.03-0.04-0.01}$
	$0.979 \pm 0.008 \pm 0.007 \pm 0.002$		$0.93^{+0.01+0.02+0.00}_{-0.01-0.02-0.01}$
$\overline{B}_s^0 \to K^0\overline{K}^0$	—	—	0.04
	—	—	1.00
$\overline{B}_s^0 \to \pi^0\eta$	$0.45 \pm 0.14 \pm 0.42 \pm 0.30$	$0.38 \pm 0.20 \pm 0.42 \pm 0.37$	$0.17^{+0.04+0.10+0.01}_{-0.04-0.12-0.01}$
	$-0.89 \pm 0.07 \pm 0.21 \pm 0.15$	$-0.92 \pm 0.08 \pm 0.17 \pm 0.15$	$0.99^{+0.00+0.01+0.00}_{-0.01-0.02-0.00}$
$\overline{B}_s^0 \to \pi^0\eta'$	$0.45 \pm 0.14 \pm 0.42 \pm 0.30$	$0.38 \pm 0.20 \pm 0.42 \pm 0.37$	$-0.17^{+0.00+0.07+0.03}_{-0.01-0.08-0.05}$
	$-0.89 \pm 0.07 \pm 0.21 \pm 0.15$	$-0.92 \pm 0.08 \pm 0.17 \pm 0.15$	$0.96^{+0.00+0.01+0.01}_{-0.00-0.01-0.01}$
$\overline{B}_s^0 \to K_S\eta$	$0.82 \pm 0.32 \pm 0.11 \pm 0.04$	$0.63 \pm 0.61 \pm 0.16 \pm 0.08$	$-0.43^{+0.03+0.22+0.02}_{-0.04-0.21-0.03}$
	$0.07 \pm 0.56 \pm 0.17 \pm 0.05$	$0.49 \pm 0.68 \pm 0.21 \pm 0.03$	$-0.70^{+0.04+0.13+0.01}_{-0.05-0.21-0.01}$
$\overline{B}_s^0 \to K_S\eta'$	$0.38 \pm 0.08 \pm 0.10 \pm 0.04$	$0.24 \pm 0.09 \pm 0.15 \pm 0.05$	$-0.68^{+0.01+0.06+0.00}_{-0.02-0.05-0.00}$
	$-0.92 \pm 0.04 \pm 0.04 \pm 0.02$	$-0.90 \pm 0.05 \pm 0.05 \pm 0.03$	$-0.70^{+0.02+0.06+0.00}_{-0.02-0.07-0.00}$
$\overline{B}_s^0 \to \eta\eta$	$-0.026 \pm 0.040 \pm 0.030 \pm 0.014$	$-0.077 \pm 0.061 \pm 0.022 \pm 0.026$	$0.03^{+0.00+0.01+0.00}_{-0.00-0.01-0.00}$
	$0.9965 \pm 0.0041 \pm 0.0019 \pm 0.0015$	$0.9970 \pm 0.0048 \pm 0.0017 \pm 0.0021$	$1.00^{+0.00+0.00+0.00}_{-0.00-0.00-0.00}$
$\overline{B}_s^0 \to \eta\eta'$	$0.041 \pm 0.004 \pm 0.002 \pm 0.051$	$0.015 \pm 0.010 \pm 0.008 \pm 0.069$	$0.04^{+0.00+0.00+0.00}_{-0.00-0.00-0.00}$
	$0.9992 \pm 0.0002 \pm 0.0001 \pm 0.0021$	$0.9996 \pm 0.0003 \pm 0.0003 \pm 0.0007$	$1.00^{+0.00+0.00+0.00}_{-0.00-0.00-0.00}$
$\overline{B}_s^0 \to \eta'\eta'$	$0.049 \pm 0.005 \pm 0.005 \pm 0.031$	$0.051 \pm 0.009 \pm 0.017 \pm 0.039$	$0.04^{+0.00+0.01+0.00}_{-0.00-0.01-0.00}$
	$0.9988 \pm 0.0003 \pm 0.0002 \pm 0.0017$	$0.9980 \pm 0.0007 \pm 0.0009 \pm 0.0041$	$1.00^{+0.00+0.00+0.00}_{-0.00-0.00-0.00}$
$\overline{B}_s^0 \to \pi^+\pi^-$	—	—	$0.14^{+0.02+0.08+0.09}_{-0.00-0.02-0.05}$
	—	—	$0.99^{+0.00+0.00+0.00}_{-0.00-0.01-0.01}$
$\overline{B}_s^0 \to \pi^0\pi^0$	—	—	$0.14^{+0.02+0.08+0.09}_{-0.00-0.02-0.05}$
	—	—	$0.99^{+0.00+0.00+0.00}_{-0.00-0.01-0.01}$

one obtains R_1 and R_2:

$$R_1 = 4.69 \pm 0.94, \quad R_2 = 1.24 \pm 0.24. \tag{76}$$

We have calculated the branching ratios for the related $\overline{B_d^0} \to \pi^+\pi^-, \pi^+K^-$ decays in the pQCD approach, getting:

$$BR(\overline{B_d^0} \to \pi^+\pi^-) = (5.8^{+3.0+0.5+0.4}_{-2.1-0.4-0.3}) \times 10^{-6}, \quad BR(\overline{B_d^0} \to \pi^+K^-) = (11.6^{+5.0+5.2+0.7}_{-3.5-2.9-0.3}) \times 10^{-6}. \tag{77}$$

Taking into account the correlated errors in the numerator and the denominator, we get:

$$R_1 = 2.35^{+0.45+0.99+0.19}_{-0.36-0.59-0.15}, \quad R_2 = 1.18^{+0.11+0.10+0.01}_{-0.11-0.08-0.01}. \tag{78}$$

Adding the theoretical errors in quadrature, we get $R_1 = 2.35^{+1.10}_{-0.71}$ and $R_2 = 1.18^{+0.15}_{-0.14}$. Hence, in the pQCD approach, the ratio R_1 is smaller compared to the current data. This originates from the fact that $BR(\overline{B_d^0} \to \pi^+\pi^-)$ is somewhat larger in the pQCD approach compared to the data, and $BR(\overline{B_s^0} \to K^+K^-)$ is smaller than the currently measured branching ratio (see Table III). Furthermore, the value of R_1 also depends on the s quark mass through the chiral scale parameter $m_0^K = m_K^2/(m_s + m_{u,d})$. If we use $m_0^K = (1.9 \pm 0.2)$ GeV, where the errors reflects the uncertainty in the quark masses, we find that R_1 has an additional uncertainty $R_1 = 2.35^{+0.62}_{-0.49}$. Adding this error with the one quoted above in quadrature yields $R_1 = 2.35^{+1.26}_{-0.86}$. It would be interesting to investigate how the NLO contributions modify the ratio R_1 as the tree and penguin amplitudes are expected to be renormalized differently including the $O(\alpha_s^2)$ corrections, as shown in [52] in the context of the $B_d^0 \to PP$ decays.

The ratio R_2, on the other hand, comes out just about right in pQCD, as in this ratio both the numerator and denominator are dominated by QCD penguin amplitudes. One also expects that this ratio is stable under $O(\alpha_s^2)$ corrections, as the denominator in R_2 is itself stable against such corrections (see Table III in [52]) and very similar arguments apply to the decay rate for the numerator. The stability of the color-allowed QCD penguin amplitudes against one-loop corrections to the hard spectator scattering is also borne out in the QCD factorization framework [8]. The SU(3)-breaking effects in R_2 are of the same size as the corresponding effects in the form factors, typically $\pm$ 30%, and this likely is the dominant theoretical uncertainty in this ratio. In Fig. 5, we plot the ratio R_2 vs. $A_{CP}^{\text{dir}}(K^+\pi^-)$ for the LO pQCD-based calculations worked out by us and compare them with the current data on these observables. The experimental value of R_2 has already been given earlier, and we use $A_{CP}^{dir}(B_d^0 \to K^+\pi^-) = -0.093 \pm 0.015$ [57]. We
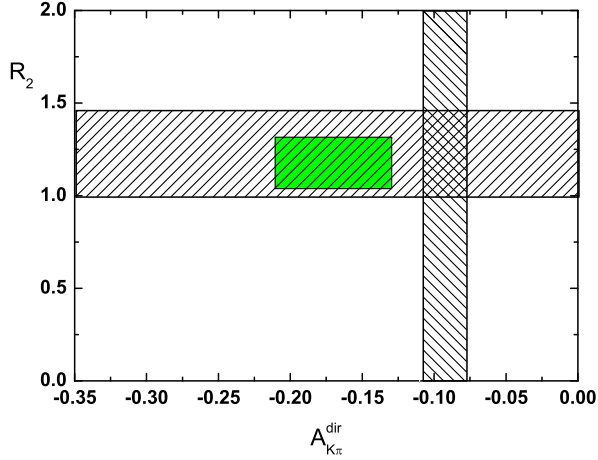
FIG. 5: R_2 vs $A_{CP}^{dir}(\pi K)$. The region inside the solid (red) box is the pQCD calculation in the LO. The experimental results are shown as bands within their $\pm 1\sigma$ errors.

recall that the direct CP asymmetry $A_{CP}^{dir}(K^+\pi^-)$, calculated by us in the LO pQCD approach, $A_{CP}^{dir}(\overline{B_d^0} \rightarrow \pi^+K^-) = -0.17_{-0.02-0.02-0.01}^{+0.02+0.03+0.01}$ is numerically significantly different than the earlier estimates of the same in this approach (for example, the central value of this CP asymmetry in LO is quoted as -0.12 in [52]). This mismatch reflects the dependence of $A_{CP}^{dir}(K^+\pi^-)$ on the input quantities, in particular V_{ub}, which have evolved in the meanwhile. Thus, with our input values, we find good agreement with data on R_2 but not so for $A_{CP}^{dir}(K^+\pi^-)$, as shown in Fig. 5. However, taking into account the $O(\alpha_s^2)$ contributions, this CP-asymmetry is renormalized while R_2 remains practically the same. Taking the central values from Table IV of Ref. [52], one gets a K-factor of 0.75 for $A_{CP}^{dir}(K^+\pi^-)$ (the central value in NLO is -0.09 with the input values used there). Using this K-factor, and our LO calculations, we estimate $A_{CP}^{dir}(K^+\pi^-) = -0.13 \pm 0.04$ in NLO, making it compatible with the current data. This is shown in Fig. 6. It should, however, be pointed out for the sake of clarity that the NLO corrections in [52] are not complete, as the hard spectator contributions in $O(\alpha_s^2)$ are not all calculated. Hence a residual contribution to $A_{CP}^{dir}(K^+\pi^-)$ (and other observables) can not be logically excluded. However, our discussion here underscores the dominant source of the uncertainty in $A_{CP}^{dir}(K^+\pi^-)$, which is of parametric origin.

In $\overline{B_d^0} \rightarrow K^-\pi^+$ and $\overline{B_s^0} \rightarrow K^+\pi^-$, the branching ratios are very different from each other due to the differing strong and weak phases entering in the tree and penguin amplitudes. However, as shown by Gronau [59], the two relevant products of the CKM matrix elements entering in the
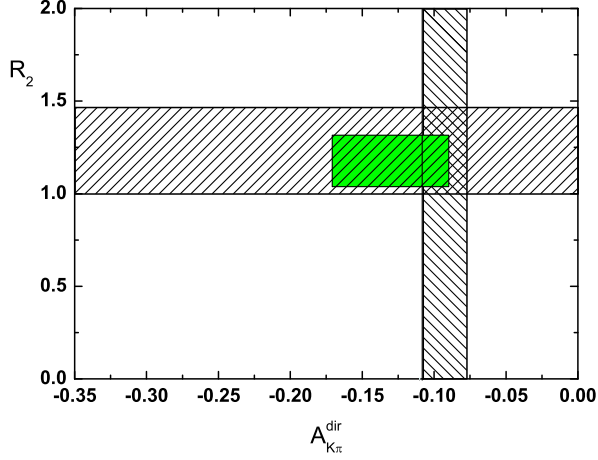
FIG. 6: R_2 vs $A_{CP}^{dir}(\pi K)$. The region inside the solid (green) box is obtained by estimating $A_{CP}^{dir}(\pi K)$ in NLO, as discussed in the text. R_2 (pQCD) and the experimental results are the same as in the previous figure.

expressions for the direct CP asymmetries in these decays are equal, and, as stressed by Lipkin [60] subsequently, the final states in these decays are charge conjugates, and the strong interactions being charge-conjugation invariant, the direct CP asymmetry in $\overline{B_s^0} \to K^- \pi^+$ can be related to the well-measured CP asymmetry in the decay $\overline{B_d^0} \to K^+ \pi^-$ using U-spin symmetry. In this symmetry limit, we have [59, 60]

$$|A(B_s \to \pi^+ K^-)|^2 - |A(\bar{B}_s \to \pi^- K^+)|^2 = |A(\bar{B}_d \to \pi^+ K^-)|^2 - |A(B_d \to \pi^- K^+)|^2, \quad (79)$$

$$A_{CP}^{dir}(\bar{B}_d \to \pi^+ K^-) = -A_{CP}^{dir}(\bar{B}_s \to \pi^- K^+) \cdot \frac{BR(B_s \to \pi^+ K^-)}{BR(\bar{B}_d \to \pi^+ K^-)} \cdot \frac{\tau(B_d)}{\tau(B_s)}. \quad (80)$$

Following the suggestions in the literature, we can test these equations and search for possible new physics effects which would likely violate these relations. To that end, one can define the following two parameters (using Eq. (65) for the definition of CP asymmetry):

$$R_3 \equiv \frac{|A(B_s \to \pi^+ K^-)|^2 - |A(\bar{B}_s \to \pi^- K^+)|^2}{|A(B_d \to \pi^- K^+)|^2 - |A(\bar{B}_d \to \pi^+ K^-)|^2}, \quad (81)$$

$$\Delta = \frac{A_{CP}^{dir}(\bar{B}_d \to \pi^+ K^-)}{A_{CP}^{dir}(\bar{B}_s \to \pi^- K^+)} + \frac{BR(B_s \to \pi^+ K^-)}{BR(\bar{B}_d \to \pi^+ K^-)} \cdot \frac{\tau(B_d)}{\tau(B_s)}. \quad (82)$$

The standard model predicts $R_3 = -1$ and $\Delta = 0$ if we assume U-spin symmetry. Since we have a detailed dynamical theory to study the SU(3) (and U-spin) symmetry violation, we can check
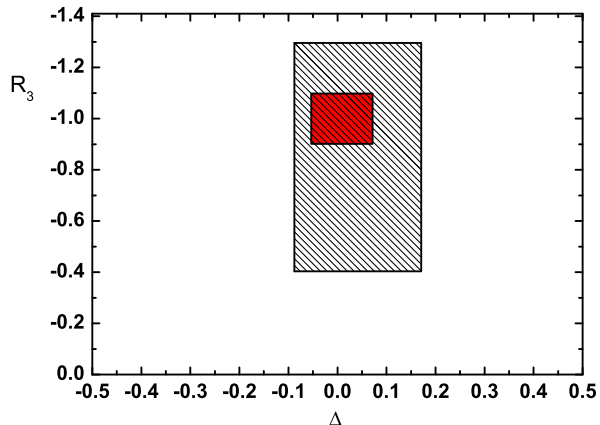
32

FIG. 7: R_3 vs Δ: The red (smaller) rectangle is the pQCD estimates worked out in this paper. The experimental results with their $\pm 1\sigma$ errors are shown as the larger rectangle.

how good quantitatively this symmetry is in the ratios R_3 and Δ. We find:

$$R_3 = -1.00^{+0.04+0.03+0.09}_{-0.04-0.04-0.08}, \quad \Delta = -0.00^{+0.03+0.03+0.06}_{-0.03-0.02-0.04}, \tag{83}$$

The differing values of ω_B and ω_{B_s}, which enter in the B_d^0 and B_s^0-meson wave functions, contribute dominantly to the first errors, whereas the current uncertainties on the CKM angle γ and V_{ts} are reflected in the third errors given above. The scale-dependent uncertainties leading to the second error are relatively small. Adding all the theoretical errors in quadrature, we get $R_3 = -1.00^{+0.10}_{-0.10}$ and $\Delta = -0.00^{+0.07}_{-0.05}$. Thus, we find that these quantities are quite reliably calculable, as anticipated on theoretical grounds. On the experimental side, the results for R_3 and Δ are [13]:

$$R_3 = -0.84 \pm 0.42 \pm 0.15, \quad \Delta = 0.04 \pm 0.11 \pm 0.08. \tag{84}$$

We conclude that the SM is in good agreement with the data, as can also be seen in Fig. 7 where we plot theoretical predictions for R_3 vs. Δ and compare them with the current measurements of the same. The measurements of these quantities are rather imprecise at present, a situation which we hope will greatly improve at the LHC (and Super-B factories).

IV. CALCULATION OF B_s TO A VECTOR AND A PSEUDO-SCALAR MESON IN THE PQCD APPROACH

A. Decay amplitudes

In the decays of B_s to a vector and a pseudo-scalar meson, only the longitudinal polarization of the vector meson can contribute, thus the decay formulas are very similar to those of the $B_s \to PP$ decays. Since the Lorentz structure of the vector meson wave functions is different from the pseudo-scalar case, there are two kinds of emission diagrams in principle. If the emitted meson is a vector meson, the decay amplitudes are the same as that of the $B_s \to PP$ case, since they are both characterized by the $B_s \to P$ transition form factors. For the non-factorizable diagrams and also those diagrams in which a pseudo-scalar meson is emitted, the distribution amplitudes of the pseudo-scalar meson will be replaced by that of the vector meson as follows:

$$\phi_2^A(x) \to \phi_2(x), \quad \phi_2^P(x) \to \phi_2^s(x), \quad \phi_2^T(x) \to \phi_2^t(x), \quad m_{02} \to M_2, \tag{85}$$

where M_2 is the mass of the vector meson. The factorizable emission topology $F_{B \to P}^{SP}$ does not contribute as the vector meson cannot be generated by the scalar or the pseudo-scalar density. Furthermore, we must add a minus sign to $\phi_3^s(x)$ and $\phi_3^t(x)$ in the annihilation diagram formulas F_{ann} and M_{ann} if the vector meson is on the light $\bar{s}$ quark side.

B. Numerical results for $B_s \to PV$ decays

The branching ratios of $B_s \to PV$ decays are listed in Table VII. The direct CP asymmetries of the $B_s \to PV$ decays are given in Table VIII. They are compared with the corresponding calculations in the QCDF approach [16], where the sources of the errors in the numerical estimates have the same origin as in the discussion of the $B \to PP$ decays. Comparison of the entries in Table VII shows that the two approaches give similar results for the tree-dominated decays and the QCD penguin- and electroweak-penguin dominated decays (except for those involving an η or η' in the final states), and they are radically different for the annihilation-dominated decays (the last four entries in this table). The branching ratios for $\bar{B}_s \to \rho\eta$ and $\bar{B}_s \to \rho\eta'$ are of the same order as the QCDF results, but there are large differences in $\bar{B}_s \to \omega(\phi)\eta$ and $\bar{B}_s \to \rho(\phi)\eta'$. In QCDF, the branching ratios for $\bar{B}_s \to \phi\eta$, $\bar{B}_s \to \phi\eta'$ and $\bar{B}_s \to \phi\pi^0$ (electro-weak penguin dominated process) are of the same magnitude, which implies that the color-suppressed QCD-penguins have a reduced

value similar to the electroweak penguins. However, in the pQCD approach, the factorization scale is low and this dynamically enhances the color-suppressed QCD penguins sizably.

Predictions for the CP-asymmetries in the two approaches given in Table VIII are, however, all quite different. The zeros shown in some cases for the pQCD approach will be lifted on including the neglected small subdominant contributions. Also, as opposed to the QCDF approach, we are able to calculate the CP asymmetries in the annihilation-dominated topologies. The mixing-induced CP asymmetries $(S_f)_{B_s}$ and the observable $(H_f)_{B_s}$, defined in the previous section, are shown in Table IX. Currently, there is no data to confront the estimates given in Tables VII, VIII and IX, and again we hope that this will be remedied at the LHC (and Super-B factories).

V. $B_s \to VV$ **DECAYS IN PQCD APPROACH**

A.   Decay amplitudes

There are three kinds of polarizations of a vector meson, namely longitudinal (L), normal (N) and transverse (T). The amplitudes for a B_s meson decay to two vector mesons are also characterized by the polarization states of these vector mesons. The amplitudes $A^{(\sigma)}$ for the decay $B_s(P_B) \to V_2(P_2, \epsilon_{2\mu}^*) + V_3(P_3, \epsilon_{3\mu}^*)$ can be decomposed as follows:

$$
\begin{aligned}
A^{(\sigma)} &= \epsilon_{2\mu}^*(\sigma)\epsilon_{3\nu}^*(\sigma)\left[a\ g^{\mu\nu} + \frac{b}{M_2 M_3}P_B^\mu P_B^\nu + i\frac{c}{M_2 M_3}\epsilon^{\mu\nu\alpha\beta}P_{2\alpha}P_{3\beta}\right] , \\
&\equiv A_L + A_N \epsilon_2^*(\sigma = T)\cdot\epsilon_3^*(\sigma = T) + i\frac{A_T}{M_{B_s}^2}\epsilon^{\alpha\beta\gamma\rho}\epsilon_{2\alpha}^*(\sigma)\epsilon_{3\beta}^*(\sigma)P_{2\gamma}P_{3\rho} ,
\end{aligned}
\tag{86}
$$

where M_2 and M_3 are the masses of the vector mesons V_2 and V_3, respectively. The definitions of the amplitudes A^i $(i = L, N, T)$ in terms of the Lorentz-invariant amplitudes a, b and c are

$$
\begin{aligned}
A_L &= a\ \epsilon_2^*(L)\cdot\epsilon_3^*(L) + \frac{b}{M_2 M_3}\epsilon_2^*(L)\cdot P_3\ \epsilon_3^*(L)\cdot P_2 , \\
A_N &= a, \\
A_T &= \frac{c}{r_2 r_3} .
\end{aligned}
\tag{87}
$$

The longitudinal polarization amplitudes for the $B_s \to VV$ decays can be obtained from those in the $B_s \to PP$ decays with the following replacement in the distribution amplitudes:

$$
\phi_{2(3)}^A(x) \to \phi_{2(3)}(x),\ \ \phi_{2(3)}^P(x) \to \phi_{2(3)}^s(x),\ \ \phi_{2(3)}^T(x) \to \phi_{2(3)}^t(x),
\tag{88}
$$

for the emission diagrams, while

$$
\phi_{2(3)}^A(x) \to \phi_{2(3)}(x),\ \ \phi_{2(3)}^P(x) \to (-)\phi_{2(3)}^s(x),\ \ \phi_{2(3)}^T(x) \to (-)\phi_{2(3)}^t(x),
\tag{89}
$$

35

TABLE VII: The CP-averaged branching ratios ($\times 10^{-6}$) of $B_s \to PV$ decays obtained in the pQCD approach (This work); the errors for these entries correspond to the uncertainties in the input hadronic quantities, from the scale-dependence, and the CKM matrix elements, respectively. For comparison, we also cite the theoretical estimates of the branching ratios in the QCD factorization framework [16].

Modes	Class	QCDF	This work
$\overline{B}_s^0 \to \pi^- K^{*+}$	T	$8.7^{+4.6+3.5+0.7+0.8}_{-3.7-2.9-1.0-0.7}$	$7.6^{+2.9+0.4+0.5}_{-2.2-0.5-0.3}$
$\overline{B}_s^0 \to \rho^- K^+$	T	$24.5^{+11.9+9.2+1.8+1.6}_{-9.7-7.8-3.0-1.6}$	$17.8^{+7.7+1.3+1.1}_{-5.6-1.6-0.9}$
$\overline{B}_s^0 \to \pi^0 K^{*0}$	C	$0.25^{+0.08+0.10+0.32+0.30}_{-0.08-0.06-0.14-0.14}$	$0.07^{+0.02+0.04+0.01}_{-0.01-0.02-0.01}$
$\overline{B}_s^0 \to \rho^0 K^0$	C	$0.61^{+0.33+0.21+1.06+0.56}_{-0.26-0.15-0.38-0.36}$	$0.08^{+0.02+0.07+0.01}_{-0.02-0.03-0.00}$
$\overline{B}_s^0 \to K^{*0}\eta$	C	$0.26^{+0.15+0.49+0.15+0.57}_{-0.13-0.22-0.05-0.15}$	$0.17^{+0.04+0.10+0.03}_{-0.04-0.06-0.01}$
$\overline{B}_s^0 \to K^{*0}\eta'$	C	$0.28^{+0.04+0.46+0.23+0.29}_{-0.04-0.24-0.10-0.15}$	$0.09^{+0.02+0.03+0.01}_{-0.02-0.02-0.01}$
$\overline{B}_s^0 \to K^0\omega$	C	$0.51^{+0.20+0.15+0.68+0.40}_{-0.18-0.11-0.23-0.25}$	$0.15^{+0.05+0.07+0.02}_{-0.04-0.03-0.01}$
$\overline{B}_s^0 \to K^+ K^{*-}$	P	$4.1^{+1.7+1.5+1.0+9.2}_{-1.5-1.3-0.9-2.3}$	$6.0^{+1.7+1.7+0.7}_{-1.5-1.2-0.3}$
$\overline{B}_s^0 \to K^{*+} K^-$	P	$5.5^{+1.3+5.0+0.8+14.2}_{-1.4-2.6-0.7-\ 3.6}$	$4.7^{+1.1+2.5+0.0}_{-0.8-1.4-0.0}$
$\overline{B}_s^0 \to K^0\overline{K}^{*0}$	P	$3.9^{+0.4+1.5+1.3+10.4}_{-0.4-1.4-1.4-\ 2.8}$	$7.3^{+2.5+2.1+0.0}_{-1.7-1.3-0.0}$
$\overline{B}_s^0 \to K^{*0}\overline{K}^0$	P	$4.2^{+0.4+4.6+1.1+13.2}_{-0.4-2.2-0.9-\ 3.2}$	$4.3^{+0.7+2.2+0.0}_{-0.7-1.4-0.0}$
$\overline{B}_s^0 \to \pi^0\phi$	P_{EW}	$0.12^{+0.03+0.04+0.01+0.02}_{-0.02-0.04-0.01-0.01}$	$0.16^{+0.06+0.02+0.00}_{-0.05-0.02-0.00}$
$\overline{B}_s^0 \to \rho^0\eta$	P_{EW}	$0.17^{+0.03+0.07+0.02+0.02}_{-0.03-0.06-0.02-0.01}$	$0.06^{+0.03+0.01+0.00}_{-0.02-0.01-0.00}$
$\overline{B}_s^0 \to \rho^0\eta'$	P_{EW}	$0.25^{+0.06+0.10+0.02+0.02}_{-0.05-0.08-0.02-0.02}$	$0.13^{+0.06+0.02+0.00}_{-0.04-0.02-0.01}$
$\overline{B}_s^0 \to \omega\eta$	P, C	$0.012^{+0.005+0.010+0.028+0.025}_{-0.004-0.003-0.006-0.006}$	$0.04^{+0.03+0.05+0.00}_{-0.01-0.02-0.00}$
$\overline{B}_s^0 \to \omega\eta'$	P, C	$0.024^{+0.011+0.028+0.077+0.042}_{-0.009-0.006-0.010-0.015}$	$0.44^{+0.18+0.15+0.00}_{-0.13-0.14-0.01}$
$\overline{B}_s^0 \to \phi\eta$	P	$0.12^{+0.02+0.95+0.54+0.32}_{-0.02-0.14-0.12-0.13}$	$3.6^{+1.5+0.8+0.0}_{-1.0-0.6-0.0}$
$\overline{B}_s^0 \to \phi\eta'$	P	$0.05^{+0.01+1.10+0.18+0.40}_{-0.01-0.17-0.08-0.04}$	$0.19^{+0.06+0.19+0.00}_{-0.01-0.13-0.00}$
$\overline{B}_s^0 \to K^0\phi$	P	$0.27^{+0.09+0.28+0.09+0.67}_{-0.08-0.14-0.06-0.18}$	$0.16^{+0.04+0.09+0.02}_{-0.03-0.04-0.01}$
$\overline{B}_s^0 \to \pi^0\omega$	ann	≈ 0.0005	$0.004^{+0.001+0.000+0.000}_{-0.001-0.001-0.000}$
$\overline{B}_s^0 \to \rho^+\pi^-$	ann	≈ 0.003	$0.22^{+0.05+0.04+0.00}_{-0.05-0.06-0.01}$
$\overline{B}_s^0 \to \pi^+\rho^-$	ann	≈ 0.003	$0.24^{+0.05+0.05+0.00}_{-0.05-0.06-0.01}$
$\overline{B}_s^0 \to \pi^0\rho^0$	ann	≈ 0.003	$0.23^{+0.05+0.05+0.00}_{-0.05-0.06-0.01}$

TABLE VIII: The direct CP asymmetries (in %) in the $B_s \to PV$ decays, obtained in the pQCD approach (This work); the errors for these entries correspond to the uncertainties in the input hadronic quantities, from the scale-dependence, and the CKM matrix elements, respectively. For comparison, we also cite the theoretical estimates of the CP asymmetries in the QCD factorization framework [16].

Modes	Class	QCDF	This work
$\overline{B}_s^0 \to \pi^- K^{*+}$	T	$0.6^{+0.2+1.4+0.1+19.9}_{-0.1-1.7-0.1-20.1}$	$-19.0^{+2.5+2.7+0.9}_{-2.6-3.4-1.4}$
$\overline{B}_s^0 \to \rho^- K^+$	T	$-1.5^{+0.4+1.2+0.2+12.1}_{-0.4-1.4-0.3-12.1}$	$14.2^{+2.4+2.3+1.2}_{-2.2-1.6-0.7}$
$\overline{B}_s^0 \to \pi^0 K^{*0}$	C	$-45.7^{+14.3+13.0+28.4+80.0}_{-16.0-11.6-28.0-59.7}$	$-47.1^{+7.4+35.5+2.9}_{-8.7-29.8-7.0}$
$\overline{B}_s^0 \to \rho^0 K^0$	C	$24.7^{+7.1+14.0+22.8+51.3}_{-5.2-12.4-17.7-52.3}$	$73.4^{+6.4+16.2+2.2}_{-11.7-47.8-3.9}$
$\overline{B}_s^0 \to K^{*0}\eta$	C	$40.2^{+17.0+24.6+\ 7.8+65.9}_{-11.5-30.8-14.0-96.3}$	$51.2^{+6.2+14.1+2.0}_{-6.4-12.4-3.3}$
$\overline{B}_s^0 \to K^{*0}\eta'$	C	$-58.6^{+16.9+41.4+19.9+44.9}_{-11.9-11.7-13.9-35.7}$	$-51.1^{+4.6+15.0+3.2}_{-6.6-18.2-4.1}$
$\overline{B}_s^0 \to K^0\omega$	C	$-43.9^{+13.6+18.0+30.6+57.7}_{-13.4-18.2-30.2-49.3}$	$-52.1^{+3.2+22.7+3.2}_{-0.0-15.1-2.0}$
$\overline{B}_s^0 \to K^+ K^{*-}$	P	$2.2^{+0.6+8.4+5.1+68.6}_{-0.7-8.0-5.9-71.0}$	$-36.6^{+2.3+2.8+1.3}_{-2.3-3.5-1.2}$
$\overline{B}_s^0 \to K^{*+} K^-$	P	$-3.1^{+1.0+3.8+1.6+47.5}_{-1.1-2.6-1.3-45.0}$	$55.3^{+4.4+8.5+5.1}_{-4.9-9.8-2.5}$
$\overline{B}_s^0 \to K^0\overline{K}^{*0}$	P	$1.7^{+0.4+0.6+0.5+1.4}_{-0.5-0.5-0.4-0.8}$	0
$\overline{B}_s^0 \to K^{*0}\overline{K}^0$	P	$0.2^{+0.0+0.2+0.1+0.2}_{-0.1-0.3-0.1-0.1}$	0
$\overline{B}_s^0 \to \pi^0\phi$	P_{EW}	$27.2^{+6.1+9.8+2.7+32.0}_{-6.8-5.6-2.4-37.1}$	$13.3^{+0.3+2.1+1.5}_{-0.4-1.7-0.7}$
$\overline{B}_s^0 \to \rho^0\eta$	P_{EW}	$27.8^{+6.4+9.1+2.6+25.9}_{-6.7-5.7-2.2-28.4}$	$-9.2^{+1.0+2.8+0.4}_{-0.4-2.7-0.7}$
$\overline{B}_s^0 \to \rho^0\eta'$	P_{EW}	$28.9^{+6.1+10.3+1.5+24.8}_{-7.5-\ 6.3-1.8-27.5}$	$25.8^{+1.3+2.8+3.4}_{-2.0-3.6-1.5}$
$\overline{B}_s^0 \to \omega\eta$	P,C	—	$-16.7^{+5.8+15.4+0.8}_{-3.2-19.1-1.7}$
$\overline{B}_s^0 \to \omega\eta'$	P,C	—	$7.7^{+0.4+4.5+9.4}_{-0.1-4.2-0.4}$
$\overline{B}_s^0 \to \phi\eta$	P	$-8.4^{+2.0+30.1+14.6+36.3}_{-2.1-71.2-44.7-59.7}$	$-1.8^{+0.0+0.6+0.1}_{-0.1-0.6-0.2}$
$\overline{B}_s^0 \to \phi\eta'$	P	$-62.2^{+15.9+132.3+80.8+122.4}_{-10.2-\ 84.2-46.8-\ 49.9}$	$7.8^{+1.5+1.2+0.1}_{-0.5-8.6-0.4}$
$\overline{B}_s^0 \to K^0\phi$	P	$-10.3^{+3.0+4.7+3.7+5.0}_{-2.4-3.0-4.1-7.5}$	0
$\overline{B}_s^0 \to \pi^0\omega$	ann	—	$6.0^{+0.0+0.5+0.8}_{-5.2-3.3-0.4}$
$\overline{B}_s^0 \to \rho^+\pi^-$	ann	—	$4.6^{+0.0+2.9+0.6}_{-0.6-3.5-0.3}$
$\overline{B}_s^0 \to \pi^+\rho^-$	ann	—	$-1.3^{+0.9+2.8+0.1}_{-0.4-3.5-0.2}$
$\overline{B}_s^0 \to \pi^0\rho^0$	ann	—	$1.7^{+0.2+2.8+0.2}_{-0.8-3.6-0.1}$

TABLE IX: The mixing-induced CP asymmetries $(S_f)_{B_s}$ and $(H_f)_{B_s}$ in $B_s \to PV$ decays obtained in the pQCD approach (This work); the errors for these entries correspond to the uncertainties in the input hadronic quantities, from the scale-dependence, and the CKM matrix elements, respectively.

Modes	Class	$(S_f)_{B_s}$	$(H_f)_{B_s}$
$\overline{B}_s^0 \to \rho^0 K_S$	C	$-0.57^{+0.22+0.51+0.02}_{-0.17-0.39-0.05}$	$-0.36^{+0.10+0.46+0.04}_{-0.13-0.15-0.04}$
$\overline{B}_s^0 \to K_S\omega$	C	$-0.63^{+0.09+0.28+0.01}_{-0.09-0.11-0.02}$	$-0.57^{+0.11+0.31+0.02}_{-0.13-0.38-0.02}$
$\overline{B}_s^0 \to \pi^0\phi$	P_{EW}	$-0.07^{+0.01+0.08+0.02}_{-0.01-0.09-0.03}$	$0.98^{+0.00+0.01+0.01}_{-0.00-0.03-0.00}$
$\overline{B}_s^0 \to \rho^0\eta$	P_{EW}	$0.15^{+0.06+0.14+0.01}_{-0.06-0.16-0.01}$	$0.98^{+0.01+0.01+0.00}_{-0.01-0.03-0.00}$
$\overline{B}_s^0 \to \rho^0\eta'$	P_{EW}	$-0.16^{+0.00+0.10+0.04}_{-0.00-0.12-0.05}$	$0.95^{+0.01+0.01+0.01}_{-0.00-0.02-0.02}$
$\overline{B}_s^0 \to \omega\eta$	P,C	$-0.02^{+0.01+0.02+0.00}_{-0.03-0.08-0.00}$	$0.99^{+0.01+0.01+0.00}_{-0.01-0.06-0.00}$
$\overline{B}_s^0 \to \omega\eta'$	P,C	$-0.11^{+0.01+0.04+0.02}_{-0.00-0.04-0.03}$	$0.99^{+0.00+0.00+0.00}_{-0.00-0.00-0.00}$
$\overline{B}_s^0 \to \phi\eta$	P	$-0.03^{+0.02+0.07+0.01}_{-0.01-0.20-0.02}$	$1.00^{+0.00+0.00+0.00}_{-0.00-0.01-0.00}$
$\overline{B}_s^0 \to \phi\eta'$	P	$0.00^{+0.00+0.02+0.00}_{-0.00-0.02-0.00}$	$1.00^{+0.00+0.00+0.00}_{-0.00-0.00-0.02}$
$\overline{B}_s^0 \to K_S\phi$	P	-0.72	-0.69
$\overline{B}_s^0 \to \pi^0\omega$	ann	$-0.97^{+0.00+0.00+0.11}_{-0.01-0.00-0.02}$	$-0.22^{+0.02+0.00+0.12}_{-0.00-0.02-0.29}$
$\overline{B}_s^0 \to \pi^0\rho^0$	ann	$-0.19^{+0.00+0.02+0.01}_{-0.00-0.02-0.02}$	$0.99^{+0.00+0.00+0.00}_{-0.00-0.00-0.00}$

for the annihilation diagrams. The factorizable emission topology contribution $F^{SP,i}_{B_s \to V_3}$ ($i = L, N, T$) vanish due to the conservation of charge parity.

The normal and transverse polarization amplitudes for $B_s \to VV$ decays are displayed as

follows. For the factorizable emission diagrams shown in Fig.3(a) and (b), the formulas are

$$
\begin{aligned}
f_{V_2} F_{B_s \to V_3}^{LL,N}(a_i) =\ & 8\pi C_F M_{B_s}^4 f_{V_2} r_2 \int_0^1 dx_1 dx_3 \int_0^\infty b_1 db_1 b_3 db_3 \phi_{B_s}(x_1, b_1) \Big\{ h_e(x_1, x_3, b_1, b_3) \\
& \times E_e(t_a) a_i(t_a) [\phi_3^T(x_3) + 2r_3 \phi_3^v(x_3) + r_3 x_3 (\phi_3^v(x_3) - \phi_3^a(x_3))] \\
& + r_3 [\phi_3^v(x_3) + \phi_3^a(x_3)] E_e(t_a') a_i(t_a') h_e(x_3, x_1, b_3, b_1) \Big\},
\end{aligned}
\tag{90}
$$

$$
\begin{aligned}
f_{V_2} F_{B_s \to V_3}^{LL,T}(a_i) =\ & 16\pi C_F M_{B_s}^4 f_{V_2} r_2 \int_0^1 dx_1 dx_3 \int_0^\infty b_1 db_1 b_3 db_3 \phi_{B_s}(x_1, b_1) \Big\{ h_e(x_1, x_3, b_1, b_3) \\
& \times [\phi_3^T(x_3) + 2r_3 \phi_3^v(x_3) - r_3 x_3 (\phi_3^v(x_3) - \phi_3^a(x_3))] E_e(t_a) a_i(t_a) \\
& + r_3 [\phi_3^v(x_3) + \phi_3^a(x_3)] E_e(t_a') a_i(t_a') h_e(x_3, x_1, b_3, b_1) \Big\},
\end{aligned}
\tag{91}
$$

$$
F_{B_s \to V_3}^{LR,i}(a_i) = F_{B_s \to V_3}^{LL,i}(a_i),
\tag{92}
$$

$$
F_{B_s \to V_3}^{SP,i}(a_i) = 0,
\tag{93}
$$

with $i = L, N, T$.

The non-factorizable emission diagrams are shown in Fig.3(c) and (d). Their contributions are expressed in the formulas given below:

$$
\begin{aligned}
M_{B_s \to V_3}^{LL,N}(a_i) =\ & 32\pi C_F M_{B_s}^4 r_2 / \sqrt{6} \int_0^1 dx_1 dx_2 dx_3 \int_0^\infty b_1 db_1 b_2 db_2 \phi_{B_s}(x_1, b_1) \\
& \times \Big\{ \left[x_2 (\phi_2^v(x_2) + \phi_2^a(x_2)) \phi_3^T(x_3) - 2r_3 (x_2 + x_3)(\phi_2^v(x_2)\phi_3^v(x_3) + \phi_2^a(x_2)\phi_3^a(x_3)) \right] \\
& \quad h_n(x_1, x_2, x_3, b_1, b_2) E_e'(t_b') a_i(t_b') \\
& \quad + (1 - x_2)(\phi_2^v(x_2) + \phi_2^a(x_2))\phi_3^T(x_3) E_e'(t_b) a_i(t_b) h_n(x_1, 1 - x_2, x_3, b_1, b_2) \Big\},
\end{aligned}
\tag{94}
$$

$$
\begin{aligned}
M_{B_s \to V_3}^{LL,T}(a_i) =\ & 64\pi C_F M_{B_s}^4 r_2 / \sqrt{6} \int_0^1 dx_1 dx_2 dx_3 \int_0^\infty b_1 db_1 b_2 db_2 \phi_{B_s}(x_1, b_1) \Big\{ E_e'(t_b') a_i(t_b') \\
& \times \left[x_2 (\phi_2^v(x_2) + \phi_2^a(x_2)) \phi_3^T(x_3) - 2r_3 (x_2 + x_3)(\phi_2^v(x_2)\phi_3^a(x_3) \right. \\
& \left. + \phi_2^a(x_2)\phi_3^v(x_3)) \right] h_n(x_1, x_2, x_3, b_1, b_2) \\
& + (1 - x_2)[\phi_2^v(x_2) + \phi_2^a(x_2)]\phi_3^T(x_3) E_e'(t_b) a_i(t_b) h_n(x_1, 1 - x_2, x_3, b_1, b_2) \Big\},
\end{aligned}
\tag{95}
$$

$$
\begin{aligned}
M_{B_s \to V_3}^{LR,T}(a_i) =\ & 2 M_{B_s \to V_3}^{LR,N}(a_i) \\
=\ & 64\pi C_F M_{B_s}^4 / \sqrt{6} \int_0^1 dx_1 dx_2 dx_3 \int_0^\infty b_1 db_1 b_2 db_2 \phi_{B_s}(x_1, b_1) \\
& \times r_3 x_3 \phi_2^T(x_2)(\phi_3^v(x_3) - \phi_3^a(x_3)) \\
& \Big\{ E_e'(t_b') a_i(t_b') h_n(x_1, x_2, x_3, b_1, b_2) + E_e'(t_b) a_i(t_b) h_n(x_1, 1 - x_2, x_3, b_1, b_2) \Big\},
\end{aligned}
\tag{96}
$$

39

$$M_{B_s \to V_3}^{SP,N}(a_i) = 32\pi C_F M_{B_s}^4 / \sqrt{6} \int_0^1 dx_1 dx_2 dx_3 \int_0^\infty b_1 db_1 b_2 db_2 \phi_{B_s}(x_1, b_1) r_2$$

$$\times \Big\{ x_2(\phi_2^v(x_2) - \phi_2^a(x_2))\phi_3^T(x_3)E_e'(t_b')a_i(t_b')h_n(x_1, x_2, x_3, b_1, b_2)$$

$$+ h_n(x_1, 1-x_2, x_3, b_1, b_2)[(1-x_2)(\phi_2^v(x_2) - \phi_2^a(x_2))\phi_3^T(x_3)$$

$$- 2r_3(1-x_2+x_3)(\phi_2^v(x_2)\phi_3^v(x_3) - \phi_2^a(x_2)\phi_3^a(x_3))]E_e'(t_b)a_i(t_b) \Big\}, \qquad (97)$$

$$M_{B_s \to V_3}^{SP,T}(a_i) = 64\pi C_F M_{B_s}^4 / \sqrt{6} \int_0^1 dx_1 dx_2 dx_3 \int_0^\infty b_1 db_1 b_2 db_2 \phi_{B_s}(x_1, b_1) r_2$$

$$\times \Big\{ x_2(\phi_2^v(x_2) - \phi_2^a(x_2))\phi_3^T(x_3)E_e'(t_b')a_i(t_b')h_n(x_1, x_2, x_3, b_1, b_2)$$

$$+ h_n(x_1, 1-x_2, x_3, b_1, b_2)[(1-x_2)(\phi_2^v(x_2) - \phi_2^a(x_2))\phi_3^T(x_3)$$

$$- 2r_3(1-x_2+x_3)(\phi_2^v(x_2)\phi_3^a(x_3) - \phi_2^a(x_2)\phi_3^v(x_3))]E_e'(t_b)a_i(t_b) \Big\}. \qquad (98)$$

The factorizable annihilation diagrams are shown in Fig.4 (a) and (b), and the normal polarization contributions are:

$$f_{B_s} F_{ann}^{LL,N}(a_i) = f_{B_s} F_{ann}^{LR,N}(a_i)$$

$$= -8\pi C_F M_{B_s}^4 f_{B_s} r_2 r_3 \int_0^1 dx_2 dx_3 \int_0^\infty b_2 db_2 b_3 db_3 \Big\{ E_a(t_c)a_i(t_c)h_a(x_2, 1-x_3, b_2, b_3))$$

$$[(2-x_3)(\phi_2^v(x_2)\phi_3^v(x_3) + \phi_2^a(x_2)\phi_3^a(x_3)) + x_3(\phi_2^v(x_2)\phi_3^v(x_3) + \phi_2^a(x_2)\phi_3^v(x_3))]$$

$$- h_a(1-x_3, x_2, b_3, b_2)[(1+x_2)(\phi_2^v(x_2)\phi_3^v(x_3) + \phi_2^a(x_2)\phi_3^a(x_3))$$

$$- (1-x_2)(\phi_2^v(x_2)\phi_3^a(x_3) + \phi_2^a(x_2)\phi_3^v(x_3))]E_a(t_c')a_i(t_c') \Big\}. \qquad (99)$$

Note, that large cancellations between the two diagrams Fig.4 (a) and (b) take place, as a result of which contributions from these diagrams are suppressed.

For the transverse polarization, we have

$$f_{B_s} F_{ann}^{LL,T}(a_i) = -f_{B_s} F_{ann}^{LR,T}(a_i)$$

$$= -16\pi C_F M_{B_s}^4 f_{B_s} r_2 r_3 \int_0^1 dx_2 dx_3 \int_0^\infty b_2 db_2 b_3 db_3 \Big\{ [x_3(\phi_2^v(x_2)\phi_3^v(x_3) + \phi_2^a(x_2)\phi_3^a(x_3))$$

$$+ (2-x_3)(\phi_2^v(x_2)\phi_3^a(x_3) + \phi_2^a(x_2)\phi_3^v(x_3))]E_a(t_c)a_i(t_c)h_a(x_2, 1-x_3, b_2, b_3)$$

$$+ h_a(1-x_3, x_2, b_3, b_2)[(1-x_2)(\phi_2^v(x_2)\phi_3^v(x_3) + \phi_2^a(x_2)\phi_3^a(x_3))$$

$$- (1+x_2)(\phi_2^v(x_2)\phi_3^a(x_3) + \phi_2^a(x_2)\phi_3^v(x_3))]E_a(t_c')a_i(t_c') \Big\}. \qquad (100)$$

We remark that, although the cancellations in this case are not as severe as for the normal polarization case, the dominant contributions are still power suppressed by $r_2 r_3$, where $r_{2(3)} =$

$M_{2(3)}/M_{B_s}$. For the $(S-P)(S+P)$ operators, we have

$$
\begin{aligned}
f_{B_s}F_{ann}^{SP,T}(a_i) &= 2f_{B_s}F_{ann}^{SP,N}(a_i) \\
&= -32\pi C_F M_{B_s}^4 f_{B_s} \int_0^1 dx_2 dx_3 \int_0^\infty b_2 db_2 b_3 db_3 \Big\{ r_2(\phi_2^v(x_2) + \phi_2^a(x_2))\phi_3^T(x_3) \\
&\quad \times E_a(t_c)a_i(t_c)h_a(x_2, 1-x_3, b_2, b_3) \\
&\quad + r_3\phi_2^T(x_2)(\phi_3^v(x_3) - \phi_3^a(x_3))E_a(t_c')a_i(t_c')h_a(1-x_3, x_2, b_3, b_2) \Big\}.
\end{aligned}
\tag{101}
$$

Again, for this case, like the $B_s \to PP$ decays, no cancellations among the contributing diagrams or power suppressions are involved. The chiral enhancement here for the transverse and normal polarizations are essential for the explanation of the large transverse polarization fraction in the penguin dominant B decays, such as $B \to K^*\phi$ and $B \to K^*\rho$ decays [42, 43]. For the non-factorizable annihilation diagrams shown in Fig.4 (c) and (d), we have

$$
\begin{aligned}
M_{ann}^{LL,N}(a_i) &= M_{ann}^{SP,N}(a_i) \\
&= -64\pi C_F M_{B_s}^4 r_2 r_3/\sqrt{6} \int_0^1 dx_1 dx_2 dx_3 \int_0^\infty b_1 db_2 b_2 db_2 \phi_{B_s}(x_1, b_1)[\phi_2^v(x_2)\phi_3^v(x_3) \\
&\quad + \phi_2^a(x_2)\phi_3^a(x_3)]E_a'(t_d)a_i(t_d)h_{na}(x_1, x_2, x_3, b_1, b_2),
\end{aligned}
\tag{102}
$$

$$
\begin{aligned}
M_{ann}^{LL,T}(a_i) &= -M_{ann}^{SP,T}(a_i) \\
&= -128\pi C_F M_{B_s}^4 r_2 r_3/\sqrt{6} \int_0^1 dx_1 dx_2 dx_3 \int_0^\infty b_1 db_2 b_2 db_2 \phi_{B_s}(x_1, b_1)[\phi_2^v(x_2)\phi_3^a(x_3) \\
&\quad + \phi_2^a(x_2)\phi_3^v(x_3)]E_a'(t_d)a_i(t_d)h_{na}(x_1, x_2, x_3, b_1, b_2),
\end{aligned}
\tag{103}
$$

$$
\begin{aligned}
M_{ann}^{LR,T}(a_i) &= 2M_{ann}^{LR,N}(a_i) \\
&= -64\pi C_F M_{B_s}^4/\sqrt{6} \int_0^1 dx_1 dx_2 dx_3 \int_0^\infty b_1 db_1 b_2 db_2 \phi_{B_s}(x_1, b_1)\Big\{ h_{na}'(x_1, x_2, x_3, b_1, b_2) \\
&\quad \big[r_2 x_2(\phi_2^v(x_2) + \phi_2^a(x_2))\phi_3^T(x_3) - r_3(1-x_3)\phi_2^T(x_2)(\phi_3^v(x_3) - \phi_3^a(x_3)) \big] E_a'(t_d')a_i(t_d') \\
&\quad + \big[r_2(2-x_2)(\phi_2^v(x_2) + \phi_2^a(x_2))\phi_3^T(x_3) - r_3(1+x_3)\phi_2^T(x_2)(\phi_3^v(x_3) - \phi_3^a(x_3)) \big] \\
&\quad \times E_a'(t_d)a_i(t_d)h_{na}(x_1, x_2, x_3, b_1, b_2) \Big\}.
\end{aligned}
\tag{104}
$$

These contributions are all power-suppressed as expected.

B. Numerical results for $B_s \to VV$ decays

The decay width for $B_s \to V_2 V_3$ is given as

$$
\Gamma = \frac{P_c}{8\pi M_{B_s}^2} \sum_{i=0,\|,\perp} A_{(i)}^\dagger A_{(i)},
\tag{105}
$$

41

where P_c is the momentum of either of the two vector mesons in the final states. The sum is over the three transversity amplitudes of the two vector mesons, defined as follows:

$$A_0 \equiv -A_L,$$
$$A_\parallel \equiv \sqrt{2}a,$$
$$A_\perp \equiv r_2 r_3 \sqrt{2(\kappa^2 - 1)} A_T , \tag{106}$$

with the ratio $\kappa = P_2 \cdot P_3/(M_2 M_3)$. Note that the definitions of $A_i(i = 0, \parallel, \perp)$ are consistent with those in [18], except for an additional minus sign in A_0, so that our definitions of the relative strong phases $\phi_i(i = \parallel, \perp)$ (see text below) also differ from the ones in [18] by π. The polarization fractions $f_i(i = 0, \parallel, \perp)$ are defined as follows:

$$f_i = \frac{|A_i|^2}{|A_0|^2 + |A_\parallel|^2 + |A_\perp|^2} . \tag{107}$$

We first give the numerical results of the form factors at maximal recoil:

$$
\begin{aligned}
V^{B \to K^*} &= 0.25^{+0.05+0.00}_{-0.05-0.00}, & A_0^{B \to K^*} &= 0.30^{+0.06+0.00}_{-0.05-0.01}, & A_1^{B \to K^*} &= 0.19^{+0.04+0.00}_{-0.03-0.00}, \\
V^{B \to \rho} &= 0.21^{+0.05+0.00}_{-0.04-0.00}, & A_0^{B \to \rho} &= 0.25^{+0.05+0.00}_{-0.04-0.01}, & A_1^{B \to \rho} &= 0.17^{+0.04+0.00}_{-0.03-0.00}, \\
V^{B \to \omega} &= 0.19^{+0.04+0.00}_{-0.04-0.00}, & A_0^{B \to \omega} &= 0.23^{+0.05+0.00}_{-0.04-0.01}, & A_1^{B \to \omega} &= 0.15^{+0.03+0.00}_{-0.03-0.00}. \\
V^{B_s \to K^*} &= 0.21^{+0.04+0.00}_{-0.03-0.01}, & A_0^{B_s \to K^*} &= 0.25^{+0.05+0.00}_{-0.05-0.01}, & A_1^{B_s \to K^*} &= 0.16^{+0.03+0.00}_{-0.03-0.01}, \\
V^{B_s \to \phi} &= 0.25^{+0.05+0.00}_{-0.04-0.01}, & A_0^{B_s \to \phi} &= 0.30^{+0.05+0.00}_{-0.05-0.01}, & A_1^{B_s \to \phi} &= 0.19^{+0.03+0.00}_{-0.03-0.01}.
\end{aligned}
\tag{108}
$$

where the first error in the above entries is due to the input hadronic parameters $f_{B(B_s)}$, ω_b and the second one is from the hard scale and Λ_{QCD}. The entries in the first three lines involve the decays of the $B^\pm$ and B_d^0 mesons to two vector mesons, and as such are not required for the $B_s^0 \to VV$ decays being worked out in this paper. We list them here to see the SU(3)-breaking effects in the form factors. Within errors, these form factors are in agreement with the ones in the light cone QCD sum rules [61] and with the slightly different estimates of the same in [18]. The branching ratios of $B_s \to VV$ decays are listed in Table X. They are compared with the corresponding results in the QCDF approach [18]. A comparison shows that the tree-, penguin- and electroweak dominated decays are comparable in the two approaches, with the numerical differences reflecting the input parameters. The color-suppressed decays, but more markedly the annihilation-dominated decays, differ in these approaches, a feature which is well appreciated in the literature. The experimental upper bounds on some of the decays are also listed. Except for the decay $\overline{B}_s \to \phi\phi$, where an experimental measurement may be just around the corner, all other decay modes remain essentially unexplored.

TABLE X: The CP-averaged branching ratios in $B_s \to VV$ decays ($\times 10^{-6}$) obtained in the pQCD approach (This work); the errors for these entries correspond to the uncertainties in the input hadronic quantities, from the scale-dependence, and the CKM matrix elements, respectively. For comparison, we also cite the updated theoretical estimates in the QCD factorization framework [18]. The experimental upper limits (at 90% C.L.) are from the Particle Data Group [28].

Channel	Class	QCDF [18]	This work	Exp [28]
$\bar{B}_s \to \rho^0 K^{*0}$	C	$1.5^{+1.0+3.1}_{-0.5-1.5}$	$0.33^{+0.09+0.14+0.00}_{-0.07-0.09-0.01}$	< 767
$\bar{B}_s \to \omega K^{*0}$	C	$1.2^{+0.7+2.3}_{-0.3-1.1}$	$0.31^{+0.10+0.12+0.07}_{-0.07-0.06-0.02}$	
$\bar{B}_s \to \rho^- K^{*+}$	T	$25.2^{+1.5+4.7}_{-1.7-3.1}$	$20.9^{+8.2+1.4+1.2}_{-6.2-1.4-1.1}$	
$\bar{B}_s \to K^{*-} K^{*+}$	P	$9.1^{+2.5+10.2}_{-2.2-5.9}$	$6.7^{+1.5+3.4+0.5}_{-1.2-1.4-0.2}$	
$\bar{B}_s \to K^{*0}\overline{K}^{*0}$	P	$9.1^{+0.5+11.3}_{-0.4-6.8}$	$7.8^{+1.9+3.8+0.0}_{-1.5-2.2-0.0}$	< 1681
$\bar{B}_s \to \phi K^{*0}$	P	$0.4^{+0.1+0.5}_{-0.1-0.3}$	$0.65^{+0.16+0.27+0.10}_{-0.13-0.18-0.04}$	< 1013
$\bar{B}_s \to \phi\phi$	P	$21.8^{+1.1+30.4}_{-1.1-17.0}$	$35.3^{+8.3+16.7+0.0}_{-6.9-10.2-0.0}$	14 ± 8
$\bar{B}_s \to \rho^+ \rho^-$	ann	$0.34^{+0.03+0.60}_{-0.03-0.38}$	$1.0^{+0.2+0.3+0.0}_{-0.2-0.2-0.0}$	
$\bar{B}_s \to \rho^0 \rho^0$	ann	$0.17^{+0.01+0.30}_{-0.01-0.19}$	$0.51^{+0.12+0.17+0.01}_{-0.11-0.10-0.01}$	< 320
$\bar{B}_s \to \rho^0 \omega$	ann	< 0.01	$0.007^{+0.002+0.001+0.000}_{-0.001-0.001-0.000}$	
$\bar{B}_s \to \omega\omega$	ann	$0.11^{+0.01+0.20}_{-0.01-0.12}$	$0.39^{+0.09+0.13+0.01}_{-0.08-0.07-0.00}$	
$\bar{B}_s \to \phi\rho^0$	P_{EW}	$0.40^{+0.12+0.25}_{-0.10-0.04}$	$0.23^{+0.09+0.03+0.00}_{-0.07-0.01-0.01}$	< 617
$\bar{B}_s \to \phi\omega$	P	$0.10^{+0.05+0.48}_{-0.03-0.12}$	$0.16^{+0.09+0.10+0.01}_{-0.05-0.04-0.00}$	

The results for the longitudinal polarization fraction f_0, parallel polarization fraction $f_\parallel$ and perpendicular polarization fraction $f_\perp$, their relative phases $\phi_\parallel \equiv Arg(A_\parallel/A_0)$ and $\phi_\perp \equiv Arg(A_\perp/A_0)$ (both in radians), and the direct CP-asymmetry in the $\overline{B_s^0} \to VV$ decays are displayed in Table XI. In calculating the CP-asymmetries, we have used the definition given earlier in Eq. 65. Again, there are no data available to confront the entries in Table XI.

Two remarks on the $B_s \to \phi\phi$ decays presented above are in order.

First, $B_s \to \phi\phi$ is a $b \to s$ penguin dominated process. The CDF collaboration [62] has reported the decay branching fraction of this channel as $(14 \pm 8) \times 10^{-6}$, but a thorough angular analysis is still lacking. This channel is very similar to the decay $B \to \phi K^*$, which is well measured in the experiment. In the $B \to \phi K^*$ decays, the data show that the fraction of the

left-handed polarization reaches about 50%. This result is quite different from the expectation in the factorization assumption that the longitudinal polarization should dominate due to the quark helicity analysis. There exist lots of theoretical attempts to solve this contradiction. To distinguish, which one is the most appropriate scheme, we must investigate the decay $B_s \to \phi\phi$ and other similar channels.

In the pQCD approach, the weak annihilation diagram induced by the operator O_6 can enhance the transverse polarization sizably. In Ref. [63], the longitudinal fraction of $B \to \phi K^*$ is about 75 %, which is much smaller than that obtained based on the factorization assumption, but still larger than the data. Moreover, the branching fraction is overestimated. Li [64] has suggested a strategy to solve these two problems together, by invoking a smaller value for the form factor A_0. A smaller A_0 is also consistent with the predictions in other approaches, such as the covariant light front quark model [65]. In the pQCD approach, a smaller A_0 requires smaller Gegenbauer moments of the longitudinal polarized distribution amplitudes of the recoiling vector meson. Following this lead, and performing a calculation using the asymptotic distribution amplitude for K^*, one indeed finds that the longitudinal polarization fraction can be reduced; Ref. [64] finds that this fraction can be reduced to 59%.

Based on the above discussion, we also analyzed the $B_s \to VV$ decays adopting the asymptotic forms of the twist-3 distribution amplitudes in the pQCD approach, while keeping the leading-twist distribution amplitudes up to the second Gegenbauer moments, as done for the pseudo-scalar meson case discussed earlier. In addition, we also test the sensitivity of the branching ratio of the $B_s \to \phi\phi$ decay on the Gengenbauer moments of the twist-2 distribution amplitudes. The result of the branching ratio for this channel with asymptotic twist-2 distribution amplitudes is 22.2×10^{-6}, which is much smaller than that for the case with higher Gegenbauer moments and is closer to the experiment. However, we find that the polarization fractions do not change too much using the asymptotic forms of distribution amplitudes. The reason is that the contributions from the annihilation topology, which enhance the transverse polarization fraction, also decrease with a decreased value of the form factor A_0. This is different from the $B \to \phi K^*$ decay.

Second, it is to be noted that the longitudinal polarization of $B \to \phi K^*$ and $\bar{B}_s \to \phi\phi$ can be related to each other in the SU(3) limit. The discrepancy between them represents SU(3) symmetry breaking effects, which can be reflected in the following aspects in the pQCD approach specifically: In the first place, the shape parameter of B and B_s wavefunction in the initial state can give rise to differences in these two U-spin related process. Then, the longitudinal and

44

TABLE XI: The CP-averaged polarization fractions, relative phases and direct CP asymmetries in the $B_s \to VV$ decays obtained in the pQCD approach; the errors for these entries correspond to the uncertainties in the input hadronic quantities, from the scale-dependence, and the CKM matrix elements, respectively.

Channel	$f_0(\%)$	$f_\parallel(\%)$	$f_\perp(\%)$	$\phi_\parallel(rad)$	$\phi_\perp(rad)$	CP($\%$)
$\bar{B}_s \to \rho^0 K^{*0}$	$45.5^{+0.4+6.9+0.6}_{-0.3-4.3-0.9}$	$27.6^{+0.1+2.1+0.4}_{-0.2-3.4-0.3}$	$26.9^{+0.2+2.3+0.4}_{-0.3-3.5-0.3}$	$2.7^{+0.2+0.2+0.3}_{-0.3-0.3-0.1}$	$2.8^{+0.3+0.3+0.4}_{-0.2-0.2-0.1}$	$61.8^{+3.2+17.1+4.4}_{-4.7-22.8-2.3}$
$\bar{B}_s \to \omega K^{*0}$	$53.2^{+0.3+3.5+2.3}_{-0.2-2.9-1.3}$	$23.6^{+0.2+1.5+0.4}_{-0.1-1.7-1.0}$	$23.1^{+0.1+1.4+1.0}_{-0.2-1.7-0.6}$	$1.4^{+0.1+0.2+0.0}_{-0.1-0.2-0.1}$	$1.4^{+0.1+0.2+0.0}_{-0.1-0.2-0.0}$	$-62.1^{+4.8+19.7+5.5}_{-3.9-12.6-1.9}$
$\bar{B}_s \to \rho^- K^{*+}$	$93.7^{+0.1+0.2+0.0}_{-0.2-0.3-0.2}$	$3.4^{+0.1+0.2+0.1}_{-0.0-0.1-0.0}$	$2.9^{+0.1+0.1+0.1}_{-0.1-0.1-0.0}$	$3.0^{+0.1+0.1+0.1}_{-0.0-0.0-0.0}$	$3.1^{+0.0+0.0+0.0}_{-0.1-0.1-0.1}$	$-8.2^{+1.0+1.2+0.4}_{-1.2-1.7-1.1}$
$\bar{B}_s \to K^{*-} K^{*+}$	$43.8^{+5.1+2.1+3.7}_{-4.0-2.3-1.5}$	$30.1^{+2.1+0.9+0.8}_{-2.7-1.0-1.9}$	$26.1^{+1.8+1.4+0.7}_{-2.4-1.0-1.8}$	$1.7^{+0.2+0.1+0.1}_{-0.2-0.1-0.0}$	$1.7^{+0.2+0.1+0.1}_{-0.2-0.1-0.0}$	$9.3^{+0.4+3.3+0.3}_{-0.7-3.6-0.2}$
$\bar{B}_s \to K^{*0}\overline{K}^{*0}$	$49.7^{+5.7+0.6+0.0}_{-4.8-3.8-0.0}$	$26.8^{+2.6+2.1+0.0}_{-3.0-0.3-0.0}$	$23.5^{+2.2+1.7+0.0}_{-2.7-0.3-0.0}$	$1.4^{+0.2+0.0+0.0}_{-0.1-0.0-0.0}$	$1.4^{+0.1+0.0+0.0}_{-0.1-0.0-0.0}$	0
$\bar{B}_s \to \phi K^{*0}$	$71.2^{+3.2+2.7+0.0}_{-3.0-3.7-0.0}$	$15.5^{+1.6+2.1+0.0}_{-1.7-1.5-0.0}$	$13.3^{+1.4+1.7+0.0}_{-1.5-1.3-0.0}$	$1.4^{+0.1+0.0+0.0}_{-0.1-0.1-0.0}$	$1.4^{+0.1+0.0+0.0}_{-0.1-0.1-0.0}$	0
$\bar{B}_s \to \phi\phi$	$61.9^{+3.6+2.5+0.0}_{-3.2-3.3-0.0}$	$20.7^{+1.7+1.8+0.0}_{-2.0-1.4-0.0}$	$17.4^{+1.5+1.5+0.0}_{-1.6-1.1-0.0}$	$1.3^{+0.2+0.1+0.0}_{-0.1-0.0-0.0}$	$1.3^{+0.2+0.0+0.0}_{-0.1-0.0-0.0}$	0
$\bar{B}_s \to \rho^+\rho^-$	~ 100	~ 0	~ 0	$4.3^{+0.1+0.1+0.0}_{-0.0-0.1-0.0}$	$4.7^{+0.0+0.3+0.1}_{-0.0-0.5-0.0}$	$-2.1^{+0.2+1.7+0.1}_{-0.1-1.3-0.1}$
$\bar{B}_s \to \rho^0\rho^0$	~ 100	~ 0	~ 0	$4.3^{+0.1+0.1+0.0}_{-0.0-0.1-0.0}$	$4.7^{+0.0+0.3+0.1}_{-0.0-0.5-0.0}$	$-2.1^{+0.2+1.7+0.1}_{-0.1-1.3-0.1}$
$\bar{B}_s \to \rho^0\omega$	~ 100	~ 0	~ 0	$4.5^{+0.0+0.0+0.0}_{-0.0-0.0-0.0}$	$3.2^{+0.0+0.1+0.0}_{-0.1-0.0-0.2}$	$6.0^{+0.7+2.7+1.0}_{-0.5-3.9-0.4}$
$\bar{B}_s \to \omega\omega$	~ 100	~ 0	~ 0	$4.3^{+0.0+0.1+0.0}_{-0.0-0.1-0.0}$	$4.7^{+0.0+0.2+0.0}_{-0.0-0.5-0.0}$	$-2.0^{+0.1+1.7+0.1}_{-0.1-1.3-0.1}$
$\bar{B}_s \to \phi\rho^0$	$87.0^{+0.2+0.9+0.9}_{-0.2-0.3-0.4}$	$6.8^{+0.1+0.2+0.3}_{-0.1-0.5-0.4}$	$6.2^{+0.1+0.1+0.1}_{-0.1-0.5-0.4}$	$3.5^{+0.0+0.0+0.0}_{-0.0-0.1-0.1}$	$3.5^{+0.0+0.1+0.1}_{-0.0-0.0-0.0}$	$10.1^{+0.9+1.6+1.3}_{-0.9-1.8-0.5}$
$\bar{B}_s \to \phi\omega$	$44.3^{+0.0+5.4+0.9}_{-7.5-6.1-0.4}$	$28.5^{+3.8+3.1+0.1}_{-0.0-2.8-0.5}$	$27.2^{+3.7+3.0+0.2}_{-0.0-2.6-0.4}$	$3.0^{+0.1+0.2+0.0}_{-0.1-0.2-0.0}$	$3.0^{+0.1+0.2+0.1}_{-0.0-0.2-0.0}$	$3.6^{+0.6+2.4+0.6}_{-0.6-2.4-0.2}$

transverse decay constants as well as the Gegenbauer moments in the two vector mesons in the final state can also contribute to the SU(3) symmetry breaking effects significantly. In addition, these two decay processes also differ due to the absence of the time-like penguin annihilation in the $B \to \phi K^*$ decay.

VI. SUMMARY

With the LHC era almost upon us, where apart from the decisive searches for the Higgs boson(s) and supersymmetry (or, alternatives thereof), also dedicated studies of the B_s^0-meson physics (as well as that of the heavier b-hadrons) will be carried out. First results on the decay characteristics

of the B_s^0-mesons are already available from the Tevatron, in particular the B_s^0 - $\overline{B_s^0}$-mixing induced mass difference ΔM_s, the branching ratios for the decays $\overline{B_s^0} \to K^+\pi^-$, $\overline{B_s^0} \to K^+K^-$, $\overline{B_s^0} \to \phi\phi$, and the first direct CP asymmetry $A_{\text{CP}}^{\text{dir}}(\overline{B_s^0} \to K^+\pi^-)$. These measurements owe themselves to the two experiments CDF and D0; they are impressive and prove that cutting-edge B physics can also be carried out by general purpose hadron collider experiments. At the LHC, we will have a dedicated b-physics experiment, LHCb, but also the two main general purpose detectors ATLAS and CMS will be able to contribute handsomely to the ongoing research in b-physics. Conceivably, also at a Super-B factory with dedicated running at the $\Upsilon(5S)$-resonance, the current experimental databank on the B_s-meson will be greatly enlarged.

Anticipating these developments, we have presented in this work the results of a comprehensive study of the decays $\overline{B_s^0} \to h_1 h_2$, where h_1 and h_2 are light (i.e., charmless) pseudo-scalar and vector mesons. This study has been carried out in the context of the pQCD approach, taking into account the most recent information on the CKM matrix elements and weak phases and updating the input hadronic parameters. The decay amplitudes contain the relevant emission and annihilation diagrams of the tree and penguin nature. Explicit formulae for all these amplitudes, including the various pQCD-related functions, are provided in the Appendices. Numerical results for the charge-conjugation averaged branching ratios, the direct CP asymmetries and the mixing-induced CP-asymmetries S_f for the CP-eigenstates f, and the time-dependent observable H_f are presented in the form of tables. In addition, for the $\overline{B_s^0} \to VV$ decays, we also calculate the charge-conjugation-averaged transversity amplitudes, their relative strong phases and magnitudes. The results for the altogether 49 $\overline{B_s^0} \to h_1 h_2$ decays include also theoretical errors coming from the input hadronic parameters, variation of the hard scattering scale together with the uncertainty on Λ_{QCD}, and the combined uncertainty in the CKM matrix elements and the angles of the unitarity triangle. For the last mentioned error, we use the recently updated results from the CKMfitter [53].

Our results are compared with the available data on the decays $\overline{B_s^0} \to h_1 h_2$ from the Tevatron, and some selected $\overline{B_d^0} \to h_1 h_2$ decays from the B-factory experiments, updating the theoretical calculations in the pQCD approach with our input parameters. In particular, we revisited the well-measured direct CP asymmetry $A_{K\pi}^{dir}(B_d^0 \to K^+\pi^-)$, working out the parametric sensitivity of this observable, and argued that data can be accommodated in the pQCD approach by invoking $O(\alpha_s^2)$ contributions, which we estimated from the existing literature. The successful predictions of this direct CP-asymmetry in the pQCD approach is set forth with the first observed CP-asymmetry in the decay $\overline{B_s^0} \to K^+\pi^-$. This CP-asymmetry is experimentally large and is in good

agreement with our numerical results, within the stated errors. We have also analyzed a number of ratios of branching ratio involving the $B_s^0 \to PP$ and $B_d^0 \to PP$ decays. They include the ratios $R_1 \equiv \frac{BR(\overline{B_s^0} \to K^+ K^-)}{BR(\overline{B_d^0} \to \pi^+ \pi^-)}$, $R_2 \equiv \frac{BR(\overline{B_s^0} \to K^+ K^-)}{BR(\overline{B_d^0} \to K^- \pi^+)}$, and two more, called R_3 and Δ, defined in Eq. (72) and (73), respectively, which involve the decays $\overline{B_d^0} \to K^- \pi^+$ and $\overline{B_s^0} \to K^+ \pi^-$ and their charge conjugates. Except for the ratio R_1, for which the pQCD calculations presented here are on the lower side of the data (within large errors), the others are well accounted for. We also compare our results with the corresponding ones in the QCDF and SCET approaches. What concerns the branching ratios, we find reasonable agreement for some topological amplitudes, but also major disagreement, in particular for those decays which are dominated by the color-suppressed tree and annihilation amplitudes. There are striking differences in the CP asymmetries, in particular with the QCDF-based estimates, which will be precisely tested in the future.

Experimental precision on B_s decays will improve enormously in the coming years, thanks to dedicated experiments at the Tevatron and LHC. Many of the decay rates and CP asymmetries worked out here will be put to experimental scrutiny. They can be combined with the B-factory data on the corresponding $B \to PP, PV, VV$ decays, eliminating some of the large parametric uncertainties in theoretically well-motivated ratios to test the SM precisely in exclusive hadronic decays. In principle, theoretical predictions presented here can be systematically improved by including higher order perturbative corrections (in α_s) and sub-leading power corrections in $1/m_b$.

Acknowledgment

APPENDIX A: PQCD FUNCTIONS

In this section, we group the functions which appear in the factorization formulae. The hard scales are chosen as

$$t_a = \max\{\sqrt{x_3}M_{B_s}, 1/b_1, 1/b_3\}, \tag{A1}$$

$$t'_a = \max\{\sqrt{x_1}M_{B_s}, 1/b_1, 1/b_3\}, \tag{A2}$$

$$t_b = \max\{\sqrt{x_1 x_3}M_{B_s}, \sqrt{|1 - x_1 - x_2|x_3}M_{B_s}, 1/b_1, 1/b_2\}, \tag{A3}$$

$$t'_b = \max\{\sqrt{x_1 x_3}M_{B_s}, \sqrt{|x_1 - x_2|x_3}M_{B_s}, 1/b_1, 1/b_2\}, \tag{A4}$$

$$t_c = \max\{\sqrt{1 - x_3}M_{B_s}, 1/b_2, 1/b_3\}, \tag{A5}$$

$$t'_c = \max\{\sqrt{x_2}M_{B_s}, 1/b_2, 1/b_3\}, \tag{A6}$$

$$t_d = \max\{\sqrt{x_2(1 - x_3)}M_{B_s}, \sqrt{1 - (1 - x_1 - x_2)x_3}M_{B_s}, 1/b_1, 1/b_2\}, \tag{A7}$$

$$t'_d = \max\{\sqrt{x_2(1 - x_3)}M_{B_s}, \sqrt{|x_1 - x_2|(1 - x_3)}M_{B_s}, 1/b_1, 1/b_2\}. \tag{A8}$$

The functions h in the decay amplitudes consist of two parts: one is the jet function $S_t(x_i)$ derived by the threshold re-summation[46], the other is the propagator of virtual quark and gluon. They are defined by

$$h_e(x_1, x_3, b_1, b_3) = \left[\theta(b_1 - b_3)I_0(\sqrt{x_3}M_{B_s}b_3)K_0(\sqrt{x_3}M_{B_s}b_1) \right. \tag{A9}$$

$$\left. + \theta(b_3 - b_1)I_0(\sqrt{x_3}M_{B_s}b_1)K_0(\sqrt{x_3}M_{B_s}b_3)\right] K_0(\sqrt{x_1 x_3}M_{B_s}b_1)S_t(x_3),$$

$$h_n(x_1, x_2, x_3, b_1, b_2) = \left[\theta(b_2 - b_1)K_0(\sqrt{x_1 x_3}M_{B_s}b_2)I_0(\sqrt{x_1 x_3}M_{B_s}b_1) \right.$$

$$\left. + \theta(b_1 - b_2)K_0(\sqrt{x_1 x_3}M_{B_s}b_1)I_0(\sqrt{x_1 x_3}M_{B_s}b_2)\right]$$

$$\times \begin{cases} \frac{i\pi}{2}H_0^{(1)}(\sqrt{(x_2 - x_1)x_3}M_{B_s}b_2), & x_1 - x_2 < 0 \\ K_0(\sqrt{(x_1 - x_2)x_3}M_{B_s}b_2), & x_1 - x_2 > 0 \end{cases}, \tag{A10}$$

$$h_a(x_2, x_3, b_2, b_3) = (\frac{i\pi}{2})^2 S_t(x_3)\Big[\theta(b_2 - b_3)H_0^{(1)}(\sqrt{x_3}M_{B_s}b_2)J_0(\sqrt{x_3}M_{B_s}b_3)$$

$$+\theta(b_3 - b_2)H_0^{(1)}(\sqrt{x_3}M_{B_s}b_3)J_0(\sqrt{x_3}M_{B_s}b_2)\Big]H_0^{(1)}(\sqrt{x_2 x_3}M_{B_s}b_2) \quad (A11)$$

$$h_{na}(x_1, x_2, x_3, b_1, b_2) = \frac{i\pi}{2}\Big[\theta(b_1 - b_2)H_0^{(1)}(\sqrt{x_2(1-x_3)}M_{B_s}b_1)J_0(\sqrt{x_2(1-x_3)}M_{B_s}b_2)$$

$$+\theta(b_2 - b_1)H_0^{(1)}(\sqrt{x_2(1-x_3)}M_{B_s}b_2)J_0(\sqrt{x_2(1-x_3)}M_{B_s}b_1)\Big]$$

$$\times K_0(\sqrt{1-(1-x_1-x_2)x_3}M_{B_s}b_1), \quad (A12)$$

$$h'_{na}(x_1, x_2, x_3, b_1, b_2) = \frac{i\pi}{2}\Big[\theta(b_1 - b_2)H_0^{(1)}(\sqrt{x_2(1-x_3)}M_{B_s}b_1)J_0(\sqrt{x_2(1-x_3)}M_{B_s}b_2)$$

$$+\theta(b_2 - b_1)H_0^{(1)}(\sqrt{x_2(1-x_3)}M_{B_s}b_2)J_0(\sqrt{x_2(1-x_3)}M_{B_s}b_1)\Big]$$

$$\times \begin{cases} \frac{i\pi}{2}H_0^{(1)}(\sqrt{(x_2 - x_1)(1-x_3)}M_{B_s}b_1), & x_1 - x_2 < 0 \\ K_0(\sqrt{(x_1 - x_2)(1-x_3)}M_{B_s}b_1), & x_1 - x_2 > 0 \end{cases}, \quad (A13)$$

where $H_0^{(1)}(z) = J_0(z) + i\,Y_0(z)$.

The S_t re-sums the threshold logarithms $\ln^2 x$ appearing in the hard kernels to all orders and it has been parameterized as

$$S_t(x) = \frac{2^{1+2c}\Gamma(3/2+c)}{\sqrt{\pi}\Gamma(1+c)}[x(1-x)]^c, \quad (A14)$$

with $c = 0.4$. In the nonfactorizable contributions, $S_t(x)$ gives a very small numerical effect to the amplitude [47]. Therefore, we drop $S_t(x)$ in h_n and h_{na}.

The evolution factors $E_e^{(\prime)}$ and $E_a^{(\prime)}$ entering in the expressions for the matrix elements (see section 3) are given by

$$E_e(t) = \alpha_s(t)\exp[-S_B(t) - S_3(t)], \quad E_e'(t) = \alpha_s(t)\exp[-S_B(t) - S_2(t) - S_3(t)]|_{b_1=b_3}, (A15)$$

$$E_a(t) = \alpha_s(t)\exp[-S_2(t) - S_3(t)], \quad E_a'(t) = \alpha_s(t)\exp[-S_B(t) - S_2(t) - S_3(t)]|_{b_2=b_3}, (A16)$$

in which the Sudakov exponents are defined as

$$S_B(t) = s\left(x_1\frac{M_{B_s}}{\sqrt{2}}, b_1\right) + \frac{5}{3}\int_{1/b_1}^t \frac{d\bar{\mu}}{\bar{\mu}}\gamma_q(\alpha_s(\bar{\mu})), \quad (A17)$$

$$S_2(t) = s\left(x_2\frac{M_{B_s}}{\sqrt{2}}, b_2\right) + s\left((1-x_2)\frac{M_{B_s}}{\sqrt{2}}, b_2\right) + 2\int_{1/b_2}^t \frac{d\bar{\mu}}{\bar{\mu}}\gamma_q(\alpha_s(\bar{\mu})), \quad (A18)$$

with the quark anomalous dimension $\gamma_q = -\alpha_s/\pi$. Replacing the kinematic variables of M_2 to M_3 in S_2, we can get the expression for S_3. The explicit form for the function $s(Q, b)$ is:

$$s(Q, b) = \frac{A^{(1)}}{2\beta_1}\hat{q}\ln\left(\frac{\hat{q}}{\hat{b}}\right) - \frac{A^{(1)}}{2\beta_1}\left(\hat{q} - \hat{b}\right) + \frac{A^{(2)}}{4\beta_1^2}\left(\frac{\hat{q}}{\hat{b}} - 1\right) - \left[\frac{A^{(2)}}{4\beta_1^2} - \frac{A^{(1)}}{4\beta_1}\ln\left(\frac{e^{2\gamma_E-1}}{2}\right)\right]\ln\left(\frac{\hat{q}}{\hat{b}}\right)$$

$$+\frac{A^{(1)}\beta_2}{4\beta_1^3}\hat{q}\left[\frac{\ln(2\hat{q})+1}{\hat{q}} - \frac{\ln(2\hat{b})+1}{\hat{b}}\right] + \frac{A^{(1)}\beta_2}{8\beta_1^3}\left[\ln^2(2\hat{q}) - \ln^2(2\hat{b})\right], \quad (A19)$$

49

where the variables are defined by

$$\hat{q} \equiv \ln[Q/(\sqrt{2}\Lambda)], \quad \hat{b} \equiv \ln[1/(b\Lambda)], \tag{A20}$$

and the coefficients $A^{(i)}$ and β_i are

$$\beta_1 = \frac{33 - 2n_f}{12}, \quad \beta_2 = \frac{153 - 19n_f}{24},$$
$$A^{(1)} = \frac{4}{3}, \quad A^{(2)} = \frac{67}{9} - \frac{\pi^2}{3} - \frac{10}{27}n_f + \frac{8}{3}\beta_1\ln(\frac{1}{2}e^{\gamma_E}), \tag{A21}$$

n_f is the number of the quark flavors and γ_E is the Euler constant. We will use the one-loop running coupling constant, i.e. we pick up the four terms in the first line of the expression for the function $s(Q,b)$.

APPENDIX B: ANALYTIC FORMULAE FOR THE $B_s \to PP$ DECAY AMPLITUDES

Before we give the analytic formulae for $B_s \to PP$ decays, we analyze the amplitudes in some special cases which can simplify the formulae.

- In the non-factorizable emission diagrams, the formulae can be simplified if the emission meson M_2 is π, η or η'. Their distribution amplitudes $\phi^A(x)$ and $\phi^P(x)$ are symmetric and $\phi^T(x)$ is antisymmetric under the change $x \to 1 - x$. From Eq. (54) we can see that the amplitude is identically zero for the $(V - A)(V + A)$ operators; From Eq. (53) and Eq. (55) we can see that the $(V - A)(V - A)$ contribution is the same as the $(S - P)(S + P)$ contribution which can be simplified as

$$
\begin{aligned}
M^{LL}_{B_s \to M_3}(a_i) = & \ 32\pi C_F M_{B_s}^4/\sqrt{6} \int_0^1 dx_1 dx_2 dx_3 \int_0^\infty b_1 db_1 b_2 db_2 \phi_B(x_1, b_1)\phi_2^A(x_2) \\
& \times h_n(x_1, x_2, x_3, b_1, b_2)\Big[-x_3\phi_3^A(x_3) + 2r_3 x_3\phi_3^T(x_3)\Big]a_i(t_b')E_e'(t_b') \\
= & \ M^{SP}_{B_s \to M_3}(a_i).
\end{aligned} \tag{B1}
$$

- In the annihilation factorizable diagrams, the $(V - A)(V - A)$ and $(V - A)(V + A)$ operators give the same contribution, both from the vector current. If the final state mesons are charge conjugate with each other, the $(V - A)(V - A)$ and $(V - A)(V + A)$ operators give identically zero contributions due to the conservation of the vector current. Such operators do not contribute to the $B_s \to K\pi$ decay either, in the $SU(3)$ limit. The $SU(3)$ symmetry breaking, i.e. the difference in the distribution amplitudes of π and K meson, can

induce small deviations from zero. We expect this kind of operators can not give important contributions to the branching ratios.

- In the nonfactorizable annihilation amplitudes of $\bar{B}_s \to \pi\pi$, $B_s \to \eta(\bar{n}n)\eta(\bar{n}n)$ and $B_s \to \eta(\bar{s}s)\eta(\bar{s}s)$, the $(V-A)(V-A)$ operators and $(S-P)(S+P)$ operators give equal contributions as can be seen from the factorization formulae M_{ann} by making $x_2 \leftrightarrow 1 - x_3$.

1. The case without $\eta^{(\prime)}$

Tree operator dominant decays:

$$
\begin{aligned}
A(\bar{B}_s^0 \to \pi^- K^+) = & \frac{G_F}{\sqrt{2}} V_{ub} V_{ud}^* \left\{ f_\pi F_{B_s \to K}^{LL} [a_1] + M_{B_s \to K}^{LL} [C_1] \right\} \\
& - \frac{G_F}{\sqrt{2}} V_{tb} V_{td}^* \left\{ f_\pi F_{B_s \to K}^{LL} [a_4 + a_{10}] + f_\pi F_{B_s \to K}^{SP} [a_6 + a_8] \right. \\
& + M_{B_s \to K}^{LL} [C_3 + C_9] + f_{B_s} F_{ann}^{LL} \left[a_4 - \frac{1}{2} a_{10} \right] + f_{B_s} F_{ann}^{SP} \left[a_6 - \frac{1}{2} a_8 \right] \\
& \left. + M_{ann}^{LL} \left[C_3 - \frac{1}{2} C_9 \right] + M_{ann}^{LR} \left[C_5 - \frac{1}{2} C_7 \right] \right\},
\end{aligned} \tag{B2}
$$

$$
\begin{aligned}
\sqrt{2} A(\bar{B}_s^0 \to \pi^0 K^0) = & \frac{G_F}{\sqrt{2}} V_{ub} V_{ud}^* \left\{ f_\pi F_{B_s \to K}^{LL} [a_2] + M_{B_s \to K}^{LL} [C_2] \right\} \\
& - \frac{G_F}{\sqrt{2}} V_{tb} V_{td}^* \left\{ f_\pi F_{B_s \to K}^{LL} \left[-a_4 - \frac{3}{2} a_7 + \frac{3}{2} a_9 + \frac{1}{2} a_{10} \right] \right. \\
& + f_\pi F_{B_s \to K}^{SP} \left[-a_6 + \frac{1}{2} a_8 \right] + M_{B_s \to K}^{LL} \left[-C_3 + \frac{3}{2} C_8 + \frac{1}{2} C_9 + \frac{3}{2} C_{10} \right] \\
& + f_{B_s} F_{ann}^{SP} \left[-a_6 + \frac{1}{2} a_8 \right] + f_{B_s} F_{ann}^{LL} \left[-a_4 + \frac{1}{2} a_{10} \right] \\
& \left. + M_{ann}^{LL} \left[-C_3 + \frac{1}{2} C_9 \right] + M_{ann}^{LR} \left[-C_5 + \frac{1}{2} C_7 \right] \right\}.
\end{aligned} \tag{B3}
$$

Pure annihilation type decays:

$$
\begin{aligned}
A(\bar{B}_s^0 \to \pi^+ \pi^-) = & \sqrt{2} A(\bar{B}_s^0 \to \pi^0 \pi^0) \\
= & \frac{G_F}{\sqrt{2}} V_{ub} V_{us}^* M_{ann}^{LL} [C_2] - \frac{G_F}{\sqrt{2}} V_{tb} V_{ts}^* M_{ann}^{LL} \left[2C_4 + 2C_6 + \frac{1}{2} C_8 + \frac{1}{2} C_{10} \right]. \tag{B4}
\end{aligned}
$$

QCD penguin operator dominant decays:

$$
\begin{aligned}
A(\bar{B}_s^0 \to K^- K^+) = {}& \frac{G_F}{\sqrt{2}} V_{ub} V_{us}^* \Big\{ f_K F_{B_s \to K}^{LL}\, [a_1] + M_{B_s \to K}^{LL}[C_1] + M_{ann}^{LL}[C_2] \Big\} \\
& - \frac{G_F}{\sqrt{2}} V_{tb} V_{ts}^* \Big\{ f_K F_{B_s \to K}^{LL}\, [a_4 + a_{10}] + f_K F_{B_s \to K}^{SP}\, [a_6 + a_8] \\
& + M_{B_s \to K}^{LL}\, [C_3 + C_9] + M_{B_s \to K}^{LR}\, [C_5 + C_7] + f_{B_s} F_{ann}^{SP} \Big[a_6 - \frac{1}{2} a_8 \Big] \\
& + M_{ann}^{LL} \Big[C_3 - \frac{1}{2} C_9 + C_4 - \frac{1}{2} C_{10} \Big] + M_{ann}^{LR} \Big[C_5 - \frac{1}{2} C_7 \Big] + M_{ann}^{SP} \Big[C_6 - \frac{1}{2} C_8 \Big] \\
& + \Big(M_{ann}^{LL}\, [C_4 + C_{10}] + M_{ann}^{SP}\, [C_6 + C_8] \Big)_{K^- \leftrightarrow K^+} \Big\},
\end{aligned}
\tag{B5}
$$

$$
\begin{aligned}
A(\bar{B}_s^0 \to \bar{K}^0 K^0) = {}& -\frac{G_F}{\sqrt{2}} V_{tb} V_{ts}^* \Big\{ f_K F_{B_s \to K}^{LL} \Big[a_4 - \frac{1}{2} a_{10} \Big] + f_K F_{B_s \to K}^{SP} \Big[a_6 - \frac{1}{2} a_8 \Big] \\
& + M_{B_s \to K}^{LL} \Big[C_3 - \frac{1}{2} C_9 \Big] + M_{B_s \to K}^{LR} \Big[C_5 - \frac{1}{2} C_7 \Big] + f_{B_s} F_{ann}^{SP} \Big[a_6 - \frac{1}{2} a_8 \Big] \\
& + M_{ann}^{LL} \Big[C_3 - \frac{1}{2} C_9 + C_4 - \frac{1}{2} C_{10} \Big] + M_{ann}^{LR} \Big[C_5 - \frac{1}{2} C_7 \Big] \\
& + M_{ann}^{LL} \Big[C_4 - \frac{1}{2} C_{10} \Big]_{K^0 \leftrightarrow \bar{K}^0} + \Big(M_{ann}^{SP} \Big[C_6 - \frac{1}{2} C_8 \Big] + [K^0 \leftrightarrow \bar{K}^0] \Big) \Big\},
\end{aligned}
\tag{B6}
$$

2.   The case with $\eta^{(\prime)}$

As discussed in the last section, we use the quark flavor basis for the mixing of η and $\eta\prime$. So we divide the amplitudes into the $\eta_n = (\bar{u}u + \bar{d}d)/\sqrt{2}$ and $\bar{s}s$ component.

$$
\begin{aligned}
\sqrt{2} A(\bar{B}_s^0 \to \eta_n K^0) = {}& \frac{G_F}{\sqrt{2}} V_{ub} V_{ud}^* \Big\{ f_n F_{B_s \to K}^{LL}\, [a_2] + M_{B_s \to K}^{LL}[C_2] \Big\} \\
& - \frac{G_F}{\sqrt{2}} V_{tb} V_{td}^* \Big\{ f_n F_{B_s \to K}^{SP} \Big[a_6 - \frac{1}{2} a_8 \Big] + f_{B_s} F_{ann}^{LL} \Big[a_4 - \frac{1}{2} a_{10} \Big] \\
& + f_n F_{B_s \to K}^{LL} \Big[2a_3 + a_4 - 2a_5 - \frac{1}{2} a_7 + \frac{1}{2} a_9 - \frac{1}{2} a_{10} \Big] \\
& + M_{B_s \to K}^{LL} \Big[C_3 + 2C_4 + 2C_6 + \frac{1}{2} C_8 - \frac{1}{2} C_9 + \frac{1}{2} C_{10} \Big] \\
& + f_{B_s} F_{ann}^{SP} \Big[a_6 - \frac{1}{2} a_8 \Big] + M_{ann}^{LL} \Big[C_3 - \frac{1}{2} C_9 \Big] + M_{ann}^{LR} \Big[C_5 - \frac{1}{2} C_7 \Big] \Big\},
\end{aligned}
\tag{B7}
$$

$$A(\bar{B}_s^0 \to K^0 \eta_s) = -\frac{G_F}{\sqrt{2}} V_{tb} V_{td}^* \left\{ f_s F_{B_s \to K}^{LL} \left[a_3 - a_5 + \frac{1}{2}a_7 - \frac{1}{2}a_9 \right] + f_K F_{B_s \to \eta_s}^{LL} \left[a_4 - \frac{1}{2}a_{10} \right] \right.$$

$$+ f_K F_{B_s \to \eta_s}^{SP} \left[a_6 - \frac{1}{2}a_8 \right] + M_{B_s \to K}^{LL} \left[C_4 + C_6 - \frac{1}{2}C_8 - \frac{1}{2}C_{10} \right]$$

$$+ M_{B_s \to \eta_s}^{LL} \left[C_3 - \frac{1}{2}C_9 \right] + M_{B_s \to \eta_s}^{LR} \left[C_5 - \frac{1}{2}C_7 \right] + f_{B_s} F_{ann}^{LL} \left[a_4 - \frac{1}{2}a_{10} \right]$$

$$\left. + f_{B_s} F_{ann}^{SP} \left[a_6 - \frac{1}{2}a_8 \right] + M_{ann}^{LL} \left[C_3 - \frac{1}{2}C_9 \right] + M_{ann}^{LR} \left[C_5 - \frac{1}{2}C_7 \right] \right\}. \tag{B8}$$

The decay amplitudes for the physical states are then

$$A(\bar{B}_s \to \eta K^0) = A(\bar{B}_s^0 \to \eta_n K^0) \cos\phi - A(\bar{B}_s^0 \to K^0 \eta_s) \sin\phi, \tag{B9}$$

$$A(\bar{B}_s \to \eta' K^0) = A(\bar{B}_s^0 \to \eta_n K^0) \sin\phi + A(\bar{B}_s^0 \to K^0 \eta_s) \cos\phi. \tag{B10}$$

For $\bar{B}_s \to \eta^{(\prime)} \pi^0$ the decay amplitudes are defined similarly,

$$A(\bar{B}_s \to \pi^0 \eta) = A(\bar{B}_s^0 \to \pi^0 \eta_n) \cos\phi - A(\bar{B}_s^0 \to \pi^0 \eta_s) \sin\phi, \tag{B11}$$

$$A(\bar{B}_s \to \pi^0 \eta') = A(\bar{B}_s^0 \to \pi^0 \eta_n) \sin\phi + A(\bar{B}_s^0 \to \pi^0 \eta_s) \cos\phi, \tag{B12}$$

where

$$A(\bar{B}_s^0 \to \pi^0 \eta_n) = \frac{G_F}{\sqrt{2}} V_{ub} V_{us}^* \left\{ f_{B_s} F_{ann}^{LL} [a_2] + M_{ann}^{LL} [C_2] \right\}$$

$$- \frac{G_F}{\sqrt{2}} V_{tb} V_{ts}^* \left\{ f_{B_s} F_{ann}^{LL} \left[\frac{3}{2}a_9 + \frac{3}{2}a_7 \right] + M_{ann}^{SP} \left[\frac{3}{2}C_8 \right] + M_{ann}^{LL} \left[\frac{3}{2}C_{10} \right] \right\}, \tag{B13}$$

and

$$\sqrt{2} A(\bar{B}_s^0 \to \pi^0 \eta_s) = \frac{G_F}{\sqrt{2}} V_{ub} V_{us}^* \left\{ f_\pi F_{B_s \to \eta_s}^{LL} [a_2] + M_{B_s \to \eta_s}^{LL} [C_2] \right\}$$

$$- \frac{G_F}{\sqrt{2}} V_{tb} V_{ts}^* \left\{ f_\pi F_{B_s \to \eta_s}^{LL} \left[\frac{3}{2}a_9 - \frac{3}{2}a_7 \right] + M_{B_s \to \eta_s}^{LL} \left[\frac{3}{2}C_8 + \frac{3}{2}C_{10} \right] \right\}. \tag{B14}$$

For $\bar{B}_s \to \eta^{(\prime)}\eta^{(\prime)}$, we have

$$A(\bar{B}_s^0 \to \eta_n\eta_n) = \frac{G_F}{\sqrt{2}}V_{ub}V_{us}^* M_{ann}^{LL}[C_2] - \frac{G_F}{\sqrt{2}}V_{tb}V_{ts}^* M_{ann}^{LL}\left[2C_4 + 2C_6 + \frac{1}{2}C_8 + \frac{1}{2}C_{10}\right], \quad \text{(B15)}$$

$$\sqrt{2}A(\bar{B}_s^0 \to \eta_n\eta_s) = \frac{G_F}{\sqrt{2}}V_{ub}V_{us}^*\left\{f_n F_{B_s\to\eta_s}^{LL}[a_2] + M_{B_s\to\eta_s}^{LL}[C_2]\right\}$$
$$- \frac{G_F}{\sqrt{2}}V_{tb}V_{ts}^*\left\{f_n F_{B_s\to\eta_s}^{LL}\left[2a_3 - 2a_5 - \frac{1}{2}a_7 + \frac{1}{2}a_9\right]\right.$$
$$\left. + M_{B_s\to\eta_s}^{LL}\left[2C_4 + 2C_6 + \frac{1}{2}C_8 + \frac{1}{2}C_{10}\right]\right\}, \quad \text{(B16)}$$

$$A(\bar{B}_s^0 \to \eta_s\eta_s) = -\sqrt{2}G_F V_{tb}V_{ts}^*\left\{f_s F_{B_s\to\eta_s}^{LL}\left[a_3 + a_4 - a_5 + \frac{1}{2}a_7 - \frac{1}{2}a_9 - \frac{1}{2}a_{10}\right]\right.$$
$$+ f_s F_{B_s\to\eta_s}^{SP}\left[a_6 - \frac{1}{2}a_8\right] + M_{B_s\to\eta_s}^{LL}\left[C_3 + C_4 + C_6 - \frac{1}{2}C_8 - \frac{1}{2}C_9 - \frac{1}{2}C_{10}\right]$$
$$+ f_{B_s} F_{ann}^{SP}\left[a_6 - \frac{1}{2}a_8\right] + M_{ann}^{LL}\left[C_3 + C_4 + C_6 - \frac{1}{2}C_8 - \frac{1}{2}C_9 - \frac{1}{2}C_{10}\right]\right\}(\text{B17})$$

The decay amplitudes for the physical states are then

$$\sqrt{2}A(\bar{B}_s \to \eta\eta) = A(\bar{B}_s^0 \to \eta_n\eta_n)\cos^2\phi + A(\bar{B}_s^0 \to \eta_s\eta_s)\sin^2\phi - \sin(2\phi)A(\bar{B}_s^0 \to \eta_n\eta_s)(\text{B18})$$

$$A(\bar{B}_s \to \eta\eta') = \left[A(\bar{B}_s^0 \to \eta_n\eta_n) - A(\bar{B}_s^0 \to \eta_s\eta_s)\right]\cos\phi\sin\phi + A(\bar{B}_s^0 \to \eta_n\eta_s)\cos(2\phi)(\text{B19})$$

$$\sqrt{2}A(\bar{B}_s \to \eta'\eta') = A(\bar{B}_s^0 \to \eta_n\eta_n)\sin^2\phi + A(\bar{B}_s^0 \to \eta_s\eta_s)\cos^2\phi + \sin(2\phi)A(\bar{B}_s^0 \to \eta_n\eta_s)(\text{B20})$$

APPENDIX C: ANALYTIC FORMULAE FOR THE $B_s \to PV$ DECAY AMPLITUDES

1. The tree dominant decays

$$A(\bar{B}_s^0 \to \pi^- K^{*+}) = \frac{G_F}{\sqrt{2}}V_{ub}V_{ud}^*\left\{f_\pi F_{B_s\to K^*}^{LL}[a_1] + M_{B_s\to K^*}^{LL}[C_1]\right\}$$
$$- \frac{G_F}{\sqrt{2}}V_{tb}V_{td}^*\left\{f_\pi F_{B_s\to K^*}^{LL}[a_4 + a_{10}] - f_\pi F_{B_s\to K^*}^{SP}[a_6 + a_8]\right.$$
$$+ M_{B_s\to K^*}^{LL}[C_3 + C_9] + f_{B_s}F_{ann}^{LL}\left[a_4 - \frac{1}{2}a_{10}\right] - f_{B_s}F_{ann}^{SP}\left[a_6 - \frac{1}{2}a_8\right]$$
$$\left. + M_{ann}^{LL}\left[C_3 - \frac{1}{2}C_9\right] - M_{ann}^{LR}\left[C_5 - \frac{1}{2}C_7\right]\right\}, \quad \text{(C1)}$$

$$A(\bar{B}_s^0 \to \rho^- K^+) = \frac{G_F}{\sqrt{2}} V_{ub} V_{ud}^* \left\{ f_\rho F_{B_s \to K}^{LL} [a_1] + M_{B_s \to K}^{LL} [C_1] \right\}$$

$$- \frac{G_F}{\sqrt{2}} V_{tb} V_{td}^* \left\{ f_\rho F_{B_s \to K}^{LL} [a_4 + a_{10}] + M_{B_s \to K}^{LL} [C_3 + C_9] \right.$$

$$+ M_{B_s \to K}^{LR} [C_5 + C_7] + f_{B_s} F_{ann}^{LL} \left[a_4 - \frac{1}{2} a_{10} \right] + f_{B_s} F_{ann}^{SP} \left[a_6 - \frac{1}{2} a_8 \right]$$

$$\left. + M_{ann}^{LL} \left[C_3 - \frac{1}{2} C_9 \right] + M_{ann}^{LR} \left[C_5 - \frac{1}{2} C_7 \right] \right\}, \tag{C2}$$

$$\sqrt{2} A(\bar{B}_s^0 \to \pi^0 K^{*0}) = \frac{G_F}{\sqrt{2}} V_{ub} V_{ud}^* \left\{ f_\pi F_{B_s \to K^*}^{LL} [a_2] + M_{B_s \to K^*}^{LL} [C_2] \right\}$$

$$- \frac{G_F}{\sqrt{2}} V_{tb} V_{td}^* \left\{ f_\pi F_{B_s \to K^*}^{LL} \left[-a_4 - \frac{3}{2} a_7 + \frac{1}{2} a_{10} + \frac{3}{2} a_9 \right] \right.$$

$$- f_\pi F_{B_s \to K^*}^{SP} \left[-a_6 + \frac{1}{2} a_8 \right] + M_{B_s \to K^*}^{LL} \left[-C_3 + \frac{3}{2} C_8 + \frac{1}{2} C_9 + \frac{3}{2} C_{10} \right]$$

$$+ f_{B_s} F_{ann}^{LL} \left[-a_4 + \frac{1}{2} a_{10} \right] - f_{B_s} F_{ann}^{SP} \left[-a_6 + \frac{1}{2} a_8 \right]$$

$$\left. + M_{ann}^{LL} \left[-C_3 + \frac{1}{2} C_9 \right] - M_{ann}^{LR} \left[-C_5 + \frac{1}{2} C_7 \right] \right\}, \tag{C3}$$

$$\sqrt{2} A(\bar{B}_s^0 \to \rho^0 K^0) = \frac{G_F}{\sqrt{2}} V_{ub} V_{ud}^* \left\{ f_\rho F_{B_s \to K}^{LL} [a_2] + M_{B_s \to K}^{LL} [C_2] \right\}$$

$$- \frac{G_F}{\sqrt{2}} V_{tb} V_{td}^* \left\{ f_\rho F_{B_s \to K}^{LL} \left[-a_4 + \frac{3}{2} a_7 + \frac{1}{2} a_{10} + \frac{3}{2} a_9 \right] + M_{B_s \to K}^{LR} \left[-C_5 + \frac{1}{2} C_7 \right] \right.$$

$$+ M_{B_s \to K}^{LL} \left[-C_3 + \frac{1}{2} C_9 + \frac{3}{2} C_{10} \right] - M_{B_s \to K}^{SP} \left[\frac{3}{2} C_8 \right] + f_{B_s} F_{ann}^{LL} \left[-a_4 + \frac{1}{2} a_{10} \right]$$

$$\left. + f_{B_s} F_{ann}^{SP} \left[-a_6 + \frac{1}{2} a_8 \right] + M_{ann}^{LL} \left[-C_3 + \frac{1}{2} C_9 \right] + M_{ann}^{LR} \left[-C_5 + \frac{1}{2} C_7 \right] \right\} \tag{C4}$$

$$\sqrt{2}A(\bar{B}^0_s \to \omega K^0) = \frac{G_F}{\sqrt{2}}V_{ub}V_{ud}^* \left\{ f_\omega F^{LL}_{B_s \to K}\left[a_2\right] + M^{LL}_{B_s \to K}[C_2] \right\}$$

$$- \frac{G_F}{\sqrt{2}}V_{tb}V_{td}^* \left\{ f_\omega F^{LL}_{B_s \to K}\left[2a_3 + a_4 + 2a_5 + \frac{1}{2}a_7 + \frac{1}{2}a_9 - \frac{1}{2}a_{10}\right] \right.$$

$$+ M^{LL}_{B_s \to K}\left[C_3 + 2C_4 - \frac{1}{2}C_9 + \frac{1}{2}C_{10}\right] + M^{LR}_{B_s \to K}\left[C_5 - \frac{1}{2}C_7\right]$$

$$- M^{SP}_{B_s \to K}\left[2C_6 + \frac{1}{2}C_8\right] + f_{B_s}F^{LL}_{ann}\left[a_4 - \frac{1}{2}a_{10}\right] + f_{B_s}F^{SP}_{ann}\left[a_6 - \frac{1}{2}a_8\right]$$

$$\left. + M^{LL}_{ann}\left[C_3 - \frac{1}{2}C_9\right] + M^{LR}_{ann}\left[C_5 - \frac{1}{2}C_7\right] \right\}, \tag{C5}$$

2. The pure annihilation type decays

$$A(\bar{B}^0_s \to \pi^+\rho^-) = \frac{G_F}{\sqrt{2}}V_{ub}V_{us}^* \left\{ f_{B_s}F^{LL}_{ann}\left[a_2\right] + M^{LL}_{ann}[C_2] \right\} - \frac{G_F}{\sqrt{2}}V_{tb}V_{ts}^* \left\{ f_{B_s}F^{LL}_{ann}\left[a_3 + a_9\right] \right.$$

$$\left. - f_{B_s}F^{LR}_{ann}\left[a_5 + a_7\right] + M^{LL}_{ann}\left[C_4 + C_{10}\right] - M^{SP}_{ann}\left[C_6 + C_8\right] + [\pi^+ \leftrightarrow \rho^-] \right\}, \tag{C6}$$

$$A(\bar{B}^0_s \to \rho^+\pi^-) = \frac{G_F}{\sqrt{2}}V_{ub}V_{us}^* \left\{ f_{B_s}F^{LL}_{ann}\left[a_2\right] + M^{LL}_{ann}[C_2] \right\} - \frac{G_F}{\sqrt{2}}V_{tb}V_{ts}^* \left\{ f_{B_s}F^{LL}_{ann}\left[a_3 + a_9\right] \right.$$

$$\left. - f_{B_s}F^{LR}_{ann}\left[a_5 + a_7\right] + M^{LL}_{ann}\left[C_4 + C_{10}\right] - M^{SP}_{ann}\left[C_6 + C_8\right] + [\rho^+ \leftrightarrow \pi^-] \right\}, \tag{C7}$$

$$2A(\bar{B}^0_s \to \pi^0\rho^0) = A(\bar{B}^0_s \to \pi^+\rho^-) + A(\bar{B}^0_s \to \rho^+\pi^-), \tag{C8}$$

$$2A(\bar{B}^0_s \to \pi^0\omega) = \frac{G_F}{\sqrt{2}}V_{ub}V_{us}^* \left\{ M^{LL}_{ann}[C_2] \right\} - \frac{G_F}{\sqrt{2}}V_{tb}V_{ts}^* \left\{ M^{LL}_{ann}\left[\frac{3}{2}C_{10}\right] - M^{SP}_{ann}\left[\frac{3}{2}C_8\right] + [\pi^0 \leftrightarrow \omega] \right\} \tag{C9}$$

3. The QCD penguin dominant decays

$$A(\bar{B}_s^0 \to K^- K^{*+}) = \frac{G_F}{\sqrt{2}} V_{ub} V_{us}^* \Big\{ f_K F_{B_s \to K^*}^{LL} [a_1] + M_{B_s \to K^*}^{LL} [C_1] + f_{B_s} F_{ann}^{LL} [a_2] + M_{ann}^{LL} [C_2] \Big\}$$

$$- \frac{G_F}{\sqrt{2}} V_{tb} V_{ts}^* \Big\{ f_K F_{B_s \to K^*}^{LL} [a_4 + a_{10}] - f_K F_{B_s \to K^*}^{SP} [a_6 + a_8]$$

$$+ M_{B_s \to K^*}^{LL} [C_3 + C_9] + f_B F_{ann}^{LL} \Big[a_3 + a_4 - a_5 + \frac{1}{2} a_7 - \frac{1}{2} a_9 - \frac{1}{2} a_{10} \Big]$$

$$- M_{ann}^{LR} \Big[C_5 - \frac{1}{2} C_7 \Big] + f_{B_s} F_{ann}^{LL} [a_3 - a_5 - a_7 + a_9]_{K^* \leftrightarrow K}$$

$$- M_{B_s \to K^*}^{LR} [C_5 + C_7] - f_{B_s} F_{ann}^{SP} \Big[a_6 - \frac{1}{2} a_8 \Big]$$

$$+ M_{ann}^{LL} \Big[C_3 - \frac{1}{2} C_9 + C_4 - \frac{1}{2} C_{10} \Big] - M_{ann}^{SP} \Big[C_6 - \frac{1}{2} C_8 \Big]$$

$$+ M_{ann}^{LL} [C_4 + C_{10}]_{K^* \leftrightarrow K} - M_{ann}^{SP} [C_6 + C_8]_{K^* \leftrightarrow K} \Big\}, \tag{C10}$$

$$A(\bar{B}_s^0 \to K^{*-} K^+) = \frac{G_F}{\sqrt{2}} V_{ub} V_{us}^* \Big\{ f_{K^*} F_{B_s \to K}^{LL} [a_1] + M_{B_s \to K^*}^{LL} [C_1] + f_{B_s} F_{ann}^{LL} [a_2] + M_{ann}^{LL} [C_2] \Big\}$$

$$- \frac{G_F}{\sqrt{2}} V_{tb} V_{ts}^* \Big\{ f_{K^*} F_{B_s \to K}^{LL} [a_4 + a_{10}] + M_{B_s \to K}^{LL} [C_3 + C_9] + M_{B_s \to K}^{LR} [C_5 + C_7]$$

$$+ f_B F_{ann}^{LL} \Big[a_3 + a_4 - a_5 + \frac{1}{2} a_7 - \frac{1}{2} a_9 - \frac{1}{2} a_{10} \Big] + f_{B_s} F_{ann}^{SP} \Big[a_6 - \frac{1}{2} a_8 \Big]$$

$$+ f_{B_s} F_{ann}^{LL} [a_3 - a_5 - a_7 + a_9]_{K^* \leftrightarrow K} + M_{ann}^{LR} \Big[C_5 - \frac{1}{2} C_7 \Big]$$

$$+ M_{ann}^{LL} \Big[C_3 - \frac{1}{2} C_9 + C_4 - \frac{1}{2} C_{10} \Big] - M_{ann}^{SP} \Big[C_6 - \frac{1}{2} C_8 \Big]$$

$$+ M_{ann}^{LL} [C_4 + C_{10}]_{K^* \leftrightarrow K} - M_{ann}^{SP} [C_6 + C_8]_{K^* \leftrightarrow K} \Big\}, \tag{C11}$$

$$A(\bar{B}_s^0 \to \bar{K}^0 K^{*0}) = -\frac{G_F}{\sqrt{2}} V_{tb} V_{ts}^* \left\{ f_K F_{B_s \to K^*}^{LL} \left[a_4 - \frac{1}{2} a_{10} \right] - f_K F_{B_s \to K^*}^{SP} \left[a_6 - \frac{1}{2} a_8 \right] \right.$$

$$+ M_{B_s \to K^*}^{LL} \left[C_3 - \frac{1}{2} C_9 \right] + f_{B_s} F_{ann}^{LL} \left[a_3 + a_4 - a_5 + \frac{1}{2} a_7 - \frac{1}{2} a_9 - \frac{1}{2} a_{10} \right]$$

$$- M_{B_s \to K^*}^{LR} \left[C_5 - \frac{1}{2} C_7 \right] - f_{B_s} F_{ann}^{SP} \left[a_6 - \frac{1}{2} a_8 \right]$$

$$+ M_{ann}^{LL} \left[C_3 - \frac{1}{2} C_9 + C_4 - \frac{1}{2} C_{10} \right] + M_{ann}^{LL} \left[C_4 - \frac{1}{2} C_{10} \right]_{K^* \leftrightarrow K}$$

$$- M_{ann}^{LR} \left[C_5 - \frac{1}{2} C_7 \right] - \left(M_{ann}^{SP} \left[C_6 - \frac{1}{2} C_8 \right] + [K^* \leftrightarrow K] \right)$$

$$\left. + f_{B_s} F_{ann}^{LL} \left[a_3 - a_5 + \frac{1}{2} a_7 - \frac{1}{2} a_9 \right]_{K^* \leftrightarrow K} \right\}, \tag{C12}$$

$$A(\bar{B}_s^0 \to \bar{K}^{*0} K^0) = -\frac{G_F}{\sqrt{2}} V_{tb} V_{ts}^* \left\{ f_{K^*} F_{B_s \to K}^{LL} \left[a_4 - \frac{1}{2} a_{10} \right] + M_{B_s \to K}^{LL} \left[C_3 - \frac{1}{2} C_9 \right] \right.$$

$$+ M_{B_s \to K}^{LR} \left[C_5 - \frac{1}{2} C_7 \right] + f_{B_s} F_{ann}^{LL} \left[a_3 + a_4 - a_5 + \frac{1}{2} a_7 - \frac{1}{2} a_9 - \frac{1}{2} a_{10} \right]$$

$$+ f_{B_s} F_{ann}^{SP} \left[a_6 - \frac{1}{2} a_8 \right] + M_{ann}^{LL} \left[C_3 - \frac{1}{2} C_9 + C_4 - \frac{1}{2} C_{10} \right]$$

$$+ M_{ann}^{LR} \left[C_5 - \frac{1}{2} C_7 \right] - \left(M_{ann}^{SP} \left[C_6 - \frac{1}{2} C_8 \right] + [K^* \leftrightarrow K] \right) \tag{C13}$$

$$\left. + f_{B_s} F_{ann}^{LL} \left[a_3 - a_5 + \frac{1}{2} a_7 - \frac{1}{2} a_9 \right]_{K^* \leftrightarrow K} + M_{ann}^{LL} \left[C_4 - \frac{1}{2} C_{10} \right]_{K^* \leftrightarrow K} \right\}.$$

$$A(\bar{B}_s^0 \to K^0 \phi) = -\frac{G_F}{\sqrt{2}} V_{tb} V_{td}^* \left\{ f_\phi F_{B_s \to K}^{LL} \left[a_3 + a_5 - \frac{1}{2} a_7 - \frac{1}{2} a_9 \right] + f_K F_{B_s \to \phi}^{LL} \left[a_4 - \frac{1}{2} a_{10} \right] \right.$$

$$- f_K F_{B_s \to \phi}^{SP} \left[a_6 - \frac{1}{2} a_8 \right] + M_{B_s \to K}^{LL} \left[C_4 - \frac{1}{2} C_{10} \right] + M_{B_s \to \phi}^{LL} \left[C_3 - \frac{1}{2} C_9 \right]$$

$$- M_{B_s \to K}^{SP} \left[C_6 - \frac{1}{2} C_8 \right] - M_{B_s \to \phi}^{LR} \left[C_5 - \frac{1}{2} C_7 \right] + f_{B_s} F_{ann}^{LL} \left[a_4 - \frac{1}{2} a_{10} \right]$$

$$\left. - f_{B_s} F_{ann}^{SP} \left[a_6 - \frac{1}{2} a_8 \right] + M_{ann}^{LL} \left[C_3 - \frac{1}{2} C_9 \right] - M_{ann}^{LR} \left[C_5 - \frac{1}{2} C_7 \right] \right\}. \tag{C14}$$

4. The Electroweak penguin dominant decays

$$\sqrt{2}A(\bar{B}_s^0 \to \pi^0\phi) = \frac{G_F}{\sqrt{2}}V_{ub}V_{us}^* \left\{ f_\pi F_{B_s\to\phi}^{LL}[a_2] + M_{B_s\to\phi}^{LL}[C_2] \right\}$$
$$-\frac{G_F}{\sqrt{2}}V_{tb}V_{ts}^* \left\{ f_\pi F_{B_s\to\phi}^{LL}\left[\frac{3}{2}a_9 - \frac{3}{2}a_7\right] + M_{B_s\to\phi}^{LL}\left[\frac{3}{2}C_8 + \frac{3}{2}C_{10}\right] \right\}. \quad (C15)$$

5. The decays involving η and η'

$$\sqrt{2}A(\bar{B}_s^0 \to \eta_n K^{*0}) = \frac{G_F}{\sqrt{2}}V_{ub}V_{ud}^* \left\{ f_n F_{B_s\to K^*}^{LL}[a_2] + M_{B_s\to K^*}^{LL}[C_2] \right\}$$
$$-\frac{G_F}{\sqrt{2}}V_{tb}V_{td}^* \left\{ f_n F_{B_s\to K^*}^{LL}\left[2a_3 + a_4 - 2a_5 - \frac{1}{2}a_7 + \frac{1}{2}a_9 - \frac{1}{2}a_{10}\right] \right.$$
$$-f_n F_{B_s\to K^*}^{SP}\left[a_6 - \frac{1}{2}a_8\right] + M_{B_s\to K^*}^{LL}\left[C_3 + 2C_4 - \frac{1}{2}C_9 + \frac{1}{2}C_{10}\right]$$
$$+M_{B_s\to K^*}^{SP}\left[2C_6 + \frac{1}{2}C_8\right] + f_{B_s}F_{ann}^{LL}\left[a_4 - \frac{1}{2}a_{10}\right] + f_{B_s}F_{ann}^{SP}\left[a_6 - \frac{1}{2}a_8\right]$$
$$\left. +M_{ann}^{LL}\left[C_3 - \frac{1}{2}C_9\right] + M_{ann}^{LR}\left[C_5 - \frac{1}{2}C_7\right] \right\}, \quad (C16)$$

$$A(\bar{B}_s^0 \to K^{*0}\eta_s) = -\frac{G_F}{\sqrt{2}}V_{tb}V_{td}^* \left\{ f_s F_{B_s\to K^*}^{LL}\left[a_3 - a_5 + \frac{1}{2}a_7 - \frac{1}{2}a_9\right] + f_{K^*}F_{B_s\to\eta_s}^{LL}\left[a_4 - \frac{1}{2}a_{10}\right] \right.$$
$$+M_{B_s\to K^*}^{LL}\left[C_4 - \frac{1}{2}C_{10}\right] + M_{B_s\to\eta_s}^{LL}\left[C_3 - \frac{1}{2}C_9\right]$$
$$+M_{B_s\to K^*}^{SP}\left[C_6 - \frac{1}{2}C_8\right] + M_{B_s\to\eta_s}^{LR}\left[C_5 - \frac{1}{2}C_7\right] + f_{B_s}F_{ann}^{LL}\left[a_4 - \frac{1}{2}a_{10}\right]$$
$$\left. +f_{B_s}F_{ann}^{SP}\left[a_6 - \frac{1}{2}a_8\right] + M_{ann}^{LL}\left[C_3 - \frac{1}{2}C_9\right] + M_{ann}^{LR}\left[C_5 - \frac{1}{2}C_7\right] \right\}. \quad (C17)$$

The decay amplitudes for the physical states are then

$$A(\bar{B}_s \to \eta K^{*0}) = A(\bar{B}_s^0 \to \eta_n K^{*0})\cos\phi - A(\bar{B}_s^0 \to \eta_s K^{*0})\sin\phi, \quad (C18)$$
$$A(\bar{B}_s \to \eta' K^{*0}) = A(\bar{B}_s^0 \to \eta_n K^{*0})\sin\phi + A(\bar{B}_s^0 \to \eta_s K^{*0})\cos\phi. \quad (C19)$$

For $\bar{B}_s \to \eta^{(\prime)}\rho^0$ the decay amplitudes are defined similarly,

$$A(\bar{B}_s \to \rho^0\eta) = A(\bar{B}_s^0 \to \rho^0\eta_n)\cos\phi - A(\bar{B}_s^0 \to \rho^0\eta_s)\sin\phi, \quad (C20)$$
$$A(\bar{B}_s \to \rho^0\eta') = A(\bar{B}_s^0 \to \rho^0\eta_n)\sin\phi + A(\bar{B}_s^0 \to \rho^0\eta_s)\cos\phi, \quad (C21)$$

where

$$2A(\bar{B}_s^0 \to \rho^0 \eta_n) = -\frac{G_F}{\sqrt{2}} V_{tb} V_{ts}^* \left\{ f_{B_s} F_{ann}^{LL} \left[\frac{3}{2} a_9 - \frac{3}{2} a_7 \right] + M_{ann}^{LL} \left[\frac{3}{2} C_{10} \right] - M_{ann}^{SP} \left[\frac{3}{2} C_8 \right] \right\}$$
$$+ \frac{G_F}{\sqrt{2}} V_{ub} V_{us}^* \left\{ f_{B_s} F_{ann}^{LL} [a_2] + M_{ann}^{LL} [C_2] \right\} + \left[\rho^0 \leftrightarrow \eta_n \right], \tag{C22}$$

and

$$\sqrt{2} A(\bar{B}_s^0 \to \rho^0 \eta_s) = \frac{G_F}{\sqrt{2}} V_{ub} V_{us}^* \left\{ f_\rho F_{B_s \to \eta_s}^{LL} [a_2] + M_{B_s \to \eta_s}^{LL} [C_2] \right\} \tag{C23}$$
$$- \frac{G_F}{\sqrt{2}} V_{tb} V_{ts}^* \left\{ f_\rho F_{B_s \to \eta_s}^{LL} \left[\frac{3}{2} a_7 + \frac{3}{2} a_9 \right] + M_{B_s \to \eta_s}^{LL} \left[\frac{3}{2} C_{10} \right] - M_{B_s \to \eta_s}^{SP} \left[\frac{3}{2} C_8 \right] \right\}.$$

For decays $\bar{B}_s \to \eta^{(\prime)} \omega$, we have

$$2A(\bar{B}_s^0 \to \eta_n \omega) = \frac{G_F}{\sqrt{2}} V_{ub} V_{us}^* \left\{ f_{B_s} F_{ann}^{LL} [a_2] + M_{ann}^{LL} [C_2] \right\}$$
$$- \frac{G_F}{\sqrt{2}} V_{tb} V_{ts}^* \left\{ M_{ann}^{LL} \left[2 C_4 + \frac{1}{2} C_{10} \right] - M_{ann}^{SP} \left[2 C_6 + \frac{1}{2} C_8 \right] \right.$$
$$\left. + f_{B_s} F_{ann}^{LL} \left[2 a_3 - 2 a_5 - \frac{1}{2} a_7 + \frac{1}{2} a_9 \right] \right\} + [\eta_n \leftrightarrow \omega], \tag{C24}$$

$$\sqrt{2} A(\bar{B}_s^0 \to \omega \eta_s) = \frac{G_F}{\sqrt{2}} V_{ub} V_{us}^* \left\{ f_\omega F_{B_s \to \eta_s}^{LL} [a_2] + M_{B_s \to \eta_s}^{LL} [C_2] \right\}$$
$$- \frac{G_F}{\sqrt{2}} V_{tb} V_{ts}^* \left\{ f_\omega F_{B_s \to \eta_s}^{LL} \left[2 a_3 + 2 a_5 + \frac{1}{2} a_7 + \frac{1}{2} a_9 \right] \right.$$
$$\left. + M_{B_s \to \eta_s}^{LL} \left[2 C_4 + \frac{1}{2} C_{10} \right] - M_{B_s \to \eta_s}^{SP} \left[2 C_6 + \frac{1}{2} C_8 \right] \right\}. \tag{C25}$$

And the decay amplitudes for physical states are

$$A(\bar{B}_s \to \eta \omega) = A(\bar{B}_s^0 \to \eta_n \omega) \cos \phi - A(\bar{B}_s^0 \to \omega \eta_s) \sin \phi, \tag{C26}$$
$$A(\bar{B}_s \to \eta' \omega) = A(\bar{B}_s^0 \to \eta_n \omega) \sin \phi + A(\bar{B}_s^0 \to \omega \eta_s) \cos \phi. \tag{C27}$$

For decays $\bar{B}_s \to \eta\phi$, we have

$$\sqrt{2}A(\bar{B}_s^0 \to \eta_n\phi) = \frac{G_F}{\sqrt{2}}V_{ub}V_{us}^* \left\{ f_n F_{B_s\to\phi}^{LL}[a_2] + M_{B_s\to\phi}^{LL}[C_2] \right\}$$
$$- \frac{G_F}{\sqrt{2}}V_{tb}V_{ts}^* \left\{ f_n F_{B_s\to\phi}^{LL}\left[2a_3 - 2a_5 - \frac{1}{2}a_7 + \frac{1}{2}a_9\right] \right.$$
$$\left. + M_{B_s\to\phi}^{LL}\left[2C_4 + \frac{1}{2}C_{10}\right] + M_{B_s\to\phi}^{SP}\left[2C_6 + \frac{1}{2}C_8\right] \right\}, \tag{C28}$$

$$A(\bar{B}_s^0 \to \eta_s\phi) = -\frac{G_F}{\sqrt{2}}V_{tb}V_{ts}^* \left\{ f_s F_{B_s\to\phi}^{LL}\left[a_3 + a_4 - a_5 + \frac{1}{2}a_7 - \frac{1}{2}a_9 - \frac{1}{2}a_{10}\right] \right.$$
$$- f_s F_{B_s\to\phi}^{SP}\left[a_6 - \frac{1}{2}a_8\right] + M_{B_s\to\phi}^{LL}\left[C_3 + C_4 - \frac{1}{2}C_9 - \frac{1}{2}C_{10}\right]$$
$$+ M_{B_s\to\phi}^{SP}\left[C_6 - \frac{1}{2}C_8\right] + f_{B_s} F_{ann}^{LL}\left[a_3 + a_4 - a_5 + \frac{1}{2}a_7 - \frac{1}{2}a_9 - \frac{1}{2}a_{10}\right]$$
$$+ M_{ann}^{LL}\left[C_3 + C_4 - \frac{1}{2}C_9 - \frac{1}{2}C_{10}\right] - f_{B_s} F_{ann}^{SP}\left[a_6 - \frac{1}{2}a_8\right]$$
$$\left. - M_{ann}^{LR}\left[C_5 - \frac{1}{2}C_7\right] - M_{ann}^{SP}\left[C_6 - \frac{1}{2}C_8\right] \right\} + [\eta_s \leftrightarrow \phi]. \tag{C29}$$

And the decay amplitudes for physical states are

$$A(\bar{B}_s \to \eta\phi) = A(\bar{B}_s^0 \to \eta_n\phi)\cos\phi - A(\bar{B}_s^0 \to \eta_s\phi)\sin\phi, \tag{C30}$$

$$A(\bar{B}_s \to \eta'\phi) = A(\bar{B}_s^0 \to \eta_n\phi)\sin\phi + A(\bar{B}_s^0 \to \eta_s\phi)\cos\phi. \tag{C31}$$

APPENDIX D: ANALYTIC FORMULAE FOR THE $B_s \to VV$ DECAY AMPLITUDES

There are three kinds of polarizations in the B_s meson decays to two vector final states, namely: Longitudinal (L), parallel (N) and transverse (T). The decay amplitudes are classified accordingly, with $i = L, N, T$.

1. Tree dominant decays

$$
\begin{aligned}
A^i(\bar{B}_s^0 \to \rho^- K^{*+}) &= \frac{G_F}{\sqrt{2}} V_{ub} V_{ud}^* \Big\{ f_\rho F_{B_s \to K^*}^{LL,i}[a_1] + M_{B_s \to K^*}^{LL,i}[C_1] \Big\} \\
&\quad - \frac{G_F}{\sqrt{2}} V_{tb} V_{td}^* \Big\{ f_\rho F_{B_s \to K^*}^{LL,i}[a_4 + a_{10}] \\
&\quad + M_{B_s \to K^*}^{LL,i}[C_3 + C_9] - M_{B_s \to K^*}^{LR,i}[C_5 + C_7] \\
&\quad + f_{B_s} F_{ann}^{LL,i}\left[a_4 - \frac{1}{2}a_{10}\right] - f_{B_s} F_{ann}^{SP,i}\left[a_6 - \frac{1}{2}a_8\right] \\
&\quad + M_{ann}^{LL,i}\left[C_3 - \frac{1}{2}C_9\right] - M_{ann}^{LR,i}\left[C_5 - \frac{1}{2}C_7\right] \Big\},
\end{aligned}
\tag{D1}
$$

$$
\begin{aligned}
\sqrt{2} A^i(\bar{B}_s^0 \to \rho^0 K^{*0}) &= \frac{G_F}{\sqrt{2}} V_{ub} V_{ud}^* \Big\{ f_\rho F_{B_s \to K^*}^{LL,i}[a_2] + M_{B_s \to K^*}^{LL,i}[C_2] \Big\} \\
&\quad + \frac{G_F}{\sqrt{2}} V_{tb} V_{td}^* \Big\{ f_\rho F_{B_s \to K^*}^{LL,i}\left[-a_4 + \frac{3}{2}a_7 + \frac{3}{2}a_9 + \frac{1}{2}a_{10}\right] - M_{B_s \to K^*}^{LR,i}\left[-C_5 + \frac{1}{2}C_7\right] \\
&\quad + M_{B_s \to K^*}^{LL,i}\left[-C_3 + \frac{1}{2}C_9 + \frac{3}{2}C_{10}\right] - M_{B_s \to K^*}^{SP,i}\left[\frac{3}{2}C_8\right] \\
&\quad + f_{B_s} F_{ann}^{LL,i}\left[-a_4 + \frac{1}{2}a_{10}\right] - f_{B_s} F_{ann}^{SP,i}\left[-a_6 + \frac{1}{2}a_8\right] \\
&\quad + M_{ann}^{LL,i}\left[-C_3 + \frac{1}{2}C_9\right] - M_{ann}^{LR,i}\left[-C_5 + \frac{1}{2}C_7\right] \Big\},
\end{aligned}
\tag{D2}
$$

$$
\begin{aligned}
\sqrt{2} A^i(\bar{B}_s^0 \to \omega K^{*0}) &= \frac{G_F}{\sqrt{2}} V_{ub} V_{ud}^* \Big\{ f_\omega F_{B_s \to K^*}^{LL,i}[a_2] + M_{B_s \to K^*}^{LL,i}[C_2] \Big\} \\
&\quad - \frac{G_F}{\sqrt{2}} V_{tb} V_{td}^* \Big\{ f_\omega F_{B_s \to K^*}^{LL,i}\left[2a_3 + a_4 + 2a_5 + \frac{1}{2}a_7 + \frac{1}{2}a_9 - \frac{1}{2}a_{10}\right] \\
&\quad + M_{B_s \to K^*}^{LL,i}\left[C_3 + 2C_4 - \frac{1}{2}C_9 + \frac{1}{2}C_{10}\right] \\
&\quad - M_{B_s \to K^*}^{LR,i}\left[C_5 - \frac{1}{2}C_7\right] - M_{B_s \to K^*}^{SP,i}\left[2C_6 + \frac{1}{2}C_8\right] \\
&\quad + f_{B_s} F_{ann}^{LL,i}\left[a_4 - \frac{1}{2}a_{10}\right] - f_{B_s} F_{ann}^{SP,i}\left[a_6 - \frac{1}{2}a_8\right] \\
&\quad + M_{ann}^{LL,i}\left[C_3 - \frac{1}{2}C_9\right] - M_{ann}^{LR,i}\left[C_5 - \frac{1}{2}C_7\right] \Big\}.
\end{aligned}
\tag{D3}
$$

2. Pure annihilation type decays

$$
\begin{aligned}
A^i(\bar{B}_s^0 \to \rho^+\rho^-) &= \frac{G_F}{\sqrt{2}} V_{ub} V_{us}^* \left\{ f_{B_s} F_{ann}^{LL,i} \left[a_2\right] + M_{ann}^{LL,i}[C_2] \right\} \\
&\quad - \frac{G_F}{\sqrt{2}} V_{tb} V_{ts}^* \left\{ f_{B_s} F_{ann}^{LL,i} \left[2a_3 + \frac{1}{2}a_9\right] + f_{B_s} F_{ann}^{LR,i} \left[2a_5 + \frac{1}{2}a_7\right] \right. \\
&\quad \left. + M_{ann}^{LL,i} \left[2C_4 + \frac{1}{2}C_{10}\right] + M_{ann}^{SP,i} \left[2C_6 + \frac{1}{2}C_8\right] \right\},
\end{aligned}
\tag{D4}
$$

$$
\begin{aligned}
\sqrt{2}A^i(\bar{B}_s^0 \to \rho^0\rho^0) &= \frac{G_F}{\sqrt{2}} V_{ub} V_{us}^* \left\{ f_{B_s} F_{ann}^{LL,i} \left[a_2\right] + M_{ann}^{LL,i}[C_2] \right\} \\
&\quad - \frac{G_F}{\sqrt{2}} V_{tb} V_{ts}^* \left\{ f_{B_s} F_{ann}^{LL,i} \left[2a_3 + \frac{1}{2}a_9\right] + f_{B_s} F_{ann}^{LR,i} \left[2a_5 + \frac{1}{2}a_7\right] \right. \\
&\quad \left. + M_{ann}^{LL,i} \left[2C_4 + \frac{1}{2}C_{10}\right] + M_{ann}^{SP,i} \left[2C_6 + \frac{1}{2}C_8\right] \right\},
\end{aligned}
\tag{D5}
$$

$$
\begin{aligned}
\sqrt{2}A^i(\bar{B}_s^0 \to \omega\omega) &= \frac{G_F}{\sqrt{2}} V_{ub} V_{us}^* \left\{ f_{B_s} F_{ann}^{LL,i} \left[a_2\right] + M_{ann}^{LL,i}[C_2] \right\} \\
&\quad - \frac{G_F}{\sqrt{2}} V_{tb} V_{ts}^* \left\{ f_{B_s} F_{ann}^{LL,i} \left[2a_3 + \frac{1}{2}a_9\right] + f_{B_s} F_{ann}^{LR,i} \left[2a_5 + \frac{1}{2}a_7\right] \right. \\
&\quad \left. + M_{ann}^{LL,i} \left[2C_4 + \frac{1}{2}C_{10}\right] + M_{ann}^{SP,i} \left[2C_6 + \frac{1}{2}C_8\right] \right\},
\end{aligned}
\tag{D6}
$$

$$
\begin{aligned}
2A^i(\bar{B}_s^0 \to \rho^0\omega) &= \frac{G_F}{\sqrt{2}} V_{ub} V_{us}^* \left\{ f_{B_s} F_{ann}^{LL,i} \left[a_2\right] + M_{ann}^{LL,i}[C_2] \right\} - \frac{G_F}{\sqrt{2}} V_{tb} V_{ts}^* \left\{ f_{B_s} F_{ann}^{LL,i} \left[\frac{3}{2}a_9\right] \right. \\
&\quad \left. + f_{B_s} F_{ann}^{LR,i} \left[\frac{3}{2}a_7\right] + M_{ann}^{LL,i} \left[\frac{3}{2}C_{10}\right] + M_{ann}^{SP,i} \left[\frac{3}{2}C_8\right] \right\} + \left[\rho^0 \leftrightarrow \omega\right].
\end{aligned}
\tag{D7}
$$

3. QCD penguin dominant decays

$$
\begin{aligned}
A^i(\bar{B}_s^0 \to K^{*-}K^{*+}) = & \frac{G_F}{\sqrt{2}} V_{ub} V_{us}^* \left\{ f_{K^*} F_{B_s \to K^*}^{LL,i} [a_1] + M_{B_s \to K^*}^{LL,i} [C_1] + f_{B_s} F_{ann}^{LL,i} [a_2] \right. \\
& \left. + M_{ann}^{LL,i} [C_2] \right\} - \frac{G_F}{\sqrt{2}} V_{tb} V_{ts}^* \left\{ f_{K^*} F_{B_s \to K^*}^{LL,i} [a_4 + a_{10}] \right. \\
& + M_{B_s \to K^*}^{LL,i} [C_3 + C_9] - M_{B_s \to K}^{LR,i} [C_5 + C_7] \\
& + f_{B_s} F_{ann}^{LL,i} \left[a_3 + a_4 - \frac{1}{2} a_9 - \frac{1}{2} a_{10} \right] + f_{B_s} F_{ann}^{LR,i} \left[a_5 - \frac{1}{2} a_7 \right] \\
& - f_{B_s} F_{ann}^{SP,i} \left[a_6 - \frac{1}{2} a_8 \right] + M_{ann}^{LL,i} \left[C_3 - \frac{1}{2} C_9 + C_4 - \frac{1}{2} C_{10} \right] \\
& - M_{ann}^{LR,i} \left[C_5 - \frac{1}{2} C_7 \right] + M_{ann}^{SP,i} \left[C_6 - \frac{1}{2} C_8 \right] \\
& + \left(f_{B_s} F_{ann}^{LL,i} [a_3 + a_9] + f_{B_s} F_{ann}^{LR,i} [a_5 + a_7] \right. \\
& \left. + M_{ann}^{LL,i} [C_4 + C_{10}] + M_{ann}^{SP,i} [C_6 + C_8] \right)_{K^{*-} \leftrightarrow K^{*+}} \Bigg\},
\end{aligned}
\tag{D8}
$$

$$A^i(\bar{B}_s^0 \to \bar{K}^{*0}K^{*0}) = -\frac{G_F}{\sqrt{2}}V_{tb}V_{ts}^* \bigg\{ f_{K^*}F_{B_s\to K^*}^{LL,i}\left[a_4 - \frac{1}{2}a_{10}\right] + M_{B_s\to K^*}^{LL,i}\left[C_3 - \frac{1}{2}C_9\right]$$

$$-M_{B_s\to K^*}^{LR,i}\left[C_5 - \frac{1}{2}C_7\right] + f_{B_s}F_{ann}^{LL,i}\left[a_3 + a_4 - \frac{1}{2}a_9 - \frac{1}{2}a_{10}\right]$$

$$-f_{B_s}F_{ann}^{SP,i}\left[a_6 - \frac{1}{2}a_8\right] + M_{ann}^{LL,i}\left[C_3 - \frac{1}{2}C_9 + C_4 - \frac{1}{2}C_{10}\right]$$

$$-M_{ann}^{LR,i}\left[C_5 - \frac{1}{2}C_7\right] + M_{ann}^{SP,i}\left[C_6 - \frac{1}{2}C_8\right]$$

$$+\left(f_{B_s}F_{ann}^{LL,i}\left[a_3 - \frac{1}{2}a_9\right] + f_{B_s}F_{ann}^{LR,i}\left[a_5 - \frac{1}{2}a_7\right]\right)_{K^{*0}\leftrightarrow \bar{K}^{*0}}$$

$$+\left(M_{ann}^{LL,i}\left[C_4 - \frac{1}{2}C_{10}\right] + M_{ann}^{SP,i}\left[C_6 - \frac{1}{2}C_8\right]\right)_{K^{*0}\leftrightarrow \bar{K}^{*0}} \bigg\}, \tag{D9}$$

$$A^i(\bar{B}_s^0 \to K^{*0}\phi) = -\frac{G_F}{\sqrt{2}}V_{tb}V_{td}^* \bigg\{ f_{\phi}F_{B_s\to K^*}^{LL,i}\left[a_3 + a_5 - \frac{1}{2}a_7 - \frac{1}{2}a_9\right] + f_{K^*}F_{B_s\to \phi}^{LL,i}\left[a_4 - \frac{1}{2}a_{10}\right]$$

$$+M_{B_s\to K^*}^{LL,i}\left[C_4 - \frac{1}{2}C_{10}\right] + M_{B_s\to \phi}^{LL,i}\left[C_3 - \frac{1}{2}C_9\right] - M_{B_s\to K^*}^{SP,i}\left[C_6 - \frac{1}{2}C_8\right]$$

$$-M_{B_s\to \phi}^{LR,i}\left[C_5 - \frac{1}{2}C_7\right] + f_{B_s}F_{ann}^{LL,i}\left[a_4 - \frac{1}{2}a_{10}\right] - f_{B_s}F_{ann}^{SP,i}\left[a_6 - \frac{1}{2}a_8\right]$$

$$+M_{ann}^{LL,i}\left[C_3 - \frac{1}{2}C_9\right] - M_{ann}^{LR,i}\left[C_5 - \frac{1}{2}C_7\right] \bigg\}. \tag{D10}$$

$$\sqrt{2}A^i(\bar{B}_s^0 \to \omega\phi) = \frac{G_F}{\sqrt{2}}V_{ub}V_{us}^* \bigg\{ f_{\omega}F_{B_s\to \phi}^{LL,i}[a_2] + M_{B_s\to \phi}^{LL,i}[C_2] \bigg\}$$

$$-\frac{G_F}{\sqrt{2}}V_{tb}V_{ts}^* \bigg\{ f_{\omega}F_{B_s\to \phi}^{LL,i}\left[2a_3 + 2a_5 + \frac{1}{2}a_7 + \frac{1}{2}a_9\right]$$

$$+M_{B_s\to \phi}^{LL,i}\left[2C_4 + \frac{1}{2}C_{10}\right] - M_{B_s\to \phi}^{SP,i}\left[2C_6 + \frac{1}{2}C_8\right] \bigg\}, \tag{D11}$$

$$\sqrt{2}A^i(\bar{B}_s^0 \to \phi\phi) = -\frac{2G_F}{\sqrt{2}}V_{tb}V_{ts}^* \bigg\{ f_{\phi}F_{B_s\to \phi}^{LL,i}\left[a_3 + a_4 + a_5 - \frac{1}{2}a_7 - \frac{1}{2}a_9 - \frac{1}{2}a_{10}\right]$$

$$+M_{B_s\to \phi}^{LL,i}\left[C_3 + C_4 - \frac{1}{2}C_9 - \frac{1}{2}C_{10}\right] - M_{B_s\to \phi}^{LR,i}\left[C_5 - \frac{1}{2}C_7\right]$$

$$-M_{B_s\to \phi}^{SP,i}\left[C_6 - \frac{1}{2}C_8\right] + f_{B_s}F_{ann}^{LL,i}\left[a_3 + a_4 - \frac{1}{2}a_9 - \frac{1}{2}a_{10}\right]$$

$$+f_{B_s}F_{ann}^{LR,i}\left[a_5 - \frac{1}{2}a_7\right] - f_{B_s}F_{ann}^{SP,i}\left[a_6 - \frac{1}{2}a_8\right] - M_{ann}^{LR,i}\left[C_5 - \frac{1}{2}C_7\right]$$

$$+M_{ann}^{LL,i}\left[C_3 + C_4 - \frac{1}{2}C_9 - \frac{1}{2}C_{10}\right] + M_{ann}^{SP,i}\left[C_6 - \frac{1}{2}C_8\right] \bigg\}. \tag{D12}$$

4. Electroweak penguin dominant decays

$$
\begin{aligned}
\sqrt{2} A^i(\bar{B}_s^0 \to \rho^0 \phi) \;=\; & \frac{G_F}{\sqrt{2}} V_{ub} V_{us}^* \left\{ f_\rho F_{B_s \to \phi}^{LL,i} \left[a_2\right] + M_{B_s \to \phi}^{LL,i} \left[C_2\right] \right\} \\
& - \frac{G_F}{\sqrt{2}} V_{tb} V_{ts}^* \left\{ f_\rho F_{B_s \to \phi}^{LL,i} \left[\frac{3}{2}(a_9 + a_7)\right] + M_{B_s \to \phi}^{LL,i} \left[\frac{3}{2} C_{10}\right] - M_{B_s \to \phi}^{SP,i} \left[\frac{3}{2} C_8\right] \right\} .
\end{aligned}
$$
(D13)

REFERENCES

[1] M. Wirbel, B. Stech, M. Bauer, Z. Phys. C**29**, 637 (1985); M. Bauer, B. Stech, M. Wirbel, Z. Phys. C**34**, 103 (1987).

[2] A. Ali and C. Greub, Phys. Rev. D**57**, 2996 (1998) [hep-ph/9707251]; G. Kramer, W. F. Palmer and H. Simma, Nucl. Phys. B**428**, 77 (1994); Z. Phys. C**66**, 429 (1995).

[3] A. Ali, G. Kramer, and C. -D. Lü, Phys. Rev. D**58**, 094009 (1998) [hep-ph/9804363]; Phys. Rev. D**59**, 014005 (1999) [hep-ph/9805403]; Y. H. Chen, H. Y. Cheng, B. Tseng, and K. C. Yang, Phys. Rev. D**60**, 094014 (1999) [hep-ph/9903453].

[4] M. Beneke, G. Buchalla, M. Neubert and C. T. Sachrajda, Phys. Rev. Lett. **83**, 1914 (1999) [hep-ph/9905312]; Nucl. Phys. B**591**, 313 (2000) [hep-ph/0006124].

[5] Y. Y. Keum, H. -n. Li, and A. I. Sanda, Phys. Lett. **B504**, 6 (2001) [hep-ph/0004004]; Phys. Rev. D**63**, 054008 (2001) [hep-ph/0004173]; C.-D. Lü, K. Ukai and M.-Z. Yang, Phys. Rev. D**63**, 074009 (2001) [hep-ph/0004213].

[6] C. W. Bauer, D. Pirjol, I. W. Stewart, Phys. Rev. Lett. **87** (2001) 201806 [hep-ph/0107002]; Phys. Rev. D**65**, 054022 (2002) [hep-ph/0109045].

[7] M. Ciuchini, E. Franco, G. Martinelli and L. Silvestrini, Nucl. Phys. B**501**, 271 (1997) [hep-ph/9703353].

[8] M. Beneke, [hep-ph/0612353].

[9] M. Beneke and T. Feldmann, Nucl. Phys. B**685**, 249 (2004) [hep-ph/0311335].

[10] C. W. Bauer, D. Pirjol, I. Z. Rothstein and I. W. Stewart, Phys. Rev. D**70**, 054015 (2004) [hep-ph/0401188].

[11] The use of charge conjugate modes in all the decays and branching ratios are implied in this paper.

[12] A. Abulencia *et al.* [CDF Collaboration], Phys. Rev. Lett. **97**, 211802 (2006) [hep-ex/0607021].

[13] M. Morello [CDF Collaboration], FERMILAB-PUB-06-471-E (2006) [hep-ex/0612018].

[14] G. Kramer and W. F. Palmer, Phys. Rev. D**46**, 3197 (1992); A. Deandrea, N. Di Bartolomeo, R. Gatto and G. Nardulli, Phys. Lett. B**318**, 549 (1993) [hep-ph/9308210]; A. Deandrea, N. Di Bartolemeo, R. Gatto, F. Feruglio and G. Nardulli, Phys. Lett. B**320**, 170 (1994) [hep-ph/9310326]; D. S. Du and Z. Z. Xing, Phys. Rev. D**48**, 3400 (1993); D. S. Du and M. Z. Yang, Phys. Lett. B**358**, 123 (1995) [hep-ph/9503278].

[15] B. Tseng, Phys. Lett. B**446**, 125 (1999) [hep-ph/9807393]; Y. H. Chen, H.Y. Cheng and B. Tseng, Phys. Rev. D**59**, 074003 (1999) [hep-ph/9809364].

[16] M. Beneke and M. Neubert, Nucl. Phys. B**675**, 333(2003) [hep-ph/0308039].

[17] J. F. Sun, G. H. Zhu, and D. S. Du, Phys. Rev. D**68**, 054003 (2003) [hep-ph/0211154]; X. Q. Li, G. R. Lu, Y. D. Yang, Phys. Rev. D**68**, 114015 (2003); Erratum-ibid. D**71**, 019902 (2005) [hep-ph/0309136]; Y. D. Yang, F. Su G. R. Lu, and H. J. Hao, Eur. Phys. J. C**44**, 243 (2005) [hep-ph/0507326].

[18] M. Beneke, J. Rohrer and D. Yang, Nucl. Phys. B**774**, 64 (2007) [hep-ph/0612290].

[19] C. H. Chen, Phys. Lett. B**520**, 33(2001) [hep-ph/0107189]; Y. Li, C.-D. Lü, Z.J. Xiao, X.Q. Yu, Phys. Rev. D**70**, 034009(2004) [hep-ph/0404028]; X. Q. Yu, Y. Li and C.-D. Lü, Phys. Rev. D**71**, 074026(2005); Erratum-ibid. D**72**, 119903 (2005) [hep-ph/0501152]; J. Zhu, Y. L. Shen and C.-D. Lü, J.Phys. G**32**, 101 (2006) [hep-ph/0506316]; X. Q. Yu, Y. Li and C.-D. Lü, Phys. Rev. D**73**, 017501 (2006) [hep-ph/0511269]; Z. J. Xiao, X. Liu, H. S. Wang, Phys. Rev. D**75**, 034017(2007) [hep-ph/0606177]; Z. J. Xiao, X. F. Chen and D. Q. Guo, Eur. Phys. J. C**50**, 363 (2007) [hep-ph/0608222]; J. W. Li and F. Y. You, Preprint Xu Zhou Normal University (2006) [hep-ph/0607249]; X. F. Chen, D. Q. Guo andZ. J. Xiao, Preprint NJNU-TH-07-02 [hep-ph/0701146].

[20] A. Williamson and J. Zupan, Phys. Rev. D**74**, 014003(2006); Erratum-ibid. D**74**, 039901 (2006) [hep-ph/0601214].

[21] R. Fleischer, Phys. Lett. B**459**, 306(1999) [hep-ph/9903456]; G. Barenboim, J. Bernabeu, J. Matias, and M. Raidal, Phys. Rev. D**60**, 016003(1999) [hep-ph/9901265]; M. Gronau and J. L. Rosner, Phys. Lett. B**482**, 71 (2000) [hep-ph/0003119]; C. H. Chen and C. Q. Geng, [hep-ph/0107145]; D. Atwood and A. Soni, Phys. Rev. D**65**, 073018 (2002) [hep-ph/0106083]; R. Fleischer and J. Matias, Phys. Rev. D**61**, 074004 (2000) [hep-ph/9906274]; Phys. Rev. D**66**, 054009 (2002) [hep-ph/0204101];

M. Gronau and J. L. Rosner, Phys. Rev. D**65**, 113008 (2002) [hep-ph/0203158]; A. J. Buras, R. Fleischer, S. Recksiegel and F. Schwab, Phys. Rev. Lett. **92**, 101804 (2004) [hep-ph/0312259]; Nucl. Phys. B **697**, 133 (2004) [hep-ph/0402112]; Eur. Phys. J C **45**, 701 (2006) [hep-ph/0512032]; D. London, Phys. Rev. D**70**, 031502 (2004) [hep-ph/0404009]; A. S. Safir, JHEP **0409**, 053 (2004) [hep-ph/0407015]; S. Descotes-Genon, J. Matias and J. Virto, Phys. Rev. Lett. **97**, 061801 (2006) [hep-ph/0603239]; R. Fleischer, J. Phys. G**32**, R71 (2006) [hep-ph/0512253]; M. Gronau , D. Pirjol, A. Soni and J. Zupan, Phys. Rev. D**75**, 014002 (2007) [hep-ph/0608243].

[22] D. Zhang, Z. J. Xiao, C. S. Li, Phys. Rev. D**64**, 014014 (2001) [hep-ph/0012063]; D. London, J. Matias and J. Virto, Phys. Rev. D**71**, 014024 (2005) [hep-ph/0410011]; S. Baek, D. London, J. Matias and J. Virto, JHEP **0602**, 027 (2006) [hep-ph/0511295]; JHEP **0612**, 019 (2006) [hep-ph/0610109].

[23] For a review, see G. Buchalla, A. J. Buras, M. E. Lautenbacher, Rev. Mod. Phys. **68**, 1125 (1996) [hep-ph/9512380].

[24] A. G. Grozin and M. Neubert, Phys. Rev. D**55**, 272 (1997) [hep-ph/9607366]; M. Beneke amd T. Feldmann, Nucl. Phys. B**592**, 3 (2001) [hep-ph/0008255].

[25] H. Kawamura, J. Kodaira, C. F. Qiao and K. Tanaka, Phys. Lett. B**523**, 111(2001); B **536**, 344 (2002) (E) [hep-ph/0109181]; Mod. Phys. Lett. A**18**, 799 (2003) [hep-ph/0112174].

[26] C.-D. Lü, M. Z. Yang, Eur. Phys. J. C**28**, 515 (2003) [hep-ph/0212373].

[27] H. -n. Li and S. Mishima, Phys. Rev. D**74**, 094020 (2006) [hep-ph/0608277].

[28] Particle Data Group, W.-M. Yao *et al.*, J. Phys. G**33**,1 (2006).

[29] P. Ball and R. Zwicky, Phys. Rev. D**71**, 014029 (2005) [hep-ph/0412079].

[30] P. Ball and R. Zwicky, JHEP **0604**, 046 (2006) [hep-ph/0603232].

[31] V. L. Chernyak and A.R. Zhitnitsky, Phys. Rept. **112**, 173 (1984); V. M. Braun and I. E. Filyanov, Z. Physik C**44**, 157 (1989); P. Ball, JHEP **9809**, 005 (1998) [hep-ph/9802394]; V. M. Braun and I. E. Filyanov, Z. Physik C**48**, 239 (1990); A. R. Zhitnisky, I. R. Zhitnitsky and V. L. Chernyak, Sov. J. Nucl. Phys. **41**, 284(1985), Yad. Fiz. **41**, 445 (1985).

[32] P. Ball, JHEP **9901**, 010 (1999) [hep-ph/9812375].

[33] H.-n. Li, Prog. Part. & Nucl. Phys. **51**, 85 (2003) [hep-ph/0303116], and reference therein.

[34] B. H. Hong, C.-D. Lü, Sci. China G**49**, 357-366 (2006) [hep-ph/0505020].

[35] V. M. Braun and A. Lenz, Phys. Rev. D**70**, 074020 (2004 [hep-ph/0407282]; P. Ball and A. Talbot, JHEP **0506**, 063 (2005) [hep-ph/0502115]; P. Ball and R. Zwicky, Phys. Lett. B**633**, 289 (2006) [hep-ph/0510338]; A. Khodjamirian, Th. Mannel and M. Melcher, Phys. Rev. D**70**, 094002 (2004)

[hep-ph/0407226].

[36] T. Feldmann, P. Kroll and B. Stech, Phys. Rev. D**58**, 114006 (1998) [hep-ph/9802409]; Phys. Lett. B**449**, 339 (1999) [hep-ph/9812269].

[37] Y. Y. Charng, T. Kurimoto and H.-n. Li, Phys. Rev. D**74**, 074024 (2006) [hep-ph/0609165].

[38] P. Ball, V. M. Braun, Y. Koike, and K. Tanaka, Nucl. Phys. B**529**, 323 (1998) [hep-ph/9802299]; P. Ball, V. M. Braun, Nucl. Phys. B**543**, 201(1999) [hep-ph/9810475].

[39] P. Ball, and V. M. Braun, Phys. Rev. D**54**, 2182(1996) [hep-ph/9602323]; P. Ball, and R. Zwicky, JHEP **0602**, 034 (2006) [hep-ph/0601086]; P. Ball, and M. Boglione, Phys. Rev. D**68**, 094006 (2003) [hep-ph/0307337].

[40] P. Ball and G. W. Jones, JHEP **0703**, 069 (2007) [arXiv:hep-ph/0702100].

[41] H.-n. Li, Phys. Lett. B**622**, 63 (2005) [hep-ph/0411305].

[42] H.-n Li, and S. Mishima, Phys. Rev. D**71**, 054025 (2005) [hep-ph/0411146].

[43] H.-W. Huang, *et.al*, Phys. Rev. D**73**, 014011 (2006) [hep-ph/0508080].

[44] Y. Li, C.-D. Lü, Phys. Rev. D**73**, 014024 (2006) [hep-ph/0508032].

[45] H. -n. Li and H. L. Yu, Phys. Rev. D**53**, 2480 (1996) [arXiv:hep-ph/9411308].

[46] H.-n. Li, Phys. Rev. D **66**,094010 (2002) [hep-ph/0102013].

[47] H.-n. Li and K. Ukai, Phys. Lett. B**555**, 197 (2003) [hep-ph/0211272].

[48] A. Gray *et al.* [HPQCD Collaboration], Phys. Rev. Lett. **95**, 212001 (2005) [hep-lat/0507015].

[49] A. A. Penin and M. Steinhauser, Phys. Rev. D**65**, 054006 (2002) [hep-ph/0108110].

[50] M. Jamin and B. O. Lange, Phys. Rev. D**65**, 056005 (2002) [hep-ph/0108135].

[51] P. Ball, V. M. Braun, A. Lenz, JHEP **0605**, 004 (2006) [hep-ph/0603063].

[52] H.-n. Li, S. Mishima and A. I. Sanda, Phys. Rev. D**72**, 114005 (2005) [hep-ph/0508041].

[53] J. Charles et al. (The CKMfitter Group); Eur. Phys. J. C**41**, 1 (2005) [hep-ph/0406184]. The input values for the CKM parameters are taken from the unitarity fits reported on October 4, 2006 (http://ckmfitter.in2p3.fr/).

[54] I. Dunietz, Phys. Rev. D**52**, 3048 (1995) [hep-ph/9501287].

[55] M. Beneke, G. Buchalla, C. Greub, A. Lenz and U. Nierste, Phys. Lett. B**459**, 631 (1999) [hep-ph/9808385].

[56] A. Lenz and U. Nierste, Preprint TTP06-31 [hep-ph/0612167].

[57] Heavy Flavor Averaging Group (HFAG), www.slac.stanford.edu/xorg/hfag/.

[58] D. London and J. Matias, Phys. Rev. D**70**, 031502(R) (2004) [hep-ph/0404009].

[59] M. Gronau, Phys. Lett. B**492**, 297 (2000) hep-ph/0008292].

[60] H. J. Lipkin, Phys. Lett. B**621**, 126 (2005) [hep-ph/0503022].

[61] P. Ball and R. Zwicky, Phys. Rev. D**71**, 014015 (2005) [hep-ph/0406232].

[62] D. Acosta, *et.al*, Phys. Rev. Lett **95**, 031801 (2005) [hep-ex/0502044].

[63] C.H. Chen and H.-n. Li, Phys. Rev. D**66**, 054013 (2002) [hep-ph/0204166].

[64] H.-n. Li, Phys. Lett. B**622**, 63 (2005) [hep-ph/0411305].

[65] H.Y. Cheng, C.K. Chua and C.W. Hwang, Phys. Rev. D**69**, 074025 (2004) [hep-ph/0310359].